Universität für Bodenkultur Wien
University of Natural Resources and Applied Life Sciences, Vienna

MASTERARBEIT

Titel der Masterarbeit

Mutational analysis of calnexin and calnexin-ERp57 complexes

angestrebter akademischer Grad

Diplomingenieurin

Verfasserin: Jeannine Daniela Schneider
Matrikelnummer: 0306111
Studienrichtung: Biotechnologie (H418)
Betreuer: Ao.Univ.Prof. Mag.rer.nat. Dr.rer.nat. Christian Obinger
Prof. Dr., FRSC Marek Michalak

Wien, im Mai 2009

TABLE OF CONTENTS

SUMMARY

The endoplasmic reticulum (ER), one of the organelles of all eukaryotic cells, is part of the endomembrane system. The ER has many functions; it is an important structure in protein translation and is responsible for folding and transport of proteins in the secretory pathway. By acting as a quality control center for newly synthesized proteins, it assures that only native proteins reach their final destinations. Chaperones and other factors recognize and target non-native and unassembled subunits of multimeric proteins. Subsequently, these unfunctional proteins are degraded by different measures. Among the many different chaperones in the ER, the proteins calreticulin, calnexin, and ERp57, a thiol oxidoreductase, are important players that interact to control the quality of glycoprotein folding.

The aim of this thesis was to use site-specific mutagenesis of calnexin to delineate further details about its interaction with ERp57. Six amino acid residues, Cys161, Cys195, His202, His219, Cys361, and Cys367, were selected for mutation by polymerase chain reaction based on interactions between ERp57 and calreticulin, a calnexin homologue. Mutant cDNAs were transfected into calnexin-knockout murine fibroblasts by utilizing the lentivirus method. The selected cells were investigated for expression by Western blotting and for intracellular localization by immunohistochemistry. To look for differences in structure between mutant calnexins and wildtype calnexin, trypsin digestion was performed. To investigate the binding and folding of substrates of the mutant calnexins, pulse/chase immunoprecipitation experiments were performed. The results revealed that the single and the double calnexin mutants (Cys161/195 Ala, His202/219Ala, and Cys361/367Ala) show only minor differences in behaviour when compared to the wild-type protein.

ZUSAMMENFASSUNG

Das endoplasmatische Reticulum (ER) ist eine der Organellen jeder eukaryotischen Zelle. Das ER ist eine wichtige Struktur für die Biosynthese von Proteinen und für die Faltung und den Transport von Proteinen, die in der Plasmamembran gebraucht oder aus der Zelle sekretiert werden sollen. Als Ort der Qualiltätskontrolle für neu synthetisierte Proteine stellt es sicher, dass nur native Proteine ihre Destination erreichen. Chaperone und andere Faktoren erkennen unter anderem ungefaltete Proteine und freie Untereinheiten multimerer Proteine. Als Folge der Qualitätskontrolle im ER werden diese unfunktionellen Proteine abgebaut. Neben vielen anderen Chaperonen im ER sind die Proteine Calreticulin, Calnexin und ERp57, eine Thiol Oxidoreductase, wichtige Spieler deren Interaktion die Glykoproteinfaltung überprüft und kontrolliert.

Um weitere Details dieser Interaktionen untersuchen zu können, war es daher das Ziel dieser Arbeit, sowohl mutante Calnexin Proteine zu generieren, als auch deren Bindung an ERp57 zu analysieren. Aufgrund bekannter Interaktionen zwischen ERp57 und dem Calnexin-homologen Calreticulin wurden 6 Aminosäuren, Cys161, Cys195, His202, His219, Cys361, und Cys367, identifiziert, welche mittels PCR mutiert wurden. Mutante cDNA wurde in Calnexin-defiziente murine Fibroblasten mittels der Lentivirus Methode, einem auch für stabile Integration von DNA in embryonale Stammzellen eingesetzten System, transfiziert. Die Expression der mutanten Proteine und ihre Lokalisation in selektierten Zellen wurden mit Western blotting bzw. Immunohistochemie analysiert. Um strukturelle Unterschiede zwischen den mutanten und den Wildtyp-Proteinen zu eruieren, wurde ihre Trypsin-Sensitivität untersucht. Pulse/chase Experimente wurden durchgeführt, um die Bindung und Faltung von Substraten der mutanten Calnexine zu erforschen. Die Ergebnisse zeigen, dass die Einzel- sowie Doppelmutanten von Calnexin keine nennenswerten Unterschiede im Vergleich zum Wildtyp zeigen.

1 INTRODUCTION

1.1 The endoplasmic reticulum

The endoplasmic reticulum (ER) is an organelle surrounded by a single membrane, that extends throughout the cytoplasm of the cell. It can be found in two different forms: the smooth ER that has no ribosomes attached is a site for lipid synthesis and other metabolic pathways. The rough ER has ribosomes bound to its cytosolic surface, which give a rough appearance in electron miscroscope images.

The ER plays a vital role in many cellular processes. These include lipid and protein synthesis, folding, and post- translational modification, and Ca^{2+} storage and release. The ER is also involved in cellular signalling and interorganellar communication, stress-dependent activation of transcriptional processes, Ca^{2+} -mediated signalling, and the so-called process of ER-associated degradation (ERAD). Fluctuating Ca^{2+} concentrations in the lumen of the ER may function as signal for many ER functions, such as protein- and lipid synthesis (Corbett et al., 2000);(Corbett and Michalak, 2000). Therefore, the ER has been defined as a multifunctional organelle able to detect and integrate incoming signals, modulate its own luminal dynamics, and generate output signals in response to environmental changes (Corbett et al., 2000); (Corbett and Michalak, 2000). These multiple functions are performed despite the fact that the ER appears to be an unlikely environment for such functions, in particular, for protein folding. The concentration of luminal proteins is ~100 mg/ml and the total Ca^{2+} concentration is 5-10 mM, which probably gives rise to a gel-like matrix (Booth and Koch, 1989);(Meldolesi and Pozzan, 1998). Nevertheless, proteins that exit the ER are, for the most part, properly folded and assembled, owing to the coordinated activities of the components of a complex machinery for quality control. In fact, the principle of quality control in the ER is the recognition of incorrectly folded proteins, which may arise by a variety of shortcomings in the biosynthetic processes that lead to mature functional proteins. In the following sections, I will summarize the current status of knowledge about protein folding.

1.2 Folding in the endoplasmic reticulum

In several aspects the ER is unique among cellular folding compartments. It differs from other folding compartments (e.g. the cytosol and mitochondria) in its high oxidizing potential, its highly fluctuating Ca^{2+} concentration, the presence of carbohydrates, and a machinery for protein-glycosylation (Corbett and Michalak,

2000). The glycosylation of nascent proteins as well as disulphide bond formation are essentially unique for the ER. Both processes play important roles in the maturation and folding of proteins and need to be monitored by the quality control system in the ER. Furthermore, since the ER is the major Ca^{2+} store in the cell and undergoes quite rapid changes in Ca^{2+} levels, protein folding must be able to adapt to Ca^{2+} fluctuations. However, this dependence has not yet been studied extensively (Corbett and Michalak, 2000). Most proteins that fold in the ER, including proteins destined for insertion into the plasma membrane and secreted proteins, are transiently binding to the ER via an N-terminal signal sequence that subsequently has to be cleaved. In many cases this may cause a delay in folding. On the other hand, because of the vast discrepancy between the rates for folding (fast) and translation (slower), a mechanism for delaying the former is necessary. Thus, as soon as about 20 amino acids, constituting a signal sequence, protrude from the large unit of the ribosome, they are bound by the signal recognition particle (SRP) that targets the ribosome to the ER membrane (Figure 1.1). Translation is temporarily stopped and resumes only after the ribosome has attached to the ER membrane, mediated by the SRP-receptor. A delay in folding is also necessary for translocation of the polypeptide across the membrane (Stevens and Argon, 1999).

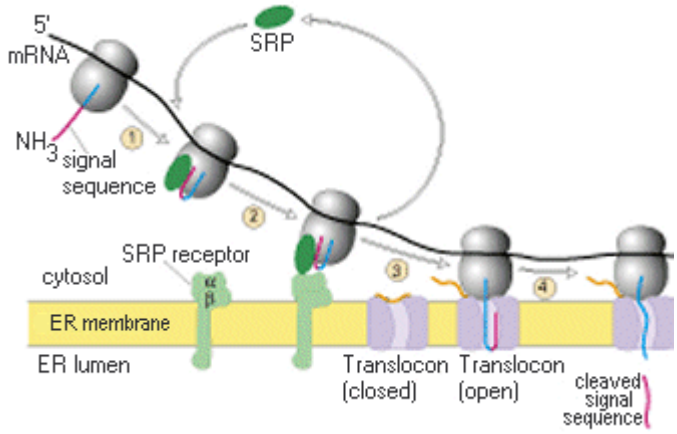

Figure 1.1. Role of the signal recognition particle (SRP) in binding to the nascent, N-terminal signal sequence of a protein destined for insertion into the plasma membrane or secretion in a eukaryotic cell. After binding the signal sequence, the SRP docks the actively synthesizing ribosome on the Translocon by first binding to a nearby SRP receptor embedded in the endoplasmic reticular membrane. In the course of targeting the ribosome to the Translocon, the SRP and the SRP receptor both hydrolyze bound GTP to GDP. The SRP exchanges GDP for GTP when it engages a new signal peptide. Excerpt from Figure 17-16 from Lodish, et al. (Molecular Cell Biology, 4th Ed.; W.H. FREEMAN, 2000; www.callutheran.edu/Academic_Programs/Departments/BioDev/omm/srp/frames/gif.htm.

Folding is assisted by a large number of folding enzymes, chaperones and folding sensors. Many of these quality control proteins interact with nascent polypeptides and continue to assist folding until a protein acquires its native conformation. As the aim of the system is that only correctly folded proteins leave the ER, exit is strictly regulated so as to inhibit the secretion of incompletely folded or misfolded proteins. This prevents the cell from using potentially malfunctioning proteins that could be harmful for the cell or the organism, reviewed by (Ellgaard and Helenius, 2001).

Quality control acts at several levels and by multiple mechanisms. Association with ER folding factors provides a primary quality control that applies to all newly synthesised proteins. It depends on general biophysical properties of incompletely folded proteins, such as exposed hydrophobic patches or lack of compactness, as for instance in globular proteins. Chaperones selectively associate with proteins that display such features and thereby promote their folding and assembly. An important aspect is that as long as proteins are associated with chaperones, they are prevented from being exported (Ellgaard et al., 1999).

The lumen of the ER contains a wide variety of chaperones and lectins involved in primary quality control. The most abundant ones are BiP, the calnexin/calreticulin system, GRP94, protein disulphide isomerase (PDI), ERp57, and ERp72. Binding of any one of these factors, even if only in an on-and-off cycle, seems to be sufficient to prevent further transport. In mammalian cells, chaperones and folding factors are highly abundant. If one chaperone fails to recognize a misfolded substrate protein, another one most likely will (Zhang et al., 1997).

A second level of quality control is specific for individual proteins, such as e.g., the association of collagens with Hsp47 (Nagata and Hosokawa, 1996). Other examples are special escort proteins, as for instance receptor-associated protein (RAP) for the LDL receptor family (Bu et al., 1995) and retention factors such as TAP (transporter associated with antigen processing) and tapasin for MHC class I antigens (Ortmann et al., 1997) and see section 1.3.1.3.

1.3 Chaperones

As indicated above, the basic paradigm of molecular chaperones is that they recognize and selectively, yet reversibly, bind non-native polypeptides to form relatively stable complexes. Chaperones comprise a group of families of unrelated proteins found in all organisms from bacteria to humans; many chaperones are also

heat shock (stress) proteins. They are located in every cellular compartment, bind a wide range of proteins, and are part of the general mechanism for protein-folding.

Chaperones may also keep newly synthesised proteins in an unfolded conformation in order to translocate them across membranes, and they bind non-native proteins during cellular stress. Alternatively or in addition, chaperones often participate in the elimination of polypeptides that become irreversibly misfolded. As classical catalysts, chaperones transiently interact with their substrate proteins, but are not present in the final folded product, and also do increase the yield of “correct” protein (Fink, 1999);(Li and Srivastava, 2004).

The major classes of chaperones are:

• *Small heat shock proteins,* which prevent protein aggregation in an ATP-independent manner. They are produced only under stress conditions and bind denatured proteins tightly, but so far there is little evidence that they subsequently release bound material (reviewed by Haslbeck, 2002).

• *40-kDa heat shock proteins (Hsp40; the DnaJ family)*, a large family defined by the presence of a highly conserved region with similarity to the initial 73 amino acids of the *Escherichia coli* protein DnaJ, hence termed the J domain (Kelley et al 1998). The J domain of DnaJ-like proteins is involved in regulating the adenosine triphosphatase (ATPase) activity of heat shock proteins (Cheetham and Caplan, 1998). The best known function of Hsp40 is that of being a co-chaperone of Hsp70, although there is also evidence that Hsp40 family members are chaperones in their own right (Hendershot et al., 1996);(Kelley, 1998);(Kelley, 1999).

• *60-kDa heat shock proteins (Hsp 60)* are large oligomeric ring-shaped proteins also known as chaperonins that bind partially folded intermediates in a large central cavity. Hsp60 members are found in all biological compartments except the ER. At least in bacteria, Hsp60 (there called GroEL) requires a cochaperone (GroES) and binds ATP (reviewed by Walter and Buchner, 2002).

• *70-kDa heat shock proteins (Hsp70)* bind to nascent polypeptide chains on ribosomes and prevent their premature folding, misfolding, and aggregation. Moreover, they bind to newly synthesised proteins in the process of translocation from the cytosol into mitochondria and the ER. Hsp70 proteins bind ATP and exhibit weak ATPase activity (reviewed by Mayer et al., 2001).

• *90-kDa heat shock proteins (Hsp90)*. Members of the Hsp90 family are highly conserved proteins found in all organisms from bacteria to humans. Mammalian

Hsp90 proteins exist as dimmers, and are frequently found in complexes with other chaperones as well (reviewed by Picard, 2002).

- *100-kDa heat shock proteins* help organisms to survive extreme stress. They perform several functions, including proteolysis (reviewed by Feng and Gierasch, 1998).

All of these chaperones prevent the aggregation of many substrate proteins. A number of other proteins involved in protein maturation and folding are also often considered chaperones. These include the members of the protein disulphide isomerase (PDI) family, the protein pair calnexin (cnx) and calreticulin (crt), and peptidyl prolyl isomerase (Fink, 1999), as well as ER degradation-enhancing α -mannosidase-like lectins (EDEMs), recently found mannose-specific lectins reviewed in (Olivari and Molinari, 2007);(Vembar and Brodsky, 2008).

1.3.1 Chaperones in the endoplasmic reticulum

The ER is a major site for protein synthesis with many nascent polypeptides being cotranslationally translocated into and across its membrane. These polypeptides pass through the translocation sites of the ER as partially unfolded polypeptide chains. Therefore, the lumen functions as a specialized folding environment and contains a number of molecular chaperones and folding factors (Ni and Lee, 2007).

The most abundant and best-characterised molecular chaperones of the ER are:

- *BiP* (Kar2p in yeast), the only member of the Hsp70 family in the ER,
- *Calnexin/calreticulin*, chaperone-lectins that recognize sugar moieties and act in association with *ERp57*, a member of the protein disulphide isomerase family,
- *Protein disulphide isomerase (PDI),* a member of the thioredoxin superfamily,
- *GRP94*, a member of the Hsp90 family and
- *EDEMs*, newly discovered mannose-specific lectins.

1.3.1.1 BiP/GRP78

BiP is a member of the Hsp70 heat shock protein family and has originally been described independently as the immunoglobulin heavy-chain binding protein (Haas and Wabl, 1983) and as the glucose-regulated protein, GRP78 (Quinones et al., 2008). It is the only member of the Hsp70 protein family found so far in the lumen of the ER, and in the mammalian and the yeast proteins, ER retrieval signal sequences at the carboxy-terminus have been found (KDEL and HDEL, respectively). Like other Hsp70 proteins, BiP binds ATP with high affinity and displays weak ATPase activity that is stimulated by binding unfolded proteins (reviewed by Gething and Sambrook,

1992). Addition of ATP, but not of nonhydrolyzable homologues, causes the dissociation of BiP from its substrate protein, which initially lead to the conclusion that ATP hydrolysis provides a timer mechanism for substrate release. However, it was later shown that dissociation from Hsp70 molecules follows rapidly after ATP binding, and before ATP hydrolysis takes place (Palleros et al., 1993).

BiP transiently associates with many, if not all, newly synthesized wild-type transmembrane and secretory proteins until they fold or assemble in the ER, and more permanently with misfolded, underglycosylated or unassembled proteins whose export form the ER is blocked. BiP binds in the nascent or misfolded proteins to sequences which in the native protein would be buried inside the three-dimensional structure, such as hydrophobic and aromatic residues or clusters thereof (Kleizen and Braakman, 2004).

Another important role for BiP apart from being a chaperone is the gating of the translocation channel (see Figure 1.1). BiP has been found to be responsible for sealing the luminal side of the mammalian translocon (Hamman et al., 1998). BiP is bound to the luminal end of the aqueous pore immediately after ribosomal targeting is completed and until the nascent chain reaches a length of approx. 70 amino acids. When no ribosome is bound to the translocon, the diameter of the pore is considerably smaller than in the functioning translocon, but BiP still binds at the luminal side to seal off the ER lumen from the cytosol. However, only a nucleotide-bound form of BiP is able to act as a gating protein. The mechanism by which BiP closes the ribosome-free translocon is not known; neither are the interaction partners of BiP in or in proximity of the translocon. Since BiP seals the translocon only in the presence of ATP or ADP, it can be speculated that the binding is conformation-dependent (Hamman et al., 1998).

Hsp70 often associates with members of the DnaJ family of proteins (see section 1.3). In the yeast ER, the BiP homologue Kar2p has been shown to interact with three DnaJ-like proteins: Jem1p and Scj1p (Nishikawa and Endo, 1997);(Schlenstedt et al., 1995) involved in protein folding and assembly, and Sec63p (see below). Jem1p and Scj1p were found to be involved in ERAD in yeast by interacting with BiP via their J-domains and facilitating the export of luminal ERAD substrates to the cytosol by preventing their aggregation (Nishikawa et al., 2001).

Post-translational import into the ER requires hydrolyzable ATP, and to date the only identified ATPases in the translocon are the Hsp70s, suggesting that they can directly couple ATP hydrolysis with protein transport. Sec63p is an integral

membrane protein with homology to DnaJ proteins. BiP interacts with the J-domain, which may activate BiP for substrate binding in a manner similar to that by which other J proteins activate their Hsp70 partners (Brodsky et al., 1995);(Lyman and Schekman, 1995). Two models have been proposed for the function of BiP in protein translocation. In the first model, it acts as a molecular motor, anchored at the membrane by its interaction with Sec63p and actively pulling the substrate into the lumen. In the other model, it acts like a ratchet: following a transient interaction with Sec63p, BiP would be transferred to the substrate and prevent it from sliding back into the cytosol (Matlack et al., 1998).

Under normal growth conditions, BiP is synthesised abundantly and constitutively, comprising about 5% of the luminal content of the ER. In a process termed unfolded protein response (UPR; see also section 1.5), its synthesis can be further induced by the appearance of high levels of mutant proteins in the ER or by a variety of stress conditions, like glucose starvation, treatment with drugs that inhibit glycosylation (e.g. tunicamycin), or treatment with calcium ionophores and amino acid analogs (Gething and Sambrook, 1992).

1.3.1.2 Calreticulin and calnexin

These chaperones bind to ATP, Ca^{2+}, Zn^{2+} and to one of the many thiol oxidoreductases of the ER, ERp57 (Williams, 2006);(Corbett and Michalak, 2000); (Oliver et al., 1997). They have co-evolved with Asn-linked glycosylation in eukaryotes; their binding preference for glycoproteins is due to the fact that cnx and crt are lectins specific for a transient oligosaccharide-processing intermediate that possesses a single terminal glucose residue: $Glc_1Man_9GlcNAc_2$ (Figure 1.2.A) (Hammond et al., 1994);(Ou et al., 1993);(Ware et al., 1995). Finally, they can associate with polypeptide segments of non-native glycoprotein conformers in a manner similar to other molecular chaperones, although the importance of this mode of association is controversial (Ihara et al., 1999);(Saito et al., 1999).

ERp57 (see section 1.3.1.3) is an oxidoreductase that forms functional complexes with crt and cnx (Hebert and Molinari, 2007). Crt and cnx show a high degree of structural and functional similarities, including similar domains. For example, the two proteins exhibit 40% amino acid sequence similarity and 30% amino acid sequence identity (Wada et al., 1991);(Fliegel et al., 1989);(Smith and Koch, 1989). Crt is a 46 kDa ER luminal Ca^{2+}-binding protein. It contains an N-terminal cleavable signal sequence signal (Figure 1.2.A). Cnx is a 90 kDa ER integral membrane protein and homologue of crt (Wada et al., 1991);(Michalak et al., 2009). Cnx (Figure 1.2.B) also

has a cleavable N-terminal amino acid signal sequence that directs it to the ER, a transmembrane domain and a cytoplasmic C-terminal RKPRRE (Arg-Lys-Pro-Arg-Arg-Glu) ER-retention signal (Wada et al., 1991).

Crt, together with cnx and ERp57 (ER protein of 57 kDa), is involved in the chaperoning of nascent polypeptides that traverse through the ER (Hebert and Molinari, 2007). Functionally, both proteins efficiently suppress the aggregation of glycosylated and non-glycosylated proteins via protein–oligosaccharide and protein–protein interactions (Hebert and Molinari, 2007). As crt and cnx facilitate protein folding in conjunction with ERp57 (Leach et al., 2002);(Oliver et al., 1997), using NMR spectroscopy techniques ERp57-binding sites have been identified at the tip of the P-domain in crt and cnx (Frickel et al., 2002);(Pollock et al., 2004). The interaction of crt with ERp57 is disrupted by mutations of Glu239, Asp241, Glu243 and Trp244 in the tip of the P-domain (Martin et al., 2006).

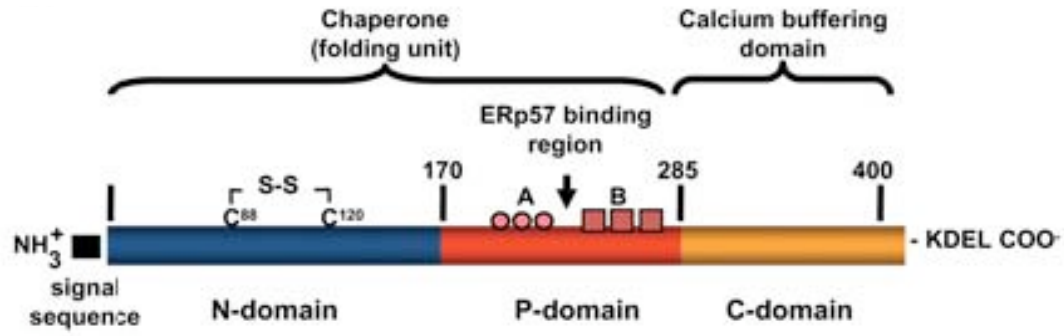

Figure 1.2.A: Linear representation of calreticulin domains. The protein contains an N-terminal amino acid signal sequence (black box), N-domain (blue box), P-domain (red box; Credle et al., 2005), C-domain (orange box) and a C-terminal KDEL ER retrieval signal. Repeats A (amino acid sequence PXXIXDPDAXKPEDWDE) and B (amino acid sequence GXWXPPXIXNPXYX) are indicated by pink circles and squares, respectively. The amino acids involved in the thiol linkage are indicated and connected with an S–S, and the numbers delineate the amino acid residues at the transition between the various domains. Figure 1 from (Michalak et al., 2009).

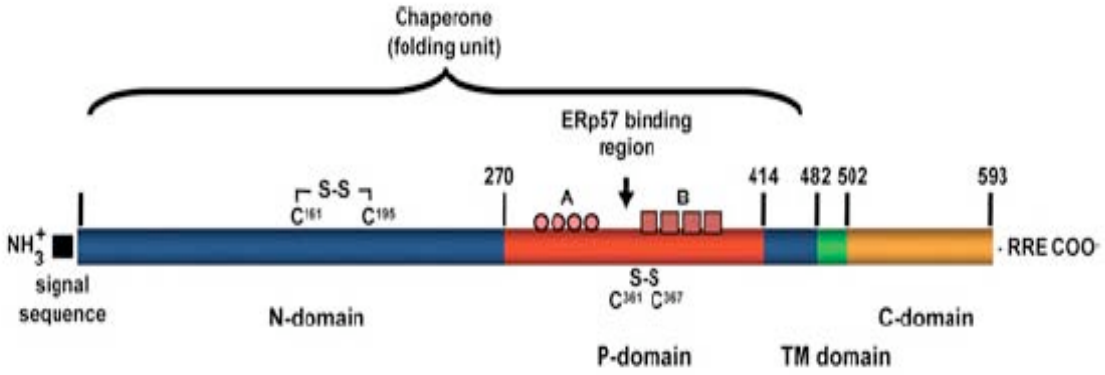

Figure 1.2.B: Linear representation of cnx domains. The protein contains an N-terminal amino acid signal sequence (black box), N-domain (blue boxes), P-domain (red box; Credle et al., 2005), transmembrane domain (green box), C-domain (orange box) and a C-terminal RKPRRE ER retrieval signal. Repeats A (amino acid sequence PXXIXDPDAXKPEDWDE) and B (amino acid sequence GXWXPPXIXNPXYX) are indicated by pink circles and squares, respectively. The amino acids involved in the thiol linkages are connected with an S–S, with the numbers delineating the amino acid residues at the transition between the various domains. Figure 1 from (Michalak et al., 2009).

Functions of Cnx and Crt in quality control of glycoproteins: Glycosylation

In eukaryotic cells, a wide variety of secretory and membrane-bound proteins have one or more N-linked glycans covalently attached. These N-linked oligosaccharides are very diverse, but the pathways by which they are formed all have a common first step in which an N-glycan moiety consisting of three N-acetylglucosamines, nine mannose and three glucose residues (see Fig. 1.3.A) is transferred en bloc from an activated lipid carrier, dolichol pyrophosphate, to the growing polypeptide chain by oligosaccharyltransferase. The acceptor site is an asparagine in the consensus sequence of Asn-X-Ser/Thr, where X can be each amino acid except proline. However, not every asparagine in such a sequence becomes glycosylated (reviewed by Helenius and Aebi, 2001).

The core oligosaccharide, $Glc_3Man_9GlcNAc_2$, is built on the phosphate group of dolichol phosphate by the successive addition of activated monosaccharides. The first steps occur on the cytosolic side of the ER membrane up to a structure of $Man_5GlcNAc_2$, and after a translocation step across the membrane, the core oligosaccharide is completed in the lumen of the ER (reviewed by Helenius and Aebi, 2002). After the addition of the core oligosaccharide to the protein, it is further modified in the ER and the Golgi apparatus. In the ER, the three glucoses are removed by glucosidases I and II, and one mannose gets cleaved by ER

mannosidase I before the protein is transported further. In the Golgi more mannoses are removed while other sugar residues such as N-acetylglucosamine, galactose or N-acetylneuraminic acid are added, so that the final version of N-linked sugars in diverse glycoproteins differs notably, except for a structure of $Man_3GlnNAc_2$, which is common to all N-linked oligosaccharides (see Figure 1.3.B).

The biological advantage of adding sugar moieties to proteins is not yet fully understood. Apart from playing a role in protein folding and the quality control in the ER, the very hydrophilic clusters of carbohydrates alter the polarity and solubility of the proteins they are attached to and may also influence their folding. Moreover, glycan moieties are crucial in many molecular recognition events (Varki, 1993).

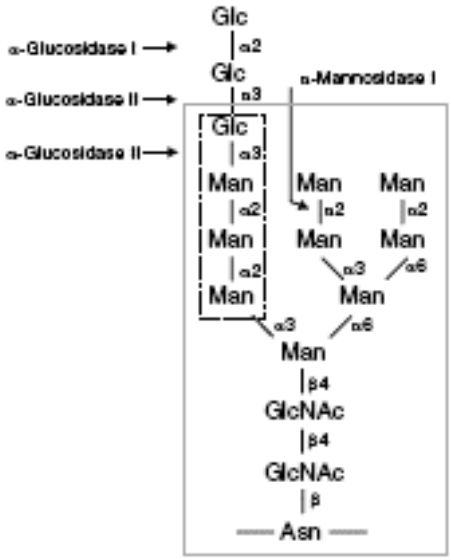

Figure 1.3.A: Composition of the $Glc_3Man_9GlcNAc_2$ oligosaccharide initially transferred to nascent glycoproteins. The box shows the monoglucosylated $Glc_1Man_9GlcNAc_2$ oligosaccharide recognized by cnx and crt. It is formed by the initial action of alpha-glucosidase I followed by cleavage of a second glucose by alpha-glucosidase II. The lectin sites of cnx and crt bind to the terminal glucose residue of the $Glc_1Man_9GlcNAc_2$ oligosaccharide as well as to three underlying mannose residues (dashed box). Also indicated is the terminal mannose residue cleaved by alpha-mannosidase I to create a signal associated with rapid degradation of misfolded glycoproteins. Glc, glucose; Man, mannose; GlcNAc, N-acetylglucosamine.

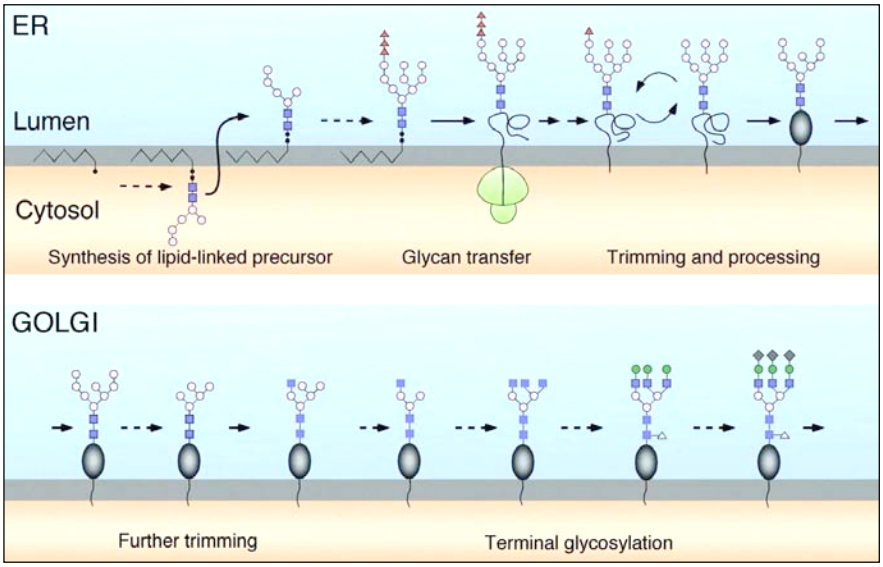

Figure 1.3.B: Biosynthesis of N-linked oligosaccharides (Helenius and Aebi, 2001): The maturation of N-linked glycans starts after the calnexin quality control cycle (2 curved arrows, for details, see below) with the trimming and processing of $Man_8GlcNAc_2$, and proceeds to terminal glycosylation reactions that generate highly diverse and yet specific mature carbohydrate structures. Δ Glucose, ○ Mannose, ■ GlcNAc, ● Galactose, △ Fucose, ◆ Sialic acid.

The calnexin cycle for quality control

Cnx and crt share the same substrate specificity and bind monoglucosylated structures. The terminal glucose in $Glc_1Man_9GlcNAc_2$ is crucial for binding, but some mannose residues also contribute to the binding specificity, since $Glc_1Man_{5-7}GlcNAc_2$ are relatively poor substrates (Fig. 1.3.A and Ware et al., 1995). Cnx and crt are part of the quality control system in the lumen of the ER that ensures that correctly folded proteins leave the ER, while incorrectly folded proteins are targeted for degradation. The lectin-assisted glycoprotein folding involves a cycle of deglucosylation and reglucosylation known as **calnexin cycle**, (reviewed by Parodi, 2000a and Vembar and Brodsky, 2008) (see Figure 1.4). Newly synthesised glycoproteins carrying three glucose residues on each glycan are co-translationally trimmed by the sequential action of ER glucosidase I and II. The monoglucosylated glycoproteins bind to cnx and/or crt (Trombetta and Helenius, 1999), together with the oxidoreductase ERp57. The last glucose is then removed by glucosidase II, and thus the interaction between the lectins and the glycoprotein is abolished. If the protein is folded correctly, it can now exit the ER; if not, the protein is reglucosylated by the ER enzyme UDP-glucose:glycoprotein glucosyltransferase (UGGT). UGGT recognizes only incompletely folded glycoproteins as its substrate, and so it is UGGT that acts as a folding sensor. After reglucosylation, the glycoprotein rebinds to cnx/crt, and the cycle is repeated until the protein is folded correctly. However, if the glycoprotein

persistently fails to fold, it gets marked for degradation due to the action of ER mannosidase I. The α1,2-linked mannose from the inner branch of the N-glycan is cleaved to yield $Man_8GlcNAc_2$. After reglucosylation by UGGT, the protein rebinds cnx/crt. Since $Glc_1Man_8GlcNAc_2$ is a poor substrate for glucosidase II, the proteins stays associated with cnx/crt longer. Two distinct complexes (OS-9 or XTP3-B) recognize substrates bearing trimmed glycans and transfer them to the Hrd1 complex. The retrotranslocon pore is either formed by Derlin-1, which is linked to Hrd1 through HERP, or the Sec61 complex. Segments in the cytosol are ubiquitinated, and ERASIN or VIMP recruits the p97 ATPase complex to the ER membrane and extracts the ubiquitinated substrate. Once in the cytosol, the substrate is degraded by the 26S proteasomes. The 26S proteasome consists of a 20S particle in its the core and, in most cases, two 19S particles on either side of the cylindrical core. Both components have been shown to be involved in the degradation of proteins released from the ER in yeast (Hampton et al., 1996);(Hiller et al., 1996).

Proteasomes are the final destination of proteins that are going to be degraded by ERAD. They mostly reside free in the cytosol (Palmer et al., 1996); however, a sub-population of proteasomes may be attached to the cytosolic face of the ER membrane (Rivett et al., 1992);(Palmer et al., 1996). These membrane-bound proteasomes could be interacting with the Sec61 complex or with other proteins involved in retro-translocation. Alternatively, proteasomes could be interacting directly with the lipid bilayer. In support of this notion, it has been demonstrated that proteasomes bind to lipid monolayers with the proteasome channel oriented perpendicular to the monolayer (Newman et al., 1996). Therefore, membrane-bound proteasomes are ideally suited to degrade membrane-bound ERAD substrates as well as proteins emerging from the translocon channel. There is also evidence that the proteasome itself provides the energy for retrograde transport by ATP hydrolysis, catalysed by its own subunits (Mayer et al., 1998).

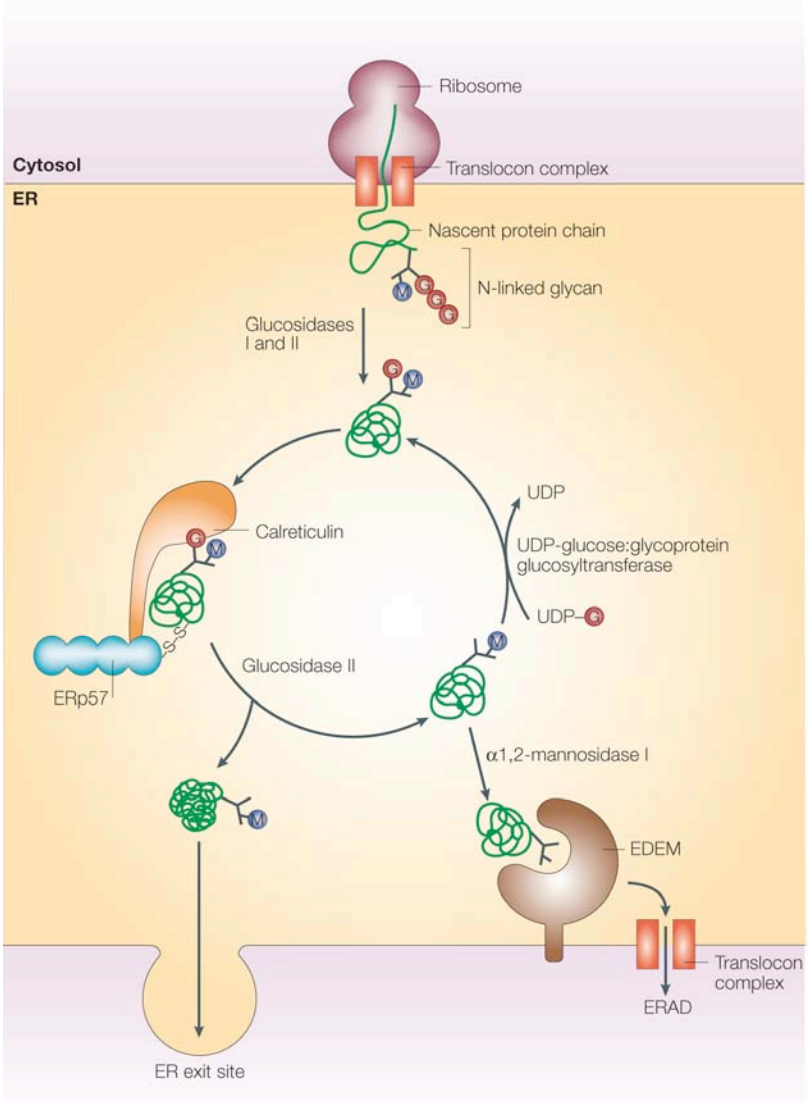

Figure 1.4: Models for the roles of cnx and crt in the calnexin cycle. As a nascent polypeptide enters the ER lumen via the translocon pore, Asn residues within Asn-X-Ser(Thr) sequences may be recognized by oligosaccharyl transferase (OST) and glycosylated with the preassembled $Glc_3Man_9GlcNAc_2$ oligosaccharide. The outer two glucoses are then rapidly removed by glucosidases I and II to generate the $Glc_1Man_9GlcNAc_2$ oligosaccharide recognized by cnx and crt. In the lectin-only model, cycles of glycoprotein release and rebinding are controlled solely by the removal and re-addition of the terminal glucose residue by glucosidase II and UDP-glucose:glycoprotein glucosyltransferase (UGGT), respectively. UGGT is the folding sensor because it only reglucosylates non-native glycoprotein forms. Chaperone binding serves to retain non-native glycoproteins within the ER and also recruits ERp57 to promote disulfide-bond formation and isomerization. It is unclear whether binding to glycoproteins only through the lectin site is sufficient to suppress aggregation. In the dual binding model, cnx and crt recognize non-native glycoproteins through their lectin sites as well as through a polypeptide binding site specific for non-native forms. This allows them to prevent off-pathway aggregation reactions similarly to other molecular chaperones. Binding via the polypeptide binding site is influenced by ATP and by the free Ca^{2+} concentration, either of which may regulate the interaction. In both models, folding takes place upon release from the chaperone, followed by further oligosaccharide trimming and export to the Golgi apparatus. For misfolded glycoproteins that remain for prolonged periods in the cnx/crt cycle, trimming by alpha-mannosidase I generates a $Man_8GlcNAc_2$ structure that may be recognized by putative lectins termed EDEM (see section 1.3.1.6) as part of a signal leading to retrotranslocation and proteasomal degradation [ER-associated degradation (ERAD)].

Of the ~100 newly synthesized glycoproteins that associate with cnx or crt (David et al., 1993);(van Leeuwen and Kearse, 1996), some interact only with one chaperone whereas others may bind both either simultaneously or sequentially. Initial association can be cotranslational (Chen et al., 1995) and the interaction is maintained during subsequent folding and assembly steps. Release from cnx or crt is often closely coupled to export of the glycoprotein out of the ER to the Golgi complex (Anderson and Cresswell, 1994);(Degen et al., 1992);(Hammond et al., 1994);(Ou et al., 1993). The functional consequences of the interaction have been assessed in a variety of ways. Since the $Glc_1Man_9GlcNAc_2$ oligosaccharide recognized by cnx and crt is formed by the combined action of glucosidases I and II on the initially transferred $Glc_3Man_9GlcNAc_2$ oligosaccharide, glucosidase-deficient cells or inhibitors of these enzymes such as castanospermine (CST) have been extensively used to prevent cnx/crt interactions. Since not all interactions with cnx or crt are blocked by this treatment, alternative approaches include the use of cnx- or crt-deficient cell lines and expression of glycoproteins of interest in heterologous systems that lack cnx/crt interactions. The studies using glucosidase inhibitors indicate that the folding and assembly of many, but not all, glycoproteins is influenced by cnx and crt, (see Danilczyk and Williams, 2001 and Parodi, 2000a, b). In some cases these observations have been confirmed in cnx- or crt-deficient cell lines or in expression systems lacking functional chaperones. For example, Semliki forest virus glycoprotein maturation is accelerated in crt-deficient cells, but is less efficient (Molinari et al., 2004). In the case of class I major histocompatibility complex (MHC) molecules, their assembly into mature ternary complexes is impaired in the absence of crt, as is their expression at the cell surface (Gao et al., 2002).

In contrast to being generally accepted that cnx/crt are important for glycoprotein folding, it is still uncertain whether they act solely as lectins [“lectin only” hypothesis; (Trombetta and Helenius, 1998)], or if they act as lectins and as classic chaperones [“dual binding” model; (Ware et al., 1995)] (see also Figure 1.4). In vitro, it has been shown that cnx/crt are able to bind both unglycosylated and glycosylated proteins, prevent their aggregation and keep them in a folding- competent state (Ihara et al., 1999);(Saito et al., 1999).

1.3.1.3 ERp57- a thiol oxidoreductase with diverse modes of substrate recognition

ERp57, in concert with cnx and crt, plays an important and complex role in glycoprotein folding. ERp57 is a member of the protein disulphide isomerase (PDI) family and contains two thioredoxin motifs like PDI itself. ERp57 harbours four thioredoxin-like domains: a, b, b' and a'. The a and a' domains contain the active site – CXXC – motifs. The N-terminal cysteine residue of the motif forms mixed disulfides with substrate proteins during oxidation and isomerization reactions. Interaction of ERp57 with the arm domains of cnx and crt is mediated primarily through its b' domain (see Figure 1.5) and to some extent through its positively charged C-terminus (Russell et al., 2004);(Silvennoinen et al., 2004). Since the association of ERp57 with glycoprotein substrates can be prevented by treatment with CST or expression in cnx-deficient cells, the commonly held view is that ERp57 is always recruited to folding glycoproteins through its interactions with cnx or crt (Lindquist et al., 2001);(Molinari and Helenius, 1999);(Oliver et al., 1997). This view is supported by the in vitro finding that the oxidative folding of monoglucosylated RNAse B by ERp57 is dramatically enhanced by the presence of cnx or crt (Zapun et al., 1998).

Despite clear in vitro evidence that ERp57 acts as a thiol oxidase, reductase, and isomerase (Frickel et al., 2004), demonstrating these functions in cells has been difficult. Along with crt, ERp57 has been shown to associate with the SERCA2b Ca^{2+} pump and to inhibit pump function in a process dependent on cysteines within an intraluminal loop of SERCA2b (Li and Camacho, 2004). Furthermore, ERp57 forms mixed disulfide complexes with viral glycoproteins and probably also with class I heavy chains (Antoniou et al., 2002);(Lindquist et al., 2001);(Molinari and Helenius, 1999). Since mixed disulfides are normal intermediates in oxidation and isomerization reactions, this implicates ERp57 in the catalysis of these processes. Such a role during MHC class I biogenesis was confirmed by depleting ERp57 more than 90% by RNA interference (Zhang et al., 2009). This markedly reduces the rate of formation of heavy-chain disulfide bonds as well as the folding of one of the heavy-chain domains.

ERp57 has possibly been best studied in the context of catalyzing disulfide formation in heavy chains of class I histocompatibility molecules (Zhang et al., 2009). Recent experiments studying the biogenesis of MHC class I molecules have challenged the notion that ERp57 is recruited to substrates by cnx or crt (Peaper et al., 2005). Assembly of MHC class I molecules begins with binding of the cnx- and ERp57-

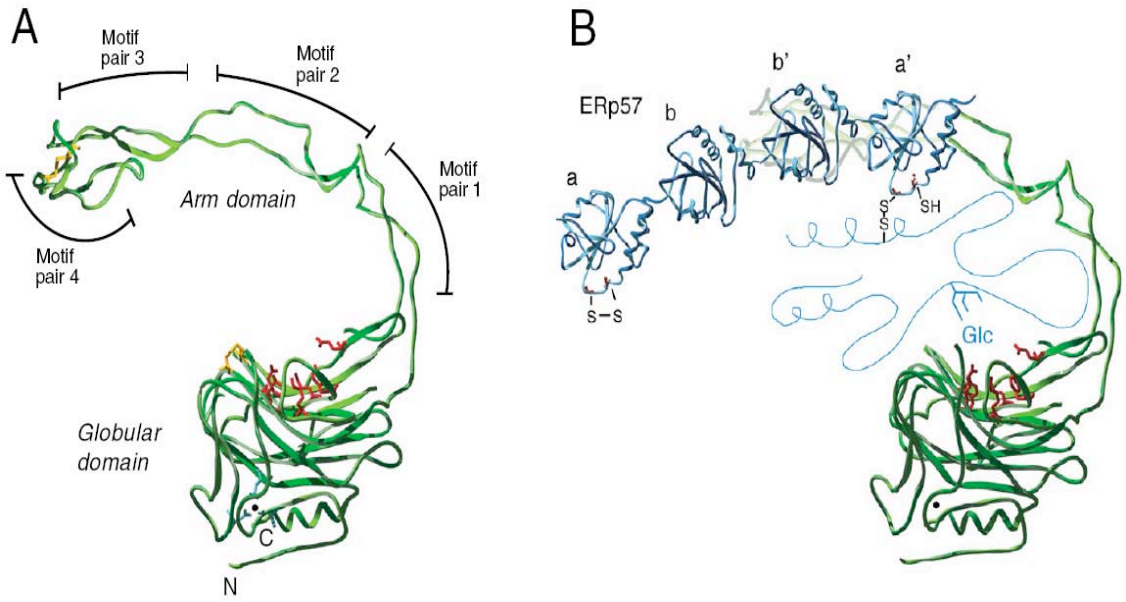

Figure 1.5: (A) Crystal structure of the ER-luminal domain of cnx. The globular domain contains the oligosaccharide-binding site with amino acids that contact the terminal glucose residue shown in red. A bound Ca^{2+} is indicated by the black sphere, residues coordinating the ion depicted in cyan. Disulfide bonds are shown in yellow. The extended arm domain consists of two strands, one containing four repeats of motif 1 [I-DP(D/E)A-KPEDWD(D/E)] and the other containing four copies of motif 2 [G-W–P-IN-P-Y]. Each motif-1-repeat is paired with a motif-2- repeat on the opposite strand. The four motif pairs are shown. **(B) Model for the interaction of a folding glycoprotein with ERp57, cnx or crt.** Cnx (green) is shown associated with a hypothetical model of ERp57 (blue) drawn on the basis of the NMR structure of the PDI 'a' domain (Kemmink et al., 1996). The four domains of ERp57 are indicated: a, b, b', a'. A folding glycoprotein (thin blue line) may enter the cavity between the arm and globular domains interacting both with the lectin site as well as a polypeptide-binding site. This may sequester it from other folding glycoproteins, thereby minimizing aggregation. Aggregation is further suppressed by the ability of the polypeptide-binding site to shield exposed hydrophobic segments. The two CGHC active sites of ERp57 (Credle et al., 2005) are well-placed to catalyze disulfide-bond formation, reduction, or isomerization. (Figure 2 from Williams, 2006).

associated class I heavy chain to a soluble subunit, alpha2-microglobulin (a2m). The heavy-chain-a2m heterodimer then enters a peptide-loading complex consisting of crt (or in some cases, with cnx), ERp57, an ABC peptide transporter termed TAP, and tapasin which, among other functions, bridges the class I heavy chain and TAP. Under normal conditions, the disulfide-linked complex of ERp57 and tapasin contains ~15% of the cellular ERp57, but upon upregulation of MHC class I molecule synthesis by interferon gamma as much as 80% of ERp57 may be covalently linked to tapasin (Peaper et al., 2005). Following the loading of a peptide antigen onto the class I molecule, the peptide loading complex disassembles and class I molecules are exported to the cell surface. Clearly, tapasin is a highly preferred substrate for ERp57. Importantly, neither CST treatment nor chaperone deficiency in cnx- or crt-

deficient cell lines has any effect on the level of the ERp57-tapasin complex, which indicates that cnx and crt do not recruit ERp57 into the peptide loading complex. Furthermore, by inactivating the redox active sites of ERp57, it was demonstrated that its enzymatic activity is dispensable in stabilizing the peptide loading complex and in supporting efficient peptide loading, suggesting a specific structural rather than catalytic role role for ERp57 within the MHC class I peptide-loading complex.

ERp57 specifically interacts with N-glycosylated polypeptides, and both its binding and its release from newly synthesised glycoproteins require glucose trimming. ERp57 forms complexes with cnx and crt and promotes native disulphide bond formation, although it has been shown that it can also interact with glycoproteins that lack any cysteine residues (reviewed by High et al., 2000). Structural details for the interaction of cnx, crt, and/or ERp57 in the course of glycoprotein folding are described in Figures 1.4 and 1.5. Further insights into the full range of ERp57 functions will require experiments using additional glycoprotein substrates and RNAi as well as the development of an ERp57-knockout mouse. Moreover, the relative roles of oligosaccharide versus polypeptide binding in promoting proper folding and ER retention need to be clarified. Also, experiments are required to assess the functions of ERp57 in the folding of a variety of glycoproteins, and we should also consider its functions that are independent of cnx and crt. The relationship of ERp57 to the many other thiol oxidoreductases of the ER is another area of intense interest that should address the question why there are so many of these enzymes and to what extent their substrate specificities do overlap.

1.3.1.4 Protein disulphide isomerase

Since many secreted proteins have multiple disulphide bonds, it is important that the disulphide pairs are formed correctly during the folding process. PDI is a protein-thiol oxidoreductase that catalyses the oxidation and isomerisation of disulphides on nascent polypeptides in the ER. The catalytic reaction involves the formation of a mixed disulphide between the protein and the oxidoreductase. When PDI catalyzes the oxidation of two substrate cysteinyl sulfhydryls, it becomes reduced itself. In order to catalyze further oxidations, PDI has to be oxidized again. Although the system for maintaining the redox status of PDI has not yet been identified, it seems that it uses glutathione as a redox donor/buffer. Glutathione (GSH) and its oxidized counterpart, GSSG, are the major electron donors and acceptors of the mammalian ER (reviewed by Noiva, 1999).

Recently, Ero1p has been identified as a candidate enzyme for the maintenance of GSH redox status in the ER (reviewed by Fassio and Sitia, 2002). In addition to its activity as a protein-thiol oxidoreductase, PDI has also been shown to act as a molecular chaperone at high concentrations (Cai et al., 1994).

1.3.1.5 Grp94

Grp94 is the representative of the Hsp90 family in the ER. It is a resident ER protein with a KDEL retrieval sequence. In contrast to BiP or cnx, it binds only to a limited number of substrate proteins that are in a relatively advanced state of folding. Each of the Grp94-substrates has been shown to interact with BiP or cnx as well. It is thought that Grp94 works downstream of other chaperones or in conjunction with them. There has been a longstanding controversy as to whether Grp94 binds and hydrolyses ATP (Argon and Simen, 1999). More recently, Frey et al. concluded that Grp94 shows mechanistically important differences in the interaction with adenosine nucleotides, but the basic hydrolysis reaction seems to be conserved between cytosolic and endoplasmic members of the Hsp90 family (Frey et al., 2007).

1.3.1.6 EDEMs

EDEM (Htm1p or Mnl1p in yeast) was discovered to be directly involved in ERAD (Hosokawa et al., 2001);(Jakob et al., 2001);(Nakatsukasa et al., 2001). Its luminal region is similar to class I α1,2-mannosidases, but it does not exhibit enzymatic activity. Deletion of the gene in yeast causes retardation of the degradation of misfolded proteins. In mammalian cells, 3 EDEMs were found to act as acceptors for terminally misfolded glycoproteins released from cnx. EDEMs 1, -2, and -3 are lectins most likely specific for the isomer B of $Man_8GlcNAc_2$ that is thought to act as a signal for degradation (Molinari et al., 2003);(Oda et al., 2003).

As reviewed in (Olivari and Molinari, 2007) and (Vembar and Brodsky, 2008), the intraluminal levels of EDEM1, EDEM2 and EDEM3 are adapted to variations of ER cargo load (e.g., upon differentiation of B cells in antibody-secreting plasma cells) or in response to accumulation of misfolded polypeptides in the ER lumen. These conditions activate a transcriptional program regulated by the ER stress-sensor IRE1 and the IRE1-dependent transcription factor Xbp1. IRE1 is a multifunctional transmembrane protein characterized by a kinase and an endoribonuclease domain in its cytoplasmic C-terminal portion. In response to ER stress, IRE1 dimerizes and undergoes autophosphorylation that activates the endoribonucleolytic function (Liu et al., 2000). Activated IRE1 performs an unconventional splicing, leading to intron

removal from the mRNA coding for Xbp1, resulting in a frameshift that leads to synthesis of a more stable and potent transcription factor. The spliced Xbp1 product binds to specific ER stress-responsive *cis*-acting elements, thereby activating the transcription of select genes involved, for instance in ERAD. EDEM1, EDEM2 and EDEM3 are among the gene products induced upon activation of the IRE1/Xbp1 stress-response pathway. Overexpression of all 3 recombinant EDEMs, a condition that mimics acute ER stress, accelerates release of terminally misfolded glycoproteins from the cnx/crt chaperone system, and thereby accelerates their elimination from the ER lumen. On the other hand, reduction of the endogenous EDEM1 level obtained by RNA interference (Molinari et al., 2003), or inactivation of the IRE1/Xbp1 pathway that would induce EDEM expression upon ER stress, decrease the efficiency of ERAD and eventually compromise the cell's secretory capacity. Thus, in the following section, a short description of ERAD is provided. For further details, see section 1.5.1.

1.4 Endoplasmic reticulum associated degradation – Details about a complex degradative pathway

Misfolded or incompletely assembled proteins, which are common side products of protein synthesis in the ER, are retained in the ER and finally degraded. This quality control system is known as ER-associated protein degradation (ERAD). A most interesting aspect of ERAD is the ability of this system to distinguish not only between resident ER proteins (which need to be protected) and proteins which need to be degraded, but also between conformational variants of the same protein. As described in the previous sections, this sorting is carried out mainly by ER chaperones, such as BiP, cnx, or other factors like specific mannose lectins. When a protein is destined for degradation, it is retro-translocated across the ER membrane to the cytosol where it is degraded by the 26S proteasome, a component of the ubiquitin-proteasome pathway (Sommer and Wolf, 1997). Retrotranslocation is believed to be a reversal of the reaction by which nascent polypeptide chains enter the ER. Recent studies suggest that newly synthesized luminally disposed polypeptides are fully translocated, requiring a re-targeting step from the luminal side before retrotranslocation is initiated (Plemper and Wolf, 1999a, b). Degradation of integral membrane proteins may be initiated by a lateral assembly of components of the Sec61 complex around the substrate (Wiertz et al., 1996).

Retro-translocation is mediated by a complex consisting of the Sec61 pore and several other factors (Plemper and Wolf, 1999b). However, persistent contact with

the Sec61 channel is not needed for retrograde transport and ERAD substrates in fact reach the luminal side of the ER (Plemper and Wolf, 1999b). Sec61 is also known as the central component of the protein import complex into the ER (Rapoport et al., 1996) (see also section 1.3.1.2, calnexin cycle).

ERAD possesses high specificity for soluble as well as integral membrane proteins. One of the substrates investigated in great detail is the cystic fibrosis transmembrane conductance regulator (CFTR), a plasma membrane protein (Ward et al., 1995). It facilitates chloride transport across the apical plasma membrane of epithelial cells. Individuals suffering from cystic fibrosis frequently bear a deletion of phenylalanine 508 (ΔF508), which prevents transport of the protein to the cell membrane. 80% of the wild type protein, but 100% of common mutated forms of CFTR are degraded prior to reaching the Golgi complex (Cheng et al., 1990);(Ward et al., 1994)).
Other examples for ERAD substrates are: a mutated form of α_1-antitrypsin, which leads to accumulation of the protein in the ER of hepatocytes (Le et al., 1990);(Qu et al., 1996); 3-hydroxy-3-methylglutaryl-CoA (HMG-CoA) reductase, which is an important enzyme in sterol synthesis (Hampton et al., 1996); the major histocompatibility complex (MHC) class I molecules (Wiertz et al., 1996); a mutated pro-alpha factor, a yeast pheromone precursor (McCracken and Brodsky, 1996), and mutated forms of carboxypeptidase yscY (CPY*) and proteinase yscA (PrA*), soluble vacuolar proteins in *S. cerevisiae* (Hiller et al., 1996).
Cytosolic proteins are also mainly degraded by the 26S proteasome (Rubin and Finley, 1995);(Jentsch and Schlenker, 1995). Degradation by the 26S proteasome complex usually requires prior poly-ubiquitination of the substrate, but not always (Coux et al., 1996). The poly-ubiquitination of proteins depends on ubiquitin-activating enzymes (E1), ubiquitin-conjugating enzymes (E2) and ubiquitin-protein ligases (E3) (Hochstrasser, 1996).

For illustrating the above considerations, Figure 1.6 depicts a comprehensive model of the pathways for luminal quality control incorporating ubiquitination and ERAD in mammalian cells as summarized by (Christianson et al., 2008).

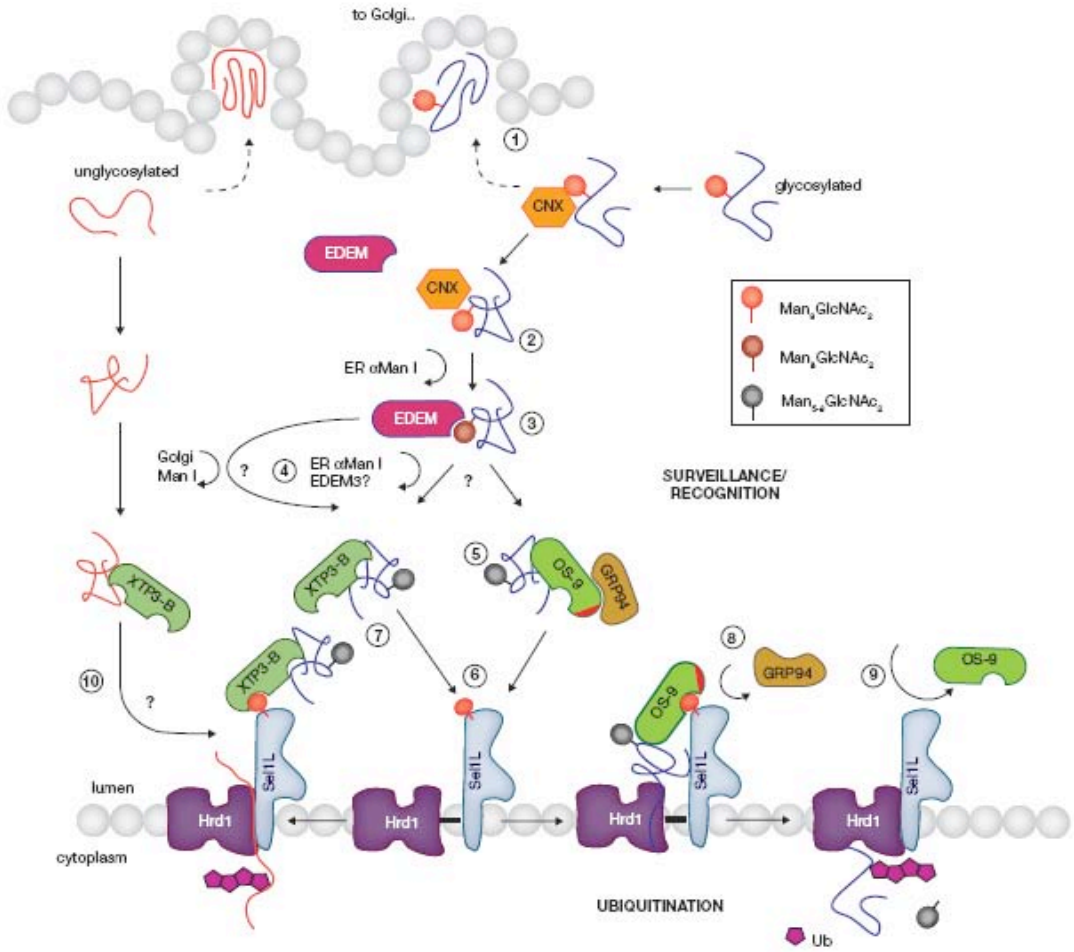

Figure 1.6. A comprehensive model for coordinating luminal surveillance with ubiquitination in mammalian ERAD. Figure 7 from (Christianson et al., 2008). Nascent glycoproteins interact with the ER-resident chaperone calnexin (cnx) where they are either folded correctly and are released for subsequent trafficking to the Golgi apparatus (**1**) or in the case of misfolded proteins, re-enter the CNX cycle in an attempt to facilitate their maturation. If folding remains unproductive, the substrate becomes the target for demannosylation by ER α-mannosidase I to a $Man_8GlcNac_2$ form (Wada et al.). The trimmed mannose structure is recognized by EDEM and displaced from the CNX cycle (**3**). Further demannosylation to a Man5 or Man6 form occurs by the actions of either ER-resident mannosidases (α-mannosidase I or possibly EDEM3), or in the case of cycling between the ER and the Golgi apparatus, Golgi Mannosidase I (**4).** These lower mannose structures may be part of the signal recognized by XTP3-B and OS-9 (**5**). OS-9 scaffolds the ER chaperones GRP94 and BiP, which may also help to prevent aggregation or facilitate unfolding of the substrate. OS-9/XTP3-B complexes bound to substrate subsequently interact with the lumenal domain of SEL1L (potentially through their MRH domains) which may facilitate the release of substrate in the case of OS-9 (**6**). XTP3-B forms a stable ternary complex with SEL1L and Hrd1 (**7**). For OS-9, binding to SEL1L displaces GRP94 and the substrate is transferred to the Hrd1–SEL1L complex (**8**). The final step is release of OS-9 and dislocation of the substrate by the dislocation apparatus and subsequent ubiquitination in the cytoplasm (**9**). In an alternative pathway, misfolded, non-glycosylated proteins may also enter this pathway, perhaps through interactions with XTP3-B (**10**).

1.5 Medical Relevance of Protein Quality Control

1.5.1 Regulation of stress signaling by endoplasmic reticulum chaperones

Cells have developed an evolutionarily conserved integrated intracellular signaling cascade, referred to as the Unfolded protein response (UPR), to reduce the unfolded protein load and increase folding capacity. For survival, the UPR stimulates pathways attenuating protein synthesis, upregulating the transcription of chaperone genes that increase ER capacity of folding and degradation, and retro-translocating misfolded proteins to the cytosol for degradation. There are three major UPR pathways with the transmembrane ER proteins PERK (see 1.5.3), ATF6, and IRE1 (see section 1.3.1.6) as signal sensors. Molecular chaperones play regulatory roles in the UPR. The best characterized of these is BiP/GRP78 which directly interacts with all three ER stress sensors and maintains them in inactive forms in non-stressed cells (Schroder and Kaufman, 2005). When accumulation of misfolded proteins occurs, BiP is titrated away, allowing the activation and transduction of the UPR signals across the ER membrane to cytosol and nucleus. The glycosylation and disulphide bond status of the luminal domain of ATF6 can be utilized as sensing mechanisms for the activation of the UPR (Hong et al., 2004);(Nadanaka et al., 2007). These studies show that ER stress-induced underglycosylation and reduction favor the transport of ATF6 from ER to Golgi.

Different mechanisms have been reported for activation involved in IRE1 signaling. Dimerization of the cLD region (the core region of luminal domain) of the yeast IRE1 retains the full function of the IRE1 luminal domain, but is insufficient for the activation. Rather, the cLD dimer presents an MHC-like groove that is proposed to interact with unfolded proteins and initiate the IRE1 activation (Credle et al., 2005). The monomer of the human IRE1α N-terminal luminal domain is able to form a dimer that exhibits an MHC-like groove at the interface (Zhou et al., 2006) and that can activate both the kinase and RNase activities of IRE1α. The MHC-like groove is too narrow to bind any peptide, implicating that unfolded protein binding is not required for the activation of IRE1α. Therefore, BiP/GRP78 likely is the primary mechanism for regulating IRE1α activation, whereas studies in yeast imply that peptide interaction is the key triggering event. Further studies are required to resolve these apparent differences. Another ER stress-inducible chaperone, P58IPK, is proposed to be a negative regulator by inhibiting eIF2α phosphorylation and attenuating the UPR (Yan et al., 2002). P58IPK contains a functional ER targeting signal consisting of 26

hydrophobic amino acids at the N-terminus, and thus may enter the ER. The precise orientation of the protein complexes and how P58IPK facilitates extraction of the stalled proteins from the ER requires further investigation.

1.5.2 Endoplasmic reticulum chaperone function is obligatory for early mammalian development

Several diseases are due to glycosylation deficiencies, the failure of mutated proteins to fold correctly, and protein transport failures that appear to be linked to ERAD. Cystic fibrosis (CF) is an autosomal recessive genetic disease caused by mutations in the cystic fibrosis conductance regulator (CFTR) gene which codes for a plasma membrane chloride channel. As described in section 1.4, the deletion of phenylalanine 508 (ΔF508) causes the protein to be retained in the ER and to become a substrate for ER degradation (Cheng et al., 1990). However, functional studies showed that CFTRΔF508 still forms a functional chloride channel. However, the mutation has been found to be temperature-sensitive. At the permissive temperature of 30°C, the transport of the mutated CFTR to the cell surface is not drastically impaired (Lukacs et al., 1993). The quality control mechanism that retains mutated CFTR in the ER has been shown to involve cnx, as normal CFTR dissociates from cnx, but the mutated form remains associated until it is degraded (Pind et al., 1994). Tay-Sachs disease is a hereditary disorder that is due to a missing or mutant N-acetylhexosaminidase A that usually removes the terminal N-acetylglucosamine residue from gangliosides (Lau and Neufeld, 1989). Another example is familial hypercholesterolemia, where in some cases the LDL-receptor fails to reach the cell surface and is removed by ERAD (Lehrman et al., 1987).

In more recent studies, the application of gene knockout technology has allowed definitive tests for the requirement of specific ER chaperone function *in vivo*. Traditional knockout approaches creating homozygous deletion of ER chaperones such as BiP/GRP78 (Luo et al., 2006), ERp57 (Garbi et al., 2006), crt (Mesaeli et al., 1999) and UGGT (Molinari et al., 2005) results in embryonic lethality. The phenotypes of mouse knockout models of the ER chaperones, co-chaperones and folding enzymes are summarized in Tables 1.1 and 1.2, from (Ni and Lee, 2007).

These studies provide direct evidence that the function of each of these ER chaperones cannot be compensated for during murine development. Thus, heterozygous mutants and/or tissue-specific knockout mouse models are required to elucidate the critical contribution of these chaperones to mammalian development.

Protein	Localization	Function	Knockout mouse model	Diseases
GRP78/ BiP	ER lumen ER transmembrane Cell surface Nucleus	Chaperone, Ca^{2+} -binding, ER stress sensor, UPR regulator Anti-apoptosis	Embryonic lethality at E3.5 due to failure of embryo peri-implantation	Cancer Alzheimer's disease Parkinson's disease Prion diseases Atherosclerosis
SIL1	ER lumen	Co-chaperone, nucleotide exchange factor for GRP78	Woozy mouse associated with cerebellar purkinje cell degeneration and ataxia	Marinesco-Sjögren syndrome
GRP94/ gp96	ER lumen Cell surface transmembrane	Chaperone, Ca^{2+}-binding Anti-apoptosis Tumor immunity	Embryonic lethality	Cancer Prion diseases Autoimmune disease
GRP170/ ORP150	ER lumen	Chaperone, potential nucleotide exchange factor for GRP78	Embryonic lethality	Alzheimer's disease
GRP58/ ERp57	ER lumen Nucleus Cytosol	Thio-oxidoreductase to catalyze disulfide bond formation of glycoprotein	Embryonic lethality (traditional knockout); *Grp58−/−* B cells are defective in antigen Presentation (conditional knockout in B cells).	Prion diseases Alzheimer's disease
PDI	ER lumen Cell surface	Thio-oxidoreductase to catalyze disulfide bond formation	N.D.	Alzheimer's disease Parkinson's disease

Table 1.1: Summary of function and disease relevance of ER chaperones, co-chaperones and folding enzymes. Modified from (Ni and Lee, 2007)

Protein	Localization	Function	Knockout mouse model	Diseases
Calnexin	ER transmembrane Cell surface	Chaperone, glycoprotein folding	Postnatal death and motor disorders	Alzheimer's disease
Calreticulin	ER lumen Cytosol Cell surface	Chaperone, glycoprotein folding, Ca2+-binding	Embryonic lethality at E14.5 due to defective embryonic cardiac development	Cardiac hypertrophy Alzheimer's disease Autoimmune diseases
EDEM	ER lumen	Chaperone, recognition and targeting of unfolded glycoprotein for degradation	N.D.	N.D.
ERp72	ER lumen	Thio-oxidoreductase to catalyze disulfide bond formation	N.D.	N.D.
Herp	ER transmembrane	Ubiquitin-like protein involved in ERAD	N.D.	Atherosclerosis Alzheimer's disease
$P58^{IPK}$	Cytosol ER membrane	Co-chaperone, negative regulator of eIF2α kinase PERK and PKR, cotranslocational degradation	Development of diabetes associated with increased β-cell death	Diabetes (mouse)
UGGT	ER lumen	Glucosyltransferase, recognition of misfolded glycoprotein and reglucosylation of N-glycan	Embryonic lethality at E13	N.D.

Table 1.2: Summary of function and disease relevance of ER chaperones, co-chaperones and folding enzymes. Modified from (Ni and Lee, 2007)

It has recently been shown that complete depletion of BiP/Grp78 leads to lethality in 3.5 day old embryos (E3.5) due to the failure of embryo peri-implantation (Luo et al., 2006). The *Grp78−/−* embryos cannot hatch from the zona pellucida *in vitro*, fail to grow in culture, and exhibit proliferation defects and a massive increase of apoptosis in the inner cell mass, which are precursors of embryonic stem cells. Thus, BiP/Grp78 is essential for embryonic cell growth and pluripotent cell survival. BiP/Grp78 is transcriptionally upregulated in both the trophectoderm and inner cell mass of E3.5 embryos, and this induction is largely dependent on the ERSE. Since ERSE is an essential cis-element of the BiP/Grp78 promoter for induction by ER stress, this suggests that physiological ER stress may exist at the peri-implantation stage of early development due to the increased activity of cell proliferation and protein secretion. On the other hand, *Grp78+/−* mice are viable and comparable to wild-type, although Grp78 level in the heterozgyotes is about 50% of the wildtype siblings. The levels of cnx and crt are not affected in the *Grp78+/−* mice, and therefore during normal mouse development, 50% of wild-type Grp78 level is apparently sufficient to maintain ER homeostasis. This is consistent with the view that compared to normal tissues and organs, BiP/Grp78 is more critically needed in cells undergoing physiological or pathological stress.

Embryonic lethality was also observed in the ERp57 knockout mice, whereas the conditional knockout mice with ERp57 deficiency in B cells are viable (Garbi et al., 2006). The development and proliferation of ERp57 deficient B cells are normal, but the MHC class I antigen presentation is impaired. Since ERp57 is also detected in the peptide-loading complex consisting of TAP1/TAP2, the MHC class I-specific chaperone tapasin, crt, and MHC I heterodimers (Zhang and Williams, 2006), ERp57 plays a role in loading of peptides onto MHC class I molecules (see also section 1.3.1.3). Taken together, the observations indicate that ERp57 recruits MHC class I to the peptide-loading complex and maintain the peptide-MHC I complex in a steady state. In addition, ERp57 deficiency in B cells also affects the recruitment of crt into the loading complex (Garbi et al., 2006).

Crt deficiency is lethal in mouse embryos at E14.5, resulting from a lesion in cardiac development (Mesaeli et al., 1999). Crt is highly expressed in cardiomyocytes at the early stages of heart development and downregulated after birth in the healthy mature heart. Interestingly, Grp78 and Grp94 are also upregulated during embryonic cardiac development, indicating that some ER chaperones may be essential for cardiogenesis (Barnes and Smoak 1997);(Mesaeli et al., 2001);(Mao et al., 2004);(Mao et al., 2006). In crt null-fibroblasts, the Ca^{2+} storage capacity of the ER is

reduced (Nakamura et al., 2001), whereas overexpression of crt increases the ER Ca^{2+} level (Arnaudeau et al., 2002). Since Ca^{2+} enhances the chaperoning ability of ER chaperones, changes in the ER Ca^{2+} storage capacity or impairment of Ca^{2+} binding to these chaperones affect the quality of ER protein folding and assembly.

Cnx-deficient mice are viable, but 50% of the *cnx*−/− mice die within 2 days of birth, and the surviving animals are smaller than their normal littermates and exhibit obvious motor disorders (Denzel et al., 2002). The *cnx*−/− mice are characterized by a dramatic loss of large to medium myelinated nerve fibers, thereby decreasing the size of the sciatic nerve, implying that cnx can play a tissue-specific role in mammalian physiology. Furthermore, deletions of cnx, crt, and ERp57 have very specific consequences on glycoprotein maturation. For example, defective maturation of MHC class I in cells lacking crt (Gao et al., 2002), of influenza virus hemagglutinin in cells lacking cnx (Molinari et al., 2004) or ERp57 (Solda et al., 2006) and of a series of heavily glycosylated proteins sharing common structural domains in cells lacking ERp57 (Jessop et al., 2007) have been reported.

1.5.3 A link of diabetes to unfolded protein response pathways and endoplasmic reticulum chaperone function

As outlined above, to reduce excessive protein loading, cells trigger the UPR to achieve transient attenuation of protein translation, degradation of malfolded proteins and the induction of molecular chaperones and folding enzymes to augment protein folding and degradation. In this context, a link between molecular chaperones and diabetes is just emerging.

A recent study suggests that deficiency of P58IPK (see section 1.5.1), an inhibitor of PERK activation, causes type 1 diabetes and late-stage type 2 diabetes in mice, associated with hyperglycemia and hypoinsulinemia concomitant with increasing apoptosis of pancreatic islet β-cells (Ladiges et al., 2005). Deficiency of P58IPK has no effect on the insulin secretion by viable pancreatic β-cells and insulin sensitivity of peripheral tissues. However, adult *P58IPK*−/− mice with hyperglycemia showed increased β-cell death and upregulation of pro-apoptotic genes, suggesting that loss of functional pancreatic β-cells leads to hypoinsulinemia and subsequent high blood glucose level. Although P58IPK is a known inhibitor of both PERK and the cytosolic eIF2α kinase PKR, its depletion only activates PERK, but not PKR (van Huizen et al., 2003).

The diabetic phenotypes of *P58IPK−/−* mice showed that sustained activation of PERK could lead to prolonged ER stress and induce apoptosis of pancreatic β-cells (Table 2). As a downstream effector of PERK, the heterozygous loss-of-function mutation of eIF2α in mice fed a high fat diet results in development of diabetes and obesity (Scheuner et al., 2005). This mutation substitutes Ala for Ser51, the phosphorylation site of eIF2α by PERK or PKR for translational inhibition. This diabetes mouse model is characterized by glucose intolerance, abnormal ER distension and inadequate insulin secretion in β-cells. Further, in eIF2α-mutant mice fed a high-fat diet, an increased amount of proinsulin was associated with Grp78, and production of mature insulin was decreased, suggesting that the stable association with Grp78 inhibits the processing of proinsulin into mature insulin. Thus, the Ser/Ala mutation of eIF2α abolishes the ability of β-cells to adapt to ER stress through translational attenuation in the high-fat diet fed mice. The increased expression of proinsulin exceeds the folding capacity of the ER, and Grp78 retains the proinsulin molecules in the ER for further folding or degradation through ERAD, which contributes to the reduced insulin level in islets and the diabetic symptoms.

2 MATERIALS AND METHODS

2.1 Chemicals

Chemicals used for buffers, solutions, and media were obtained from GE Healthcare, Sigma Aldrich, Fisher Scientific, Invitrogen, Pierce, Caledon, VWR International, EMD Chemicals, Inc., Multicell Wisent, Boehringer Mannheim Corp., Biorad, and Pacific.

2.2 Molecular Biology

2.2.1 Bacterial strains and vector systems

Strain	Genotype	Source
One Shot Stbl3 Chemically Competent *E.coli*	F- mcrBmrr hsdS20 (rB-, mB-) recA13 supE44 ara-14 galK2 lacY1 proA2 rpsL20 (Strr) xyl-5 - leu mtl-1	Invitrogen

Table 2.1: Bacterial strain used for transformation

The p2K7bsdEIFαCNX vector (Figure 2.1) was used as a template for the mutagenic polymerase chain reaction. It was constructed as described in (Suter et al., 2006). The cnx gene was cloned into a pDONR 221 entry vector and the promoter EIFα was cloned into a pDONR P4-P1R vector via Gateway BP clonase enzyme mix (Invitrogen). These entry vectors were then recombined into the p2K7bsd lentivector using the Gateway LR plus clonase enzyme mix (Invitrogen).

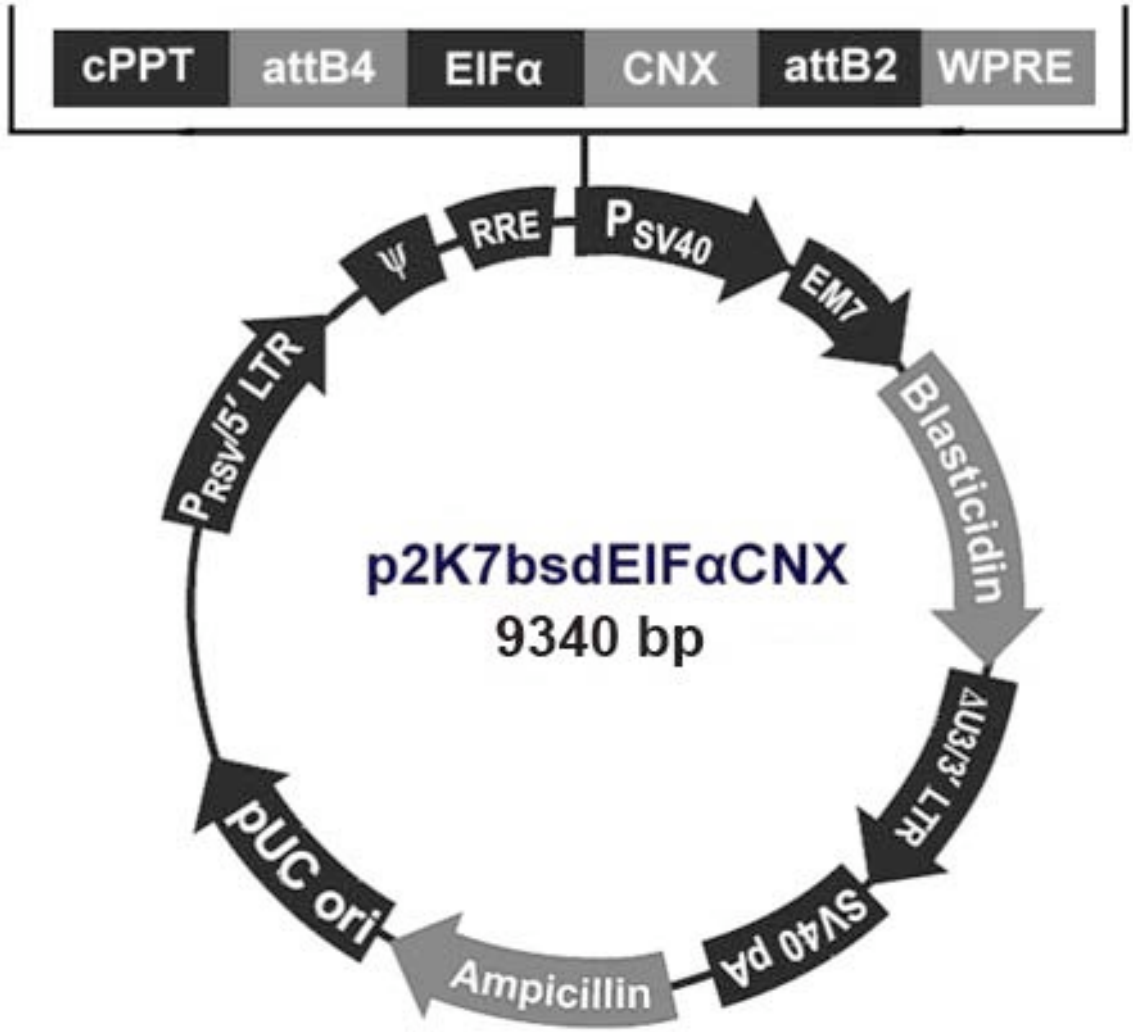

Figure 2.1: Vector used for calnexin mutatagenesis

2.2.2 Oligonucleotide primers for mutagenesis and sequencing

Oligonucleotide primers were designed using a *Mus musculus* cnx sequence derived from ENSEMBL (ENSMUSG00000020368) and according to QuikChange® XL Site-Directed Mutagenesis Kit, Stratagene.

Name	Sequence	Tm [C°] (50mM NaCl)	% GC
C161A forward	5'-GGA ATA GAA **GCT** GGT GGT GCC TAT GTG AAG CTG CTT TCC-3'	66,8	51,2
C161A reverse	5'- GGA AAG CAG CTT CAC ATA GGC ACC ACC AGC TTC TAT-3'	66,8	51,2
C195A forward	5'- GGT CCA GAT AAG **GCT** GGA GAG GAC TAC AAA CTG CAT TTC -3'	65,1	48,7
C195A reverse	5'- GAA ATG CAG TTT GTA GTC CTC TCC AGC CTT ATC TGG ACC – 3'	65,1	48,7
H202A forward	5'- GGA GAG GAC TAC AAA CTG **GCA** TTC ATC TTT CGA CAC AAA AAT CCC – 3'	65,7	44,4
H202A reverse	5'- GGG ATT TTT GTG TCG AAA GAT GAA TGC CAG TTT GTA GTC CTC TCC- 3'	65,7	44,4
H219A forward	5'- GGT GTA TAT GAA GAA AAA CAT **GCA** AAG AGG CCA GAT GCA GAT CTG – 3'	64,8	42,2
H219A reverse	5'- CAG ATC TGC ATC TGG CTT CTT TGC TCG TTT TTC TTC ATA TAC ACC-3'	64,8	42,2
C361A forward	5'- GCC AAC CCC AAG **GCT** GAG TCA GCC CCT GGG-3'	71,9	70
C361A reverse	5'- CCC AGG GGC TGA CTC AGC CTT GGG GTT GGC-3'	71,9	70
C367A forward	5'- GCC CCT GGG **GCT** GGT GTC TGG CAG CGA CCT ATG-3'	72,8	69,9
C367A reverse	5'- CAT AGG TCG CTG CCA GAC ACC AGC CCC AGG GGC-3'	72,8	69,9
Sequence primer Forward	5'- CTG AAT AAG CCC TCC CTG-3'	49,9	50
Sequence primer Reverse	5'- GTT CAC AAC AGA CTG GTC-3'	50,5	50
Sequence Primer 361/367	5'- CCA GAC CCT GAT GCA GAG AAG CCA GAG-3'	64,0	59,2

Table 2.2: Oligonucleotide primers used for mutagenic polymerase chain reaction (PCR) or sequencing of cnx mutants. Manufactured by Integrated DNA Technologies, Edmonton, Canada; in **bold** the mutations (to alanine)

2.2.3 Site-directed mutagenesis via Polymerase Chain Reaction

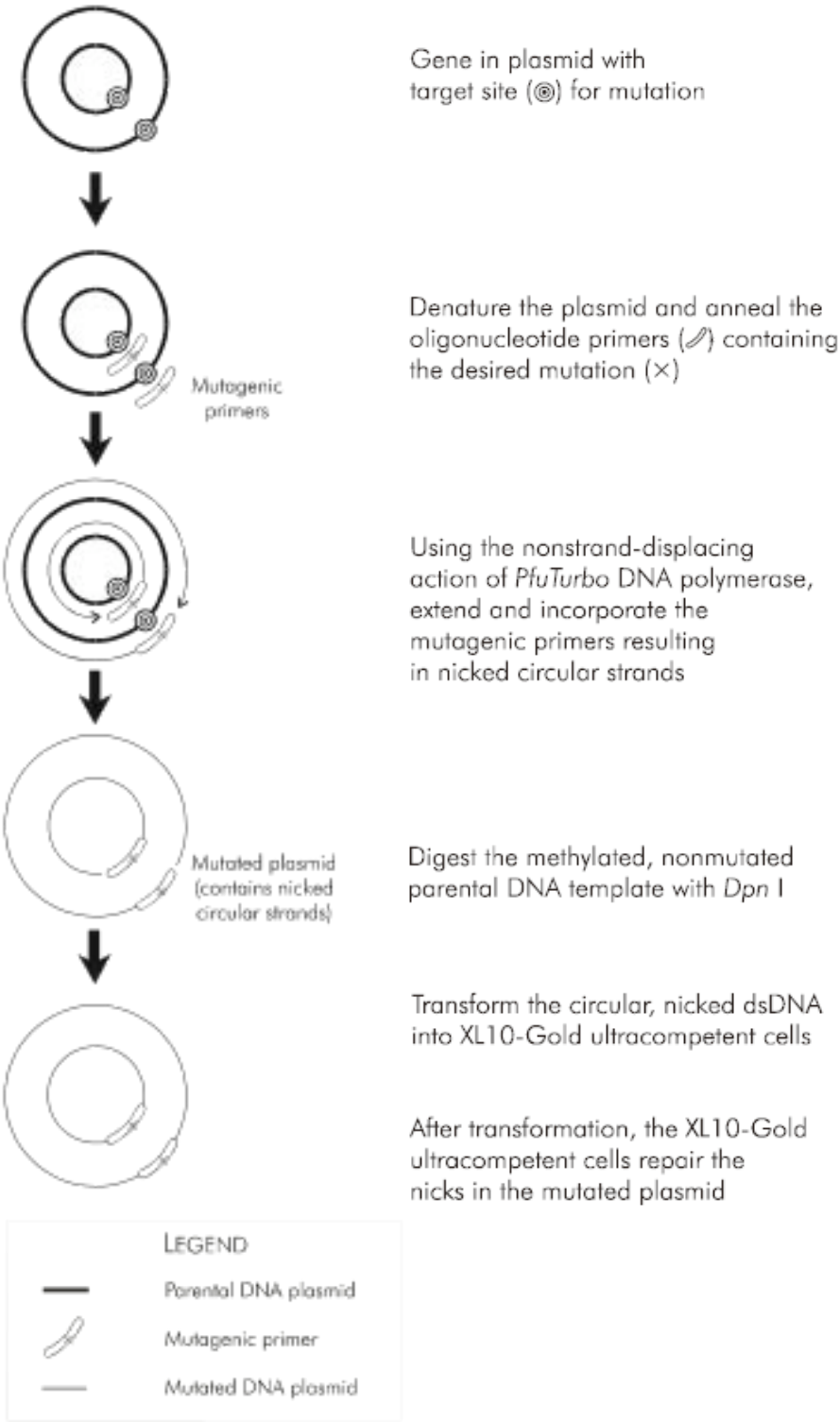

Figure 2.2: **Overview of the QuikChange® XL site-directed mutagenesis method.** (For details, see http://www.stratagene.com/manuals/200516.pdf)

Depending on the different primer sets, different PCR reaction mixtures and programs were used. The following components were pipetted on ice and gently mixed in sterile PCR reaction tubes (50 µl reaction volume):

Amount [µl]	reagent
5	10x *Pfu* reaction buffer
1,25	cDNA [0,5 µg]
1	Primer forward [25 µM]
1	Primer reverse [25 µM]
39,75	Sterile ddH_2O
1	dNTPs [10 mM each dNTP]
1	Pfu Turbo Polymerase [2.5 U/µl]

Table 2.3: PCR reaction mixture for single mutation

Amount [µl]	reagent
5	10x *Pfu* reaction buffer
1,25	cDNA [0,5 µg]
1	Primer forward 1 [25 µM]
1	Primer reverse 1 [25 µM]
1	Primer forward 2 [25 µM]
1	Primer reverse 2 [25 µM]
37,75	Sterile ddH_2O
1	dNTs [10 mM each dNTP]
1	Pfu Turbo Polymerase [2.5 U/µl]

Table 2.4: PCR reaction mixture used for double mutations

Stratagene Pfu Turbo ® Polymerase in combination with the Cloned *Pfu* reaction buffer was used for the polymerase chain reactions.

The following PCR programs were used on a GeneAmp PCR System 9700 Thermocycler PE (Applied Biosystems):

Segment	Cycles	Temperature [°C]	Time
Initial denaturation	1	95	1 min
Denaturation	18	95	50 sec
Annealing		60	50 sec
Extension		68	10 min
Last extension	1	68	7 min

Table 2.5: PCR program used for the primer set C161A forward/ reverse

Segment	Cycles	Temperature [°C]	Time
1	1	95	1 min
2	18	95	50 sec
		55	50 sec
		68	10 min
3	1	68	7 min

Table 2.6: PCR program used for the primer sets C195A forward/reverse, H219A forward/reverse, C361A forward/reverse, C367A forward/reverse

Segment	Cycles	Temperature [°C]	Time
1	1	95	1 min
2	19	95	50 sec
		60	50 sec
		68	9 min
3	1	68	7 min

Table 2.7: PCR program used for the primer set H202A forward/reverse and C361/367A forward/reverse

Segment	Cycles	Temperature [°C]	Time
1	1	95	1 min
2	18	95	50 sec
		59	50 sec
		68	10 min
3	1	68	7 min

Table 2.8: PCR program used for the primer sets C361 forward/reverse, H219A forward/reverse, and C367A forward/reverse

All PCR products were analyzed by agarose gel electrophoresis.

2.2.4 Restriction Enzyme Digestion

Dpn 1 Endonuclease digestion is used to eliminate the methylated, parental template plasmid to leave the PCR fragment. One µl of Dpn 1 from New England Biolabs [20 U/µl] was added to 50 µl PCR product, mixed, and incubated at 37°C for 90-120 min. The restriction digest pattern was checked by agarose gel electrophoresis.

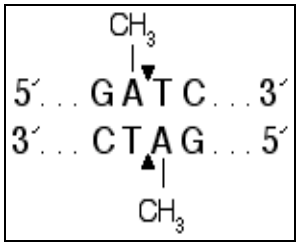

Figure 2.9: Recognition site of Dpn1

(http://www.neb.com/nebecomm/products/productR0176.asp)

2.2.5 Agarose Gel Electrophoresis

Separation of DNA fragments was performed by gel electrophoresis using 1% (w/v) agarose gels with a constant voltage of 80 V. DNA samples were mixed with 6× DNA loading buffer containing Bromophenol. 1x TAE was used as electrophoresis running buffer. The 1 kb Plus DNA Ladder from Invitrogen was used as size markers. To visualize DNA fragments under ultraviolet light (366 nm), the agarose gel contained the fluorescent intercalating dye ethidium bromide (1:10 000).

50x TAE, pH 8.0

2 M Tris-HCl

1 M Acetic acid

0.1 M EDTA

ddH_2O

Ethidium bromide stock solution

360 µg/ml ethidium bromide in ddH_2O

6x DNA loading buffer

25% Ficoll 400

25 mM EDTA, pH 8

1% SDS

0.05% Bromophenol Blue

ddH_2O

InvitrogenUltraPureAgarose

2.2.6 DNA isolation

Total DNA was isolated after PCR using the QIAquick PCR purification Kit Protocol (Quiagen), until June 6th 2008, thereafter with the GenElute PCR Clean-Up Kit from Sigma Aldrich. In the following, buffer designations are those provided with the kits.
Five volumes of Buffer PB were added to 1 volume of PCR sample and mixed. A QIAquick spin column was placed into a provided 2 ml collection tube. To bind DNA, the sample was applied to the QIAquick column and centrifuged for 60 sec (13,000 rpm). The flowthrough was discarded. 750 µl Buffer PE was added to the column and centrifuged at 13,000 rpm for 60 sec. The flow through was discarded and the column was centrifuged for 1 min (13,000 rpm). The column then was placed into a clean 2ml microcentrifuge tube. To elute the DNA, 30 µl ddH_2O were added to the center of the column and the column was incubated at room temperature for 1 min. Finally, the column was centrifuged for 1 min (13,000 rpm).

2.2.7 Transformation of Competent *Escherichia coli*

Five µl of the column eluate were carefully added to 25 µl bacterial stock (kept frozen at –80°C and slowly thawed on ice). The solution was incubated on ice for 30 min. Then, the mixture was heated for 2 min at 37°C and chilled on ice for 2 min. For regeneration, 250 µl of prewarmed LB medium (Sigma; LB-Broth, L3022) were added and the cells were incubated for 1 hr at 37°C under gentle shaking (225 rpm). 75 µl and 150 µl of the transformation mixture were plated onto pre-warmed (37°C) LB-Amp plates and incubated overnight at 37°C.

LB-Amp plates

10 g Peptone from Casein

5 g Yeast Extract

10 g NaCl

12 g Agar-Agar

1 ml Ampicillin (1 g/ml)

ddH_2O ad 1000 ml

2.2.8 Mini Preparation of Plasmid DNA

A single bacterial colony from an LB-Amp plate was transferred into 3 ml of LB-Amp medium and incubated at 37°C overnight, shaking at 225 rpm. The following day, 1.5

ml of the bacterial culture were transferred into a 2 ml Eppendorf tube and harvested by centrifugation for 1 minute at 13,000 rpm. For the following steps, reagents from a GenElute HP Endotoxin-Free Plasmid Maxiprep Kit (Sigma-Aldrich) were used.
The supernatant was removed and the pellet was resuspended in 200 µl of ice-cold resuspension solution by pipetting up and down and vortexing. The cells were lysed by adding 200 µl lysis buffer and inverting 6 times. After 3 min of incubation at room temperature, 500 µl of neutralization/binding buffer were added and the Eppendorf tube was spun for 10 min at 13,000 rpm. In the meantime the column was prepared by loading it with 500 µl column preparation solution and centrifuging for 1min at 13,000 rpm. The flowthrough was discarded. The supernatant was transferred to a new 2ml Eppendorf tube and centrifuged at the same conditions mentioned above. Then, the supernatant was loaded onto the column and spun for 1 min at 13,000 rpm. The flow through was discarded and the DNA, bound to the column, was washed with 500 µl optional wash solution and centrifuged for 1 min at 13,000 rpm. Again, the flowthrough was discarded. Then, 750 µl of wash solution were added to the column and centrifuged at 13,000 rpm for 1 min. After discarding the flowthrough, the column was centrifuged one more time for 1 min at 13,000 rpm to dry. The column was transferred to a new collection tube, and DNA was eluted by adding 50 µl ddH_2O and centrifuging for 1 min at 13,000 rpm. The DNA samples were stored at -20°C.The quality of the miniprep was checked by agarose gel electrophoresis.

2.2.9 Sequence Analysis

Nucleotide sequencing was carried out by Integrated DNA Technologies, Inc., University of Alberta, Edmonton, Canada.

2.2.10 DNA purification

To purify DNA, 50 µl of Miniprep, 250 µl Phenol and 250 µl Chloroform/Isoamylalcohol (Isoamylalcohol:Chloroform = 1:25) were added in an Eppendorf tube and mixed well by inverting. The solution was centrifuged at 13,000 rpm for 5 min and the upper phase was transferred to a new Eppendorf tube. 500 µl of Isopropanol were added and the reaction was mixed well by vortexing. Again, the solution was centrifuged, this time for 15 min at max.speed. The supernatant was discarded and the pellet was resuspended carefully with 70% Ethanol. The reaction was centrifuged at max. speed for 15 min before removing the supernatant once

again to let the pellet air dry at room temperature. Finally, the pellet was resuspended in 25 µl ddH_2O and the DNA stored at -20°C.

2.2.11 Measurement of DNA concentrations

DNA concentrations were measured by diluting the samples 1:500 in ddH_2O and measuring absorbance at 260 nm in a 1 cm quartz cuvette with an Ultraspec 2100 pro UV/Visible Spectrophotometer.

2.3 Protein methodology

2.3.1 Total protein extraction

Media of 90-100% confluent cells was aspirated. Cells were washed with 1 x PBS. The cell culture dishes were treated with 1ml trypsin solution (0.25% from Invitrogen, GIBCO) at 37°C for 1-2 min. Cells were gently washed off the dish. 100 µl were used for cell propagation, and 900 µl were transferred to a 2 ml Eppendorf tube and centrifuged at 1,200 rpm for 5 min. The supernatant was discarded and the cells were resuspended in PBS and centrifuged at 1,200 rpm for 5 min. Again, the supernatant was discarded and the pellet was resuspended in 250 µl New Radioimmunoprecipitation assay buffer (RIPA) buffer and Protease inhibitor cocktail was added. This mixture was put on ice for 15 min and then centrifuged for 15 min at 13,000 rpm.

Alternatively, following washing the cells, 150 µl of New RIPA buffer and Protease inhibitor cocktail were added to the cells in the dishes, and incubation proceeded for 15 min on ice. Then the cells were scraped off with a rubber police man. The solution was transferred into an Eppendorf tube and centrifuged 10 min at 13,000 rpm.

The supernatants were used for protein concentration determination using the Bio-Rad D C Protein Assay (BioRad) a reaction similar to the well-documented Lowry (Lowry et al., 1951) assay and were stored at -20°C.

PBS

137 mM NaCl

10 mM Phosphate, pH 7.4

2,7 mM KCl

ddH_2O

New RIPA buffer

150 mM NaCl

50 mM Tris, pH 7.5

1 mM EGTA

1 mM EDTA

1% Triton X-100

0.1% SDS

0,5% NaDOC

ddH_2O

Proteaseinhibitor cocktail

0.5 mM PMSF

0.5 mM benzamidine

0.05 µg/ml aproprotin

0.025 µg/ml phosphormidone

0.05 µg/ml TLCK

0.05 µg/ml APMSF

0.05 µg/ml E-64

0.025 g/ml leupeptin

0.01 µg/ml pepstatin

2.3.2 Antibodies used in this study

	Name, source
Primary antibody	Anti calnexin rabbit polyclonal, Stressgen Bioreagents Corp.
	Anti ß-Tubulin, (H235), rabbit polyclonal IgG, Santa Cruz Biotechnology
Secondary antibody	Alexa Fluor ® 488 goat anti rabbit IgG, Jackson Laboratories

Table 2.9: Antibodies used for immunostaining and Western blotting

2.3.3 Cell Lysis

Cells were grown to 80-100% confluency in cell culture media and washed with 2 ml 1x PBS. 250-500 µl of the various lysis buffers (RIPA, CHAPS, NEM) were added per

10 cm plate, the cells being incubated on ice for 15 min. The cells were collected with a rubber policeman and transferred into an Eppendorf tube and centrifuged at 10,000 rpm for 10 min to pellet insoluble matter. The supernatant (15 µg protein) was used for analysis by SDS-PAGE and Coomassie Blue staining.

RIPA

1 % NP-40
0.5% DOC
0.15 M NaCl
25 mM Tris pH 7.5
1 mM EDTA
1 mg/ml BSA

CHAPS

2% 3-[(3-Cholamidopropyl) dimethylammonio]-1-propanesulfonate (CHAPS)

50 mM 4-(2-hydroxyethyl)-1-piperazineethanesulfonic acid (HEPES)
200 mM NaCl
Protease Inhibitors

NEM

Buffer "**CHAPS**"
20 mM N-Ethylmaleimide (NEM)

2.3.4 SDS-Polyacrylamide Gel Electrophoresis

Protein extracts, trypsin-digested proteins, pulse/chase and immunoprecipitation samples were analyzed by sodium dodecylsulfate polyacrylamide gel electrophoresis (SDS-PAGE), followed by Coomassie Blue staining or transfer of the separated proteins to a nitrocellulose membrane for Western blotting of proteins of interest.

Protein samples were mixed with 3x sample buffer. The samples were heated in a boiling water bath for 2 min, chilled on ice immediately, spun down in a tabletop centrifuge and loaded onto sodium dodecylsulfatepolyacrylamide gels. Stacking gels had a concentration of 5% polyacrylamide, whereas separation gels of 7.5, 8, 10, 12.5% were used.

15-30 µg of total protein extracts, and 10 µg of trypsin digested samples were loaded per slot. The gel was run in 1x running buffer at 90-100 V until the Bromophenol Blue front reached the separation gel and then was turned to 130 V.

Four µl Precision plus Protein all blue Standards and 10 µl SDS-PAGE Standards, Low Range (Biorad) were loaded as markers

3x sample buffer

30% glycerol
3% Beta-mercaptoethanol
6% SDS
0.260 M Tris
0.015 mg/ml Bromophenol Blue
pH 6.8 with HCl

10x Running buffer

15 g/l Tris
5 g/l SDS
72 g/l Glycine
ddH_2O

2.3.5 Coomassie Blue staining

After SDS-PAGE the separation gel was placed in a Tupperware tray and Coomassie Brilliant Blue R-250 stain (Biorad) was added until the gel was completely covered. The gel was then incubated for 1 hr. Then, the Coomassie Blue stain was recycled and destaining solution was added to the gel. After 2 hr of incubation, protein bands were well detectable and distinguishable.
For the Pulse/Chase experiments, the gel was put onto a Whatman paper, wrapped in Saran wrap and dried at 70°C for 2-4 hr under vacuum.
For the analysis of trypsin digested samples, the gels were left in destaining buffer and water (1:1) over night and were scanned the following day.

Destaining Buffer
7,5% acetic acid
10% methanol
ddH_2O

2.3.6 Western blot analysis

After SDS-PAGE, the separated proteins were transferred to a nitrocellulose membrane (Trans-Blot Transfer Medium, Pure Nitrocellulose Membrane, 45 µm, Bio-Rad). This was performed in a Taylor Research Instruments Semidry Electro Blotter.

The nitrocellulose membrane blot was prepared as follows:
5 Whatman papers soaked in 1 x Transfer buffer were applied to the blotting unit, followed by the gel, the nitrocellulose membrane and finally, 4 more wet Whatman papers. To avoid air bubbles a glass test tube was rolled over the blot. The blot was covered with the lid of the blotting unit. Blotting was performed at 260 mA per gel for 1,5 hr at room temperature. To check transfer efficiency, the membrane was stained with Ponceau S (Sigma) for 1 min. Blotted proteins and the standards were visualized by destaining with ddH_2O. The positions of the marker proteins and the lanes of the loaded samples were marked with a pencil and excess parts of the membrane were cut off.

The membrane was blocked for 90min at 4°C with 5% skim dry milk in 1 x PBS-T (Phosphate-Buffered-Saline, 0,1% Tween 20) solution. After removing the blocking solution, the membrane was incubated overnight at 4°Cwith the primary antibodiesdiluted in 1% skim dry milk in 1 x PBS-T. The membrane was washed 3x5 min in 1 x PBS-T, followed by incubation with horse raddish peroxidase-conjugated secondary antibody, diluted in 1% skim dry milk in 1 x PBS-T. After 1-2 hr of incubation at room temperature under gentle shaking, the solution was discarded and the membrane was washed three times with 1 x PBS-T for 5-10 min. “Homemade” enhanced chemoluminescence (ECL, see below) was used to visualize the antibodies bound to proteins. The membrane was incubated 1-2 min at room temperature and placed in an exposure cassette. Films (Fujifilm) were exposed in the dark room from 30 sec to 1 hr.

1 x Semi dry transfer buffer

192 mM glycine
25 mM Tris
20% methanol
ddH_2O ad 4000 ml

PBS-T

1x PBS

0.1% Tween 20

Ponceau S

1 g Ponceau S

50 ml acetic acid

ddH_2O ad 1000 ml

ECL (as established in the Michalak laboratory)

Amount for 2 membranes	reagent
20 ml	0,1 M Tris-HCl, pH 8,5
60 µl	Luminol in DMSO (Sigma)
45 µl	90 mM p–Cumeric acid in DMSO (Sigma)
7µl	30% H_2O_2

Table 2.100: ECL reagents and volumes used

2.3.7 Pulse/Chase and Immunoprecipitation

Cells were grown to 100% confluency in cell culture media in 6 cm dishes. Under http://graphpad.com, the actual activity of the EasyTag Express Protein Labeling Mix [^{35}S] (Perkin Elmer) was determined.

2.3.7.1 Metabolic Labeling

Cells were washed with 2 ml PBS and incubated with 1.5 ml depletion media [cysteine-methionine-free DMEM (MediatechCellgro)] for 15 min at 37°C and 5% CO_2 to deplete extracellular pools of cysteine-methionine. In the meantime, protease inhibitors (see Total protein extraction) were added to the RIPA buffer. The medium was removed from the cells and fresh medium was added. The cells were pulse-labeled by incubation with 50-200 µCi of Labeling Mix for 15-30 min in a radioactivity safe box in the incubator (37°C, 5% CO_2). In the radioactivity lab, the medium was removed and the cells were washed once with chase media. Then the cells were incubated for different times with chase medium (0 and 10 min) in a radioactivity safe box in the incubator (37°C, 5% CO_2). Afterwards, the cells were washed once with 1

ml of ice cold PBS containing 20 mM NEM.

2.3.7.2 Immunoprecipitation

The cells were lysed with 150-250 µl of RIPA buffer (+ Protease inhibitors) and incubation for 15 min on ice. The cells were collected and transferred into an Eppendorf tube, which was then centrifuged at 10,000 rpm for 10 min. The supernatant (sample referred to as post nuclear supernatant, PNS) was collected and stored in 50-100 µl aliquots at -80°C after freezing in liquid nitrogen. Ten µl of each sample were stored in 20 µl 3x sample buffer at -20ºC. Adding 10% Protein-A Sepharose beads (GE Healthcare) in HEPES-buffered saline (HBS) 1:1, the sample was precleared for 30 min at 4°C, gently rotating. The sample was centrifuged for 10 sec, then the supernatant was transferred to a new Eppendorf tube. Twenty µl of sample buffer were added to the pellet of beads (sample referred to as Precleared, PC) and stored at -20°C after freezing in liquid nitrogen. Two µl of cnx-specific antibody and 10% Protein-A Sepharose beads in HBS (sample:beads = 1:1) were added to the supernatant and incubated for 3 hr at 4°C rotating. Then, the beads were spun down for 10 sec. The beads were washed twice with HBS containing 0.5% CHAPS and centrifuged for 15 sec at 10,000 rpm. Finally, the beads were washed with HBS plus 0.5% CHAPS and centrifuged for 1min. The supernatant was removed and the beads were resuspended in 20 µl 3x sample buffer and stored at -20°C (sample referred to as immunoprecipitation, IP).

The samples (10 µl PNS, 20 µl PC and 20 µl IP), as well as lysates of unlabeled wild-type and cnx-/- murine fibroblasts (20 µl), were then loaded onto a 8% separating/5% stacking sodium dodecylsulfate polyacrylamide gel after heating in boiling water for 2 min and centrifuging for 1 min at max. speed. The gels were run at 100-120 V in 1 x running buffer and then stained with Coomassie Blue for 1 hr with gentle agitation. Then the gels destained in destaining buffer over night with gentle agitation in a radioactivity safety box. The gels were scanned, impregnated with EN^{3}HANCE (autoradigraphy enhancer, NEN Life Science Products) for 30 min with gentle agitation in a radioactivity safety box, followed by washing with ddH_2O water for 30 min. Then the gels were placed on a piece of Whatman paper, wrapped in Saran wrap and dried at 70ºC for 2-4 hr. The phosphorimager plate was blanked on a general electric lamp for 1 hr. The blanked phosphorimager plate was placed into the cassette (Fujix, BAS IP Cassette 20x40) along with the dried gels and developed for ~72 hr. The phosphorimager plate was scanned by a Scanner (Storm 840, Molecular

Dynamics) with Storm 840 Scanner Control software (Version 4.1 (build 2), Phosphor Screen).

RIPA buffer

1 % NP40
0.5% DOC
0.15 M NaCl
25 mM Tris pH 7.5
1 mM EDTA
1 mg/ml BSA
ddH_2O

Cell culture medium

DMEM (Sigma, D5796)
10% BGS (Wisent)
1% Penicillin, Streptomycin (Wisent)

Chase medium

Cell culture medium
5 mM cysteine
5 mM methionine

HBS

50 mM HEPES, pH 7.4
200 mM NaCl
ddH_2O

2.3.8 Immunoprecipitation of unlabeled proteins

Cells were grown to 80-100% confluency in cell culture media. Five hundred µl RIPA buffer were added per 10 cm plate and the cells incubated on ice for 30 min. The cells were collected and then transferred into an Eppendorf tube and centrifuged at 10,000 rpm for 15 min to pellet insoluble matter. The supernatant was transferred to

a new Eppendorf tube and 2/3rd volumes of RIPA buffer were added. The lysates were precleared by rotating with 1/16th of 10% Protein-A Sepharose beads in HBS at 4°C for 30 min. The beads were centrifuged for 10 sec and the supernatant was transferred to a new Eppendorf tube. Each sample was split into two equal aliquots: to one, 2 µl of the antibody of interest was added, and to the other 2 µl pre-immune serum were added. The reaction was incubated at 4°C overnight. Hundred µl of 10% Protein A Sepharose beads in HBS were added, and rotating, the reaction was again incubated at 4°C overnight. Then the Eppendorf tube was centrifuged 10 sec at max. speed and washed 3 times with HBS, 1% CHAPS and finally with HBS.
Before applying the sample onto an 8% SDS PA gel, 30 µl sample buffer were added to the beads. Western blot analysis was carried out with the antibodies of interest.

2.3.9 Trypsin digestion of calnexin wild-type and mutant proteins

Murine His-tagged wild-type cnx and cnx mutants (H202A, H219A) were stored in storage buffer at 4°C.

Seventy µg sample were pipetted into an Eppendorf tube, adjusted with buffer A, B, C or D to 140 µl, warmed up for 2 min to 37ºC, and 0.6 µg trypsin (Sigma-Aldrich, 1 mg/ml) were added and the contents thoroughly mixed by vortexing. After incubation for 30 sec, 2 min, 5 min, 10 min, and 20 min, 20 µl aliquots were transferred to tubes containing 10 µl 3x sample buffer and kept on ice. The “0 min time point” sample was incubated on ice without the addition of trypsin during the entire duration of the experiment.

The samples were immediately analyzed by 12,5% sodium dodecylsulfate polyacrylamide gel electrophoresis and Coomassie Blue staining.

Name	Protein	Concentration [mg/ml]
1139 4B	His-CNX wild-type	7.9
1139	His-CNX wild-type	18.7
1139 pure	His-CNX wild-type	4.7
1637	His-CNX H202A	8
1638	His-CNX H219A	4.3
1139 NEW	His-CNX	7.78
1139 #2	His-CNX	14.2
1637 NEW	His-CNX H202A	18.7
1638 NEW	His-CNX H219A	19.3

Table 2.11: Proteins subjected to trypsin digestion

Storage buffer

10 mM Tris
1mM EDTA
ddH_2O

Buffer A
10 mM Tris, pH 7
1mM $MgCl_2$
100 mM KCl

Buffer B

Buffer **A** plus1 mM EGTA and 2 mM $CaCl_2$

Buffer C

Buffer **A** plus 1 mM $ZnCl_2$

Buffer D

Buffer **A** plus 1 mM Mg-ATP

2.4 Cell Culture experiments

2.4.1 Cell lines

AKO: Fibroblasts from the leg muscle of an 8 day old cnx-deficient CD1/C57Bl6 mouse embryo, propagated and immortalized by Allison Kraus of the Michalak lab, University of Alberta, Edmonton, Canada

AKW: Fibroblasts from the leg muscle of an 8 day old wild-type CD1/C57Bl6 mouse embryo, propagated and immortalized by Allison Kraus of the Michalak lab, University of Alberta, Edmonton, Canada

These cell lines have been immortalized by SV40 transfection (Allison Kraus, personal communication).

Human embryonic kidney (HEK) 293T cells: ATCC® Number: CRL-1573™

2.4.2 Cell culture

All culture dishes were incubated at 37°C and 5% CO_2. The cells were monitored for morphology and growth under the microscope.

The medium was aspirated and the cells were washed once with 1x PBS. One ml of prewarmed trypsin was distributed over the cells. For 1-2 min, the cells were put back into the incubator (37°C, 5% CO_2). Again, the cells were observed under the microscope to guarantee loss of adhesion, carefully washed off the culture dish (10 cm), and resuspended. For propagation of the cells, aliquots of the cell suspension were transferred to culture dishes with fresh cell culture medium.

If a certain cell number was required, 1 ml of cell suspension was transferred into a Falcon tube with 5 ml cell culture medium, and 10 µl of this suspension were counted in a hemacytometer. According to the cell number, a certain volume of the cell suspension was transferred to 10 ml prewarmed cell culture medium.

2.4.3 Transduction of cells with lentivirus expression plasmids

[Practical Course on HIV-derived vectors, Handbook for the design, production and titration(after Salmon P. and Trono D. : Design and Production of HIV-derived vectors In "Cell Biology: A Laboratory Handbook", 3rd Edition, Elsevier, San Diego)]

After positive nucleotide sequencing results of cnx mutants, AKO cells were transfected with the various mutant cnx forms and GFP control vectors using the lentiviral system.

2.4.3.1 Transfection for production of lentiviral particles

HEK293T cells were passaged and counted (see Cell culture). Cells were plated at 2,85 x 10^6 cells per 10 cm plate, one with cover slips, and incubated at 37ºC at 10% CO_2 overnight. The following day, cells were 70-80% confluent. The sample was prepared in an Eppendorf tube according to the following chart, resulting in 20 µg DNA per sample.

Plasmid	Concentration [µg]
1399 (pCMV 8.93, 2nd generation)	3,75
1398 (pCMV 8.92, packaging plasmid, 2nd generation)	3,75
1397 (pMD2G, envelope plasmid, 2nd generation)	2,5
sample (3rd generation, transfer vector, 2K7bsdEIFαCNX) or GFP control	10

Table 2.12: Plasmids and amounts used for lentivirus transfection. Plasmids 1397-1399 were kind gifts from Dr. Karl Heinz-Krause, Geneva.

The samples were adjusted to 250 µl each with 2.5 mM HEPES (pH 7.3). Two hundred fifty µl of 0,5 M $CaCl_2$ were added to the sample. Five hundred µl of 2x HeBS was provided in 2 ml Eppendorf tubes. Vortexing the HeBS at level 6, the DNA/$CaCl_2$ suspension was added dropwise. This reaction was incubated at room temperature for 30 min. The solution was added dropwise to the 10 cm plates of HEK293T cells while gently moving. The GFP control sample was added to the plate with cover slips. The cells were incubated at 37°C and 3% CO_2 for 20-24 hr. The cells were washed once with 1 x PBS, the medium was changed and the CO_2 level of the incubator was increased to 5%.

To test for transfection efficiency, the cover slips with cells with the GFP samples were removed from the incubator. The cover slips were withdrawn with forceps and washed with 1 x PBS. The remaining cells were put back into the incubator (37°C, 5% CO_2). The cells on the cover slips were fixed with 3.7% formaldehyde in 1x PBS for 10-15 min at room temperature. Then the cover slips were washed 3 times for 5 min with 1x PBS. About 15 µl mounting medium per cover slip were prepared on glass slides. The cover slips were dipped into ddH_2O and excess liquid was removed. Finally, the cover slips were put onto the mounting medium, cell side down, and excess liquid was removed. The cover slips were sealed with nail polish and stored at 4ºC until they were analyzed.

2.4.3.2 Transduction

AKO cells were seeded (3 wells per sample + 1 well for negative control) in 6-well plates with 2 ml cell culture medium. Again, for the GPF control, cover slips were added to the wells. The cells were approximately 60% confluent the following day.

After 48 h of incubation, the medium of the HEK293T cells containing virulent particles (see above) was harvested and transferred into Falcon tubes. The medium was

centrifuged at 1,200 rpm for 5 min. Then, the medium was filtered through 45 µm filters (Millipore) and transferred to new Falcon tubes. Following this procedure, various volumes (0.5-3 ml) of the medium was added to the seeded AKO cells. The AKO cells were incubated at 37°C at 5% CO_2. After 24 h, the medium of the AKO cells was changed and Blastacidin-S was added (4-6 µg/ml media) for selection of positively transduced cells.

To test for transduction efficiency, the cover slips with cells with the GFP samples were taken out of the incubator. The cover slips were removed and washed with 1 x PBS. The cells on the cover slips were fixed with 3.7% formaldehyde in 1x PBS for 10-15 min at room temperature. Then the cover slips were washed 3 times for 5 min with 1x PBS. About 15 µl mounting medium per cover slip were prepared on glass slides. With tweezers the cover slips were dipped in ddH_2O, and excess liquid was removed. Finally, the cover slips were put onto the mounting medium, cell side down, and excess liquid was removed. The cover slips were sealed with nail polish and stored at 4ºC until they were analyzed.

2x HeBS

0.28 M NaCl
0.05 HEPES
1.5 mM Na_2HPO_4, anhydrous
ddH_2O
pH 7.0 with NaOH

Mounting Medium

Fluorescence Preserving Media, BioFX Laboratories

2.4.4 Freezing cells

Typically, 7-9 dishes (10 cm) of cells of 80% confluency were used. The media were aspirated and the cells were washed once with 1x PBS. One ml of prewarmed trypsin was distributed over the cells. For 1-2 min, the cells were put back into the incubator (37°C, 5% CO_2). The cells were observed under the microscope to guarantee loss of adhesion. The cells were carefully washed off the culture dish, resuspended and combined. In a Falcon tube, the cell suspension was centrifuged for 5 min at 1,200 rpm. The supernatant was aspirated carefully, and the cells were resuspended in freezing media (cell suspension:freezing media = 1:2). Then 1 ml of

the suspension was transferred into 2 ml cryogenic vials (Corning), and kept at -80ºC for 24 hr before storing in liquid nitrogen.

Freezing media:

90% BGS (Hi-clone)

10% DMSO (Caledon)

2.4.5 Immunofluorescent staining

Cells were seeded onto sterile glass cover slips (diameter 22 mm) 24 hr prior to the experiment in cell culture media in 6 well plates and incubated at 37°C and 5% CO_2. The cells were washed once with 1x PBS after aspirating the media. Then, the cells were fixed for 10-15 min in 3,7% formaldehyde (Sigma Aldrich) in 1 x PBS at room temperature. The cells were washed 3 times for 5 min with 1 x PBS on ice. The cells were then permeabilized in OPAS buffer for 2 min at room temperature. Again, the cover slips were washed gently 3 times for 5 min each with 1 x PBS on ice. Incubation with the primary antibody (50 µl per cover slip) in 1 x PBS (1:200) followed for 0.5-1 hr at room temperature. The cover slips were gently washed 3 times for 5 min each with 1 x PBS on ice. The secondary antibody was also diluted 1:200 in 1 x PBS (50 µl per cover slip) and the cover slips were incubated for 0.5-1 hr at room temperature. Then the cover slips were gently washed 3 times for 5 min with 1x PBS on ice. Incubation with Texas Red labeled Concanavalin A (Invitrogen, for visualization of ER) for 0.5 – 1 hr at room temperature (1:1000 dilution in 1 x PBS). The cover slips were gently washed 3 times for 5 min each with 1 x PBS on ice. About 15 µl mounting medium per cover slip were prepared on 1 mm thick glass slides. The cover slips were dipped into ddH_2O, and excess liquid was removed. Finally, the cover slips were put onto the mounting medium, cell side down, and excess liquid was removed. The cover slips were sealed with nail polish and stored at 4ºC until analysis.

OPAS buffer

0,1% Triton X-100
100 mM PIPES
1 mM EGTA
100 mM KOH
4% w/v polyethylenglycol 8000
pH 6.9

3 RESULTS

3.1 Objectives

The aim of my diploma thesis was to create and characterize certain cnx mutants in regards to cnx as a chaperone, and its association with ERp57.

To gain better insights into the binding site of ERp57 to cnx, mutational analysis of cnx, based on the model of ERp57 binding to crt, in addition to mutations hypothesized to have a role in chaperoning was performed.

It is known that ERp57 associates with cnx; however, the exact sites for this bindig remain unsolved. NMR studies have found that ERp57 binds to cnx to a small peptide in the tip of the P-domain (Pollock et al., 2004) (see Figure 1.2.B), while immunoprecipitation studies found that ERp57 binds in the N-domain in a zinc-dependent manner (Leach et al., 2002).

Therefore, this thesis was part of a study designed to gain insight in the specific binding of ERp57 to cnx and thereby to provide further understanding of which residues are important for the function of cnx as a chaperone.

3.2 Mutagenic PCR

As shown in previous work (Guo et al., 2003);(Martin et al., 2006);(Thomson and Williams, 2005), identification of amino acid residues important for chaperone function can be determined by mutational analysis. By comparing the mutant proteins with the wildtype protein by various methods, conclusions may be drawn in terms of differences in binding to substrates or other binding partners, localization, and function.

As mentioned above, the amino acids to be mutated were mainly chosen based on the model of ERp57 binding to crt (Leach et al., 2002).

3.3 Selection of relevant amino acids and creating calnexin mutants via PCR

Located in the N-domain, cysteines 161 and 195 (Figure 1.2.B) form one of the two disulfide bonds of cnx (Schrag et al., 2001) in the globular domain, where the

polypeptide binding and lectin binding sites are located (Figure 3.2), and therefore chosen for mutational analysis.

Figure 3.1: Nucleotide sequence of mouse cnx (retrieved from www.ncbi.nlm.nih.gov, NM_001110500). In red and in boxes the mutagenic primers; in **bold** the codons that were mutated from those for cysteine (tgt) and histidine (gct and gca), respectively, (Silvennoinen et al.) to alanine.

Histidines 202 and 219 (Figure 3.2) located on the N-domain as well are thought to be important for binding of zinc, which acts as a cofactor (Baksh et al., 1995), based on the crt model, or for additional binding of ERp57 (Corbett et al., 1999);(Leach et al., 2002).

The second disulfide bond of cnx is formed by cysteines 361 and 367 shown in Figure 3.2, which are located in the arm, the so-called P-domain (Figure 1.2.B) (Schrag et al., 2001). These two amino acids were also mutated to alanines.

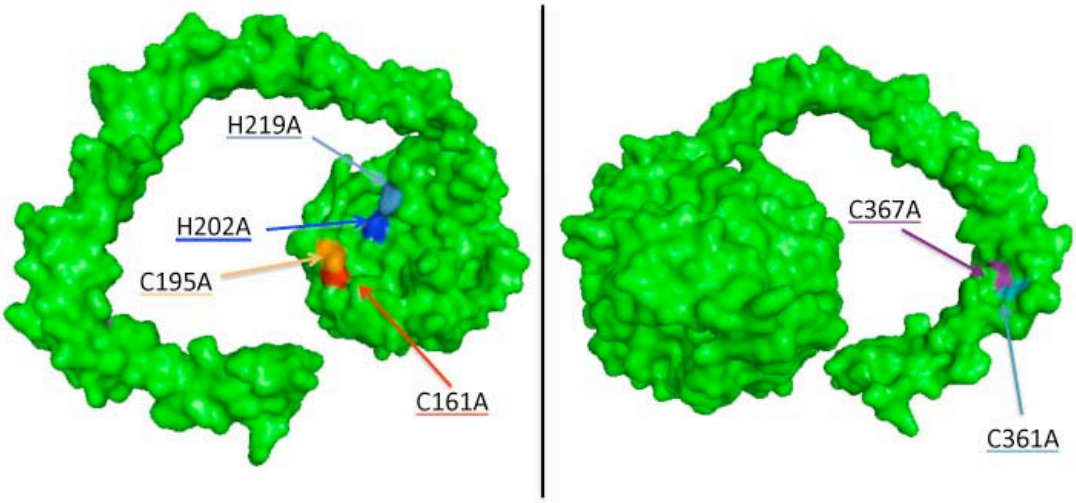

Figure 3.2: Lumenal domain of cnx (modeled with PyMol, DeLano Scientific LLC) showing the mutations generated in the globular domain. Orange: C195A; Red: C161A; Dark blue: H202A; light Blue: H219A; Cyan: C361A; Purple: C367A.

The mutations, of cysteines and histidines to alanines, were generated with the QuikChange® XL Site-Directed Mutagenesis Kit, Stratagene, to introduce single-base pair mutations (Figure 3.1). After mutagenic PCR, aliquots of the products were digested with the endonuclease Dpn1, originating from *Diplococcus pneumoniae* G41, to cleave the methylated template DNA. Dpn1 only cleaves fully-adenomethylated dam sites, so the amplified PCR product, the p2K7EIFαCNX plasmids with the cnx mutants, remained. The Dpn1 digests were then analyzed on 1% agarose gels to show the successful cleavage and the correct size (9,34 kbp) of the PCR product (Figure 3.3).

After finding optimized PCR programs, I was able to successfully generate the following mutants: C161A, C195A, H219A, C361A, C367A and C361/367A (Figure 3.2). Data for H202A and C161/195A were generously provided by Helen Coe in our laboratory.

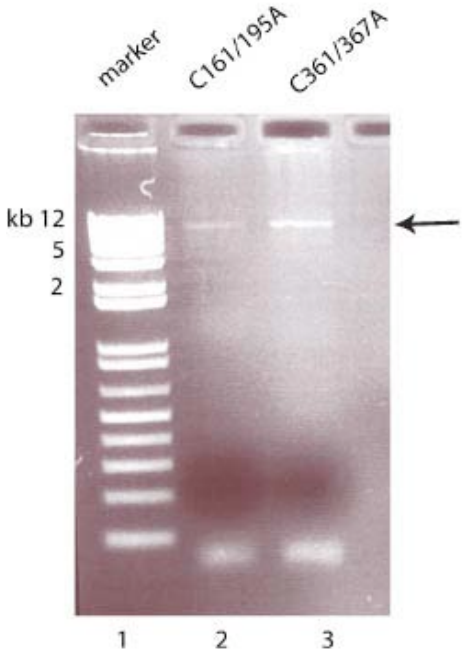

Figure 3.3: Dpn1 digestion of PCR products. PCR products were analyzed on a 1% agarose gel containing ethidium bromide. Lane 1: 1kb Plus DNA Ladder (Invitrogen); lanes 2 and 3: PCR products of double mutants C161/195A (lane 2) and C361/367A (lane 3). Arrow indicates PCR product: p2K7EIFalphaCNX plasmid of 9,34 kbp containing the indicated cnx mutants.

3.4 Cloning mutant forms of calnexin in *Escherichia coli*

Following the Dpn1 digestion, the PCR products were purified with the QIAquick PCR purification Kit Protocol, Quiagen, or with GenElute PCR Clean-Up Kit, Sigma Aldrich.

One Shot Stbl3 Chemically Competent *E. coli* were then transformed via the heat shock method. The transformed bacteria were selected on LB-Amp plates and propagated. Mini preparations were used to extract DNA containing the mutated cnx genes. After checking for correct size on a 1% agarose gel (Figure 3.4), the samples were sent for sequencing.

Comparing the output of the sequencing results with the *Mus musculus* cnx sequence derived from ENSEMBL (ENSMUSG00000020368), and confirming the substitutions with alanine(s), the transfection into AKO cells followed, as described in Materials and Methods.

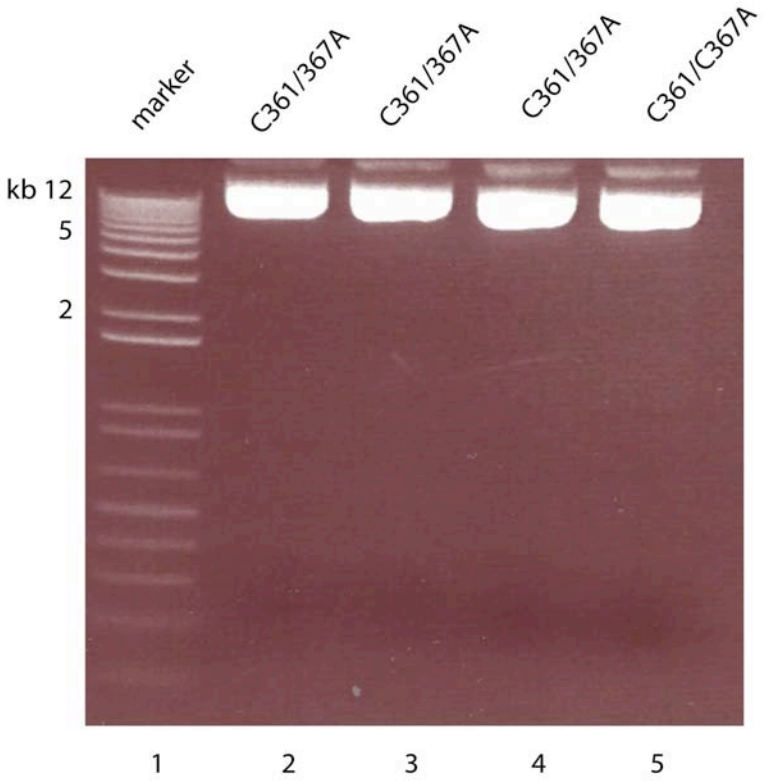

Figure 3.4: Mini preparation of double mutant DNAs. DNA was analyzed on a 1% agarose gel containing ethidium bromide. Lane 1: 1kb Plus DNA Ladder (Invitrogen); lanes 2-5: plasmid DNA of the indicated double mutant mini preps. DNA was subsequently used for transformation using the lentiviral system.

3.5 Integration of mutated cDNA encoding calnexin into calnexin -/- cells using the lentivirus system

Unlike other vectors derived from oncoretroviruses, lentiviral vectors allow stable gene delivery into most non-dividing primary cells. Since the revelation of their ability to transduce neurons in 1996 (Naldini et al., 1996b), the lentiviral vectors have greatly been improved concerning efficiency and biosafety.

In principle, replication-defective recombinant lentiviral particles are constructed from 3 different components: genomic RNA (cis-acting sequences), internal structural and enzymatic proteins (trans-acting proteins, necessary for adequate transcription, packaging, reverse transcription and integration), and the envelope glycoprotein.

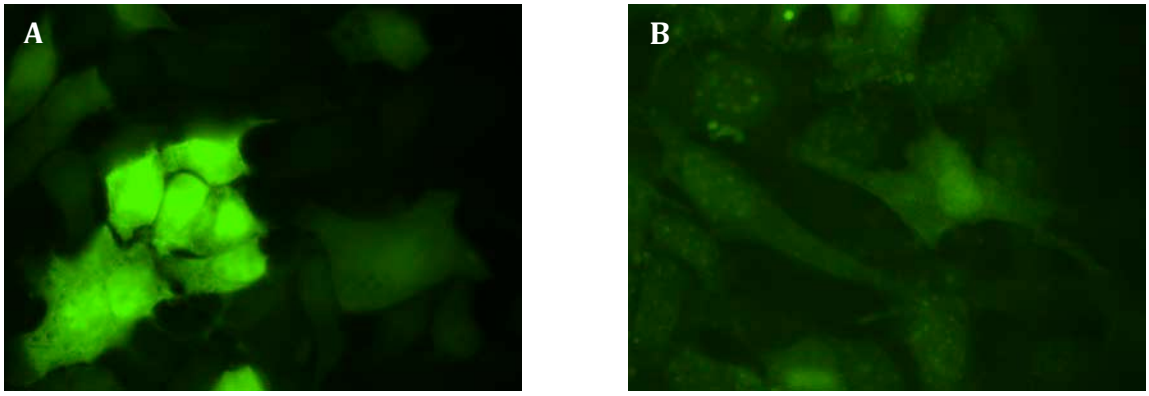

Figure 3.5: GFP control showing transfection or transduction efficiency. (A): GFP control shows transfection efficiency (~70%) for HEK293T cells with complexed DNA containing GFP vector (100x magnification, Zeiss Axioskop 2 mot plus). **(B)**: GFP control vector shows transduction efficiency (~30%) in AKO cells with lentiviral particles (1000x).

First, target DNA was introduced into host cells (in this case HEK293T cells) via calcium phosphate-mediated transfection by adapting the procedure of (Naldini et al., 1996a). After about 48 hr, the cells produced and secreted virus particles containing the target DNA (Figure 3.5). By transferring the supernatant of the HEK293T cells, containing viral particles, to AKO cells, transduction with the target DNA occurred (Figure 3.5). After this procedure, Blastacidin-S (Figure 3.6) was added to the medium. Blastacidin-S is an antibiotic that prevents growth of both eukaryotic and prokaryotic cells by inhibiting peptide bond formation by the ribosome, blocking synthesis of new proteins through translation of mRNA. Cells successfully transduced survived, as they contained the plasmid with the target DNA, which also comprised the Blastacidin-S resistance gene, bsd (see Figure 2.1). Bsd encodes a deaminase originating from *Aspergillus terreus* and can be used for selection (Kimura et al., 1994). Cells surviving this selection procedure were propagated and consequently lysed and analyzed by Western blot analysis and immunostaining.

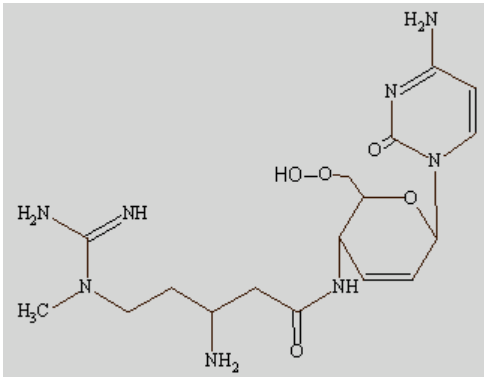

Figure 3.6: Structure of Blastacidin-S, an antibiotic used for selection of lentivirally transduced cells (http://www.blasticidin.com/datasheet.pdf)

3.6 Detection of mutant calnexin proteins

3.6.1 Analysis of transfected calnexin -/- fibroblasts by Western blotting

Next, the selected, transfected AKO cells were analyzed for expression of cnx mutants. For this purpose, cells were lysed, and 30 µg of protein were subjected to SDS-PAGE. After semi-dry transfer and incubation with primary and secondary antibodies, proteins were visualized via ECL. To normalize for protein loading, the expression of ß-tubulin (~55 kDa) was analyzed (see Figures 3.7 - 3.9). In Figure 3.7, wild-type cnx was detected at about 90 kDa in wild-type AKW cells (wild-type murine fibroblasts, lane 2; see also Figure 3.8, lane 2; Figure 3.9, lane 1). Lysates of AKWs were used as a positive control for cnx, whereas lysates of AKO cells (cnx-/- murine fibroblast), (see Figure 3.7, lane 1; Figure 3.8, lane 1; Figure 3.9, lane 2) were loaded as a negative control (i.e. not expression cnx). As shown in Figures 3.7 to 3.9, single- and double- amino acid mutant cnxs show the same size as wild type, i.e. are detected at approx. 90 kDa.

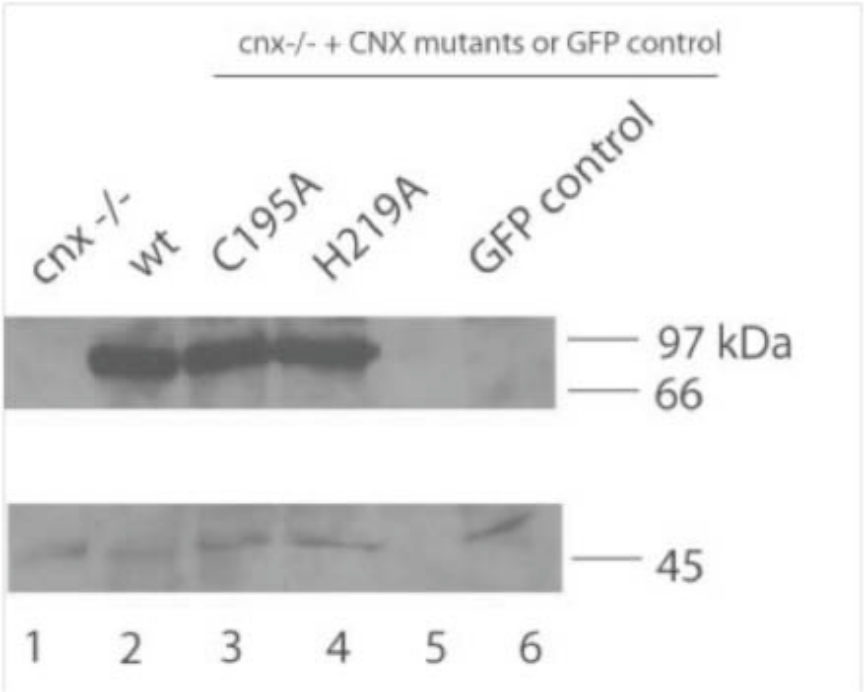

Figure 3.7: Western blot analysis showing expression of cnx mutants in *cnx*$^{-/-}$mouse fibroblasts (AKO cells). AKOs were transfected with different mutants, GFP control or wild-type using the lentivirus system. Lane 1: AKO lysates; lane 2: AKW lysates; lanes 3 and 4: AKO lysates transfected with the indicated cnx mutants; lane 5: empty; lane 6: AKO lysates transfected with GFP control plasmid; bottom panel: ß-Tubulin was visualized as a control housekeeping gene. (Anti-cnx: 1:1000; anti-ß-tubulin: 1:8000; sec. Ab: 1:500). For detection of cnx and ß-tubulin, secondary HRP-conjugated goat α-rabbit antibody was used, and visualization was done using ECL.

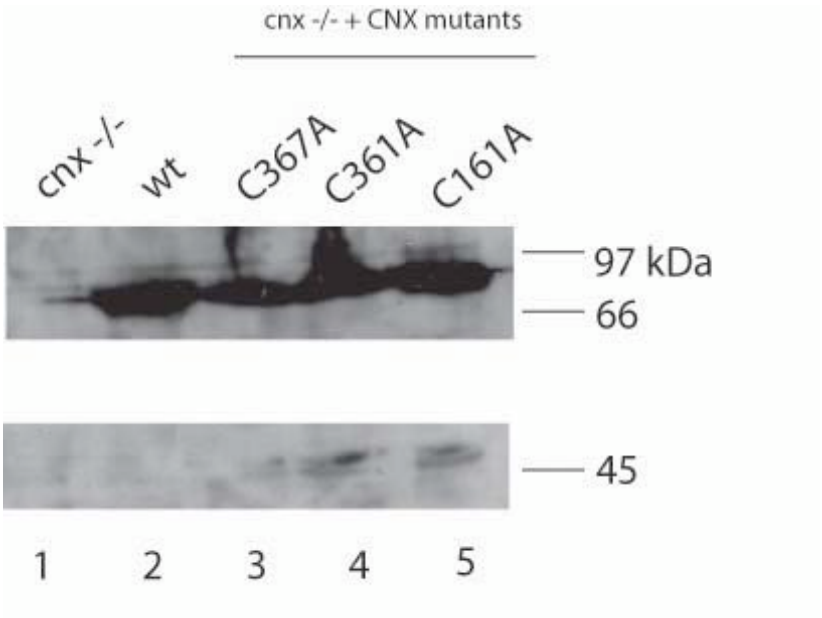

Figure 3.8: Western blot analysis showing expression of cnx mutants in *cnx*$^{-/-}$ mouse fibroblasts (AKO cells). AKOs were transfected with different mutants or wild-type using the lentivirus system. Lane 1: AKO lysates; lane 2: AKW lysates; lanes 3, 4, and 5: AKO lysates transfected with the indicated cnx mutants; bottom panel: ß-Tubulin was visualized as a control housekeeping gene product. (Anti-cnx: 1:1000; anti-ß-tubulin: 1:8000; sec. Ab: 1:750). For detection of cnx and ß-tubulin, secondary HRP-conjugated goat α-rabbit antibody was used, and visualization was performed using ECL.

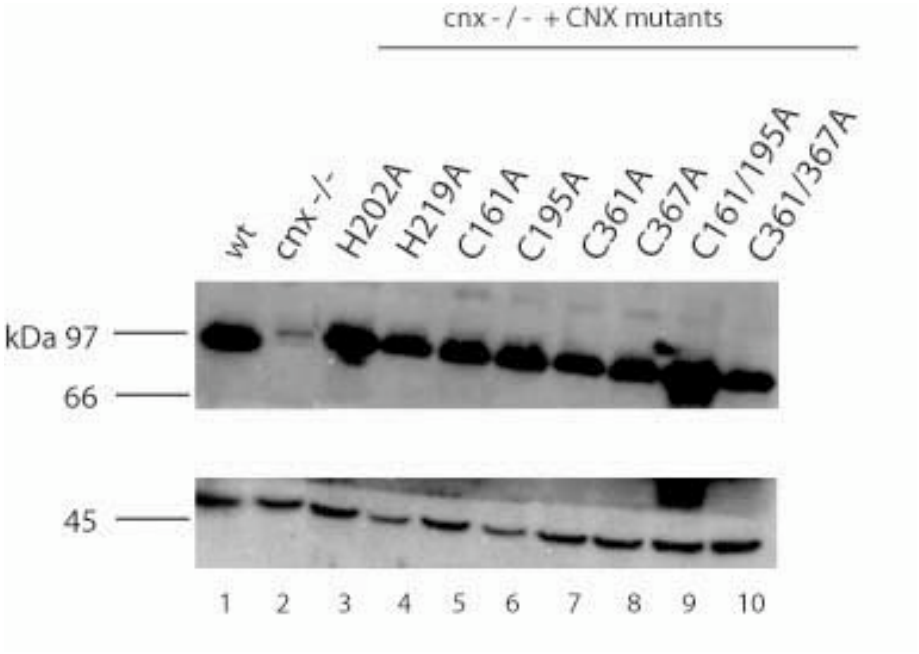

Figure 3.9: Western blot analysis showing expression of cnx mutants in *cnx*$^{-/-}$ mouse fibroblasts (AKO cells). AKOs were transfected with different mutants or wild-type using the lentivirus system. Lane 1: prestained Marker; lane 2: AKW lysates; lane 3: AKO lysates; lanes 4-9: AKO lysates transfected with the indicated cnx mutants; lanes 10 and 11: AKO lysates transfected with the indicated cnx double mutants; bottom panel: ß-tubulin was visualized as a control housekeeping gene product. Detection of cnx and ß-tubulin as described in the legend to Figure 3.8.

3.6.2 Analysis of mutated calnexins by immunofluorescent staining

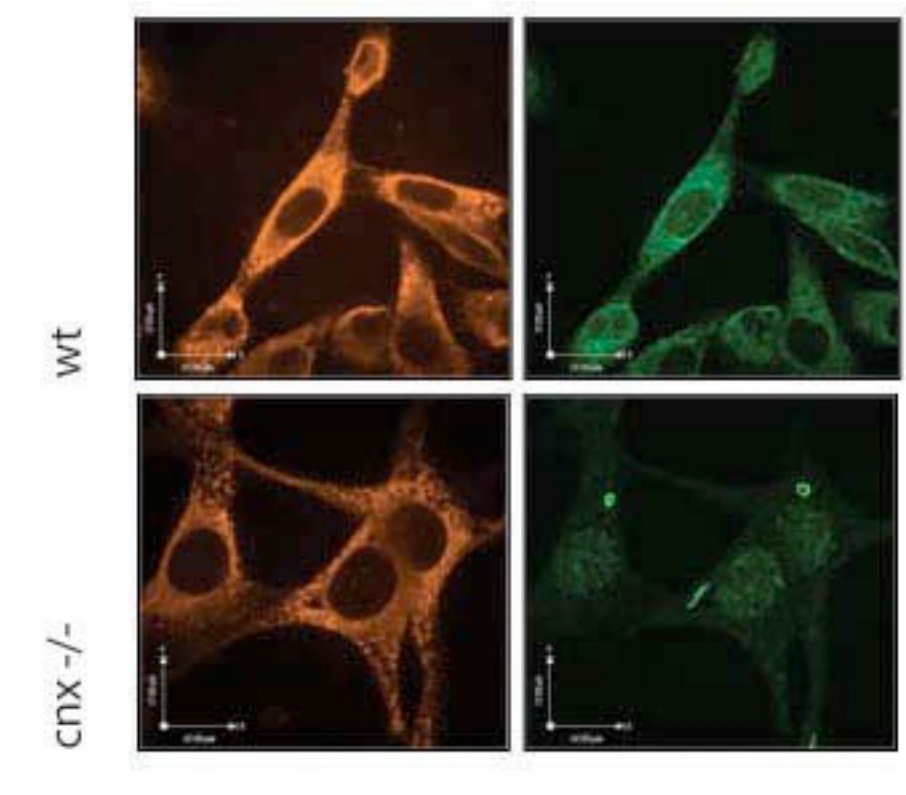

Figure 3.10: Immunostaining showing AKW and AKO cells; Concanavalin A -Texas Red; Calnexin-FITC; magnification 600x.

Transfected AKO cells, confirmed to express mutant cnxs by Western blotting, as well as AKO and AKW cells (Figure 3.10) were seeded onto cover slips in 6-well plates at concentrations of 7 x 10^5 to 1,5 x 10^6 cells per well. After performing the immunofluorescent staining protocol as described in Materials and Methods (primary antibody 1:200; secondary antibody 1:200; concanavalin A 1:1000-1:2000), slides were analyzed at with either a Zeiss Axioskop 2 mot plus (1000x) or an Olympus spinning confocal microscope (600x).

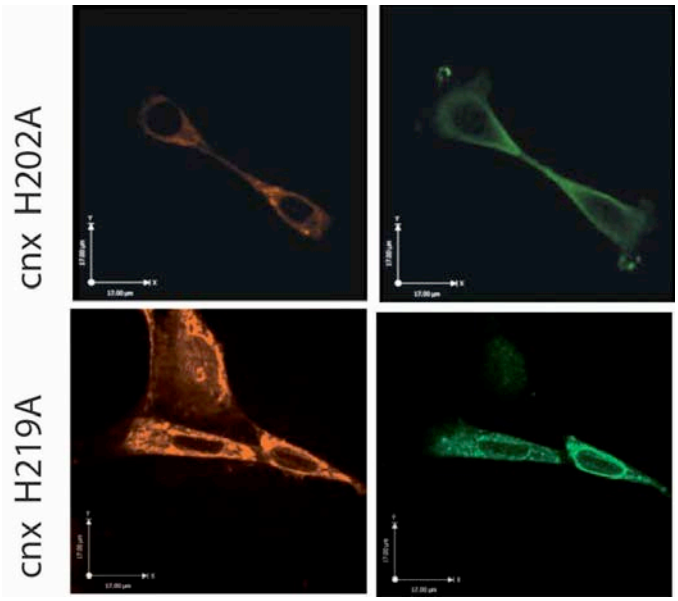

Figure 3.11: Immunostaining showing AKO cells stably expressing cnx mutants H202A and H219A; Concanavalin A -Texas Red; Calnexin-FITC; magnification 600x.

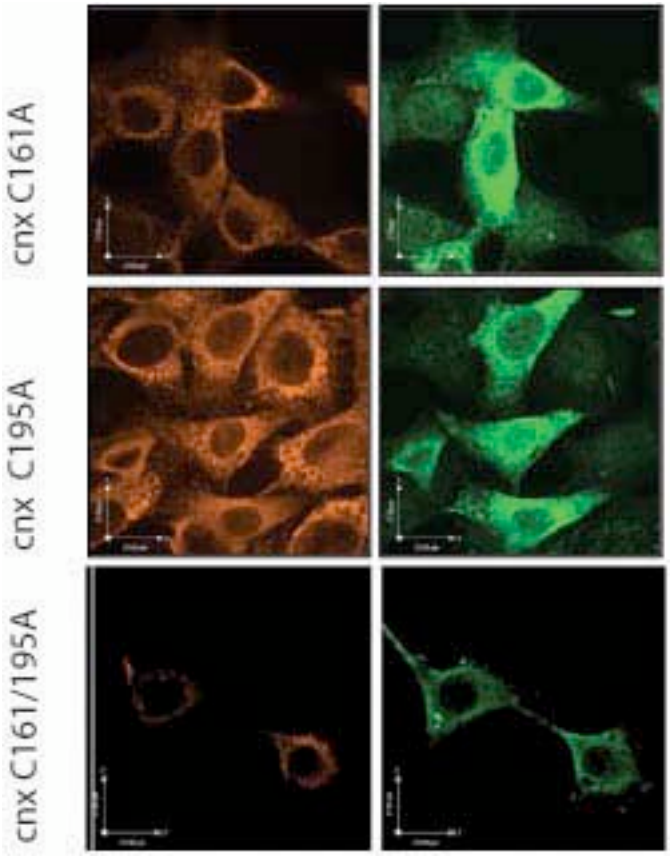

Figure 3.12: Immunostaining showing AKO cells stably expressing cnx mutants C161A, C195A or cnx double mutant cnx C161/195A; Concanavalin A -Texas Red; Calnexin-FITC; magnification 600x.

When comparing the mutant proteins to the wild-type, there appear to be no significant differences in localization of the various cnx proteins. The position of the mutated proteins (Figures 3.11 - 3.13) is indistinguishable from that of wild-type cnx in AKW cells (Figure 3.10). In both cases, cnx colocalized with concanavalin A, suggesting localization to the ER, since concanavalin A reacts with high mannose carbohydrates characteristic for ER localized glycoproteins. Most likely due to selection efficiency of less than 100%, AKO cells not expressing cnx mutants are present in all immunostaining experiments (i.e., only concanavalin A staining is visible).

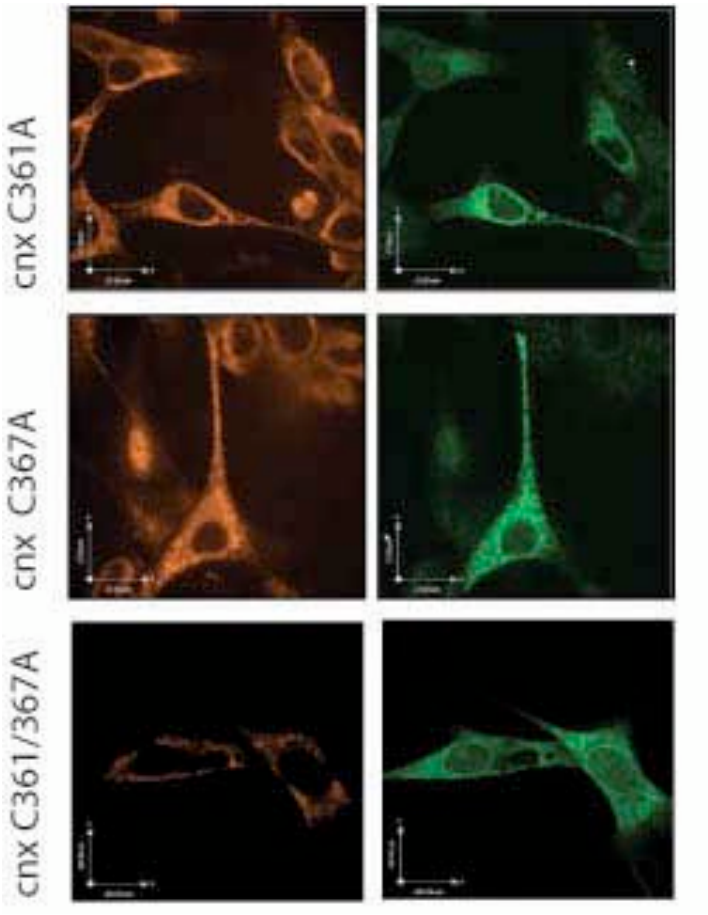

Figure 3.13: Immunostaining showing AKO cells stably expressing cnx mutants C361A, C367A or cnx double mutant cnx C361/367A; Concanavalin A -Texas Red; Calnexin-FITC; magnification 600x.

3.7 Testing for functionality and activity of mutant proteins

3.7.1 Pulse/Chase Immunoprecipitation

To test the integrity or possible irregularities in protein activity (in particular binding of substrates) of mutant cnx, we used the pulse/chase immunoprecipitation (PC IP) method.

As described in Materials and Methods, non-labeled cells (AKO and AKW as negative and positive control, respectively) and radioactively labeled cells were lysed and loaded onto 8% separating/5% stacking polyacrylamide gels. After staining with Coomassie Blue, destaining, and scanning, gels were dried. The dried gels were exposed in a cassette to a phosphorimager plate to develop. As ^{35}S-methionine and ^{35}S-cysteine are incorporated into the newly synthesized proteins during the pulse (15-30 min), they can be detected via autoradiography. The ^{35}S-isotope has a halflife of 87.4 days and emits beta radiation. The emission pattern of the beta particles is recorded as an autoradiogram by the film and can be digitalized with the help of the Storm reader. By chasing (in these experiments, for up to 10 min) the cells with media containing unlabeled cysteine and methionine, the fate of the radioactively labeled proteins can be followed.

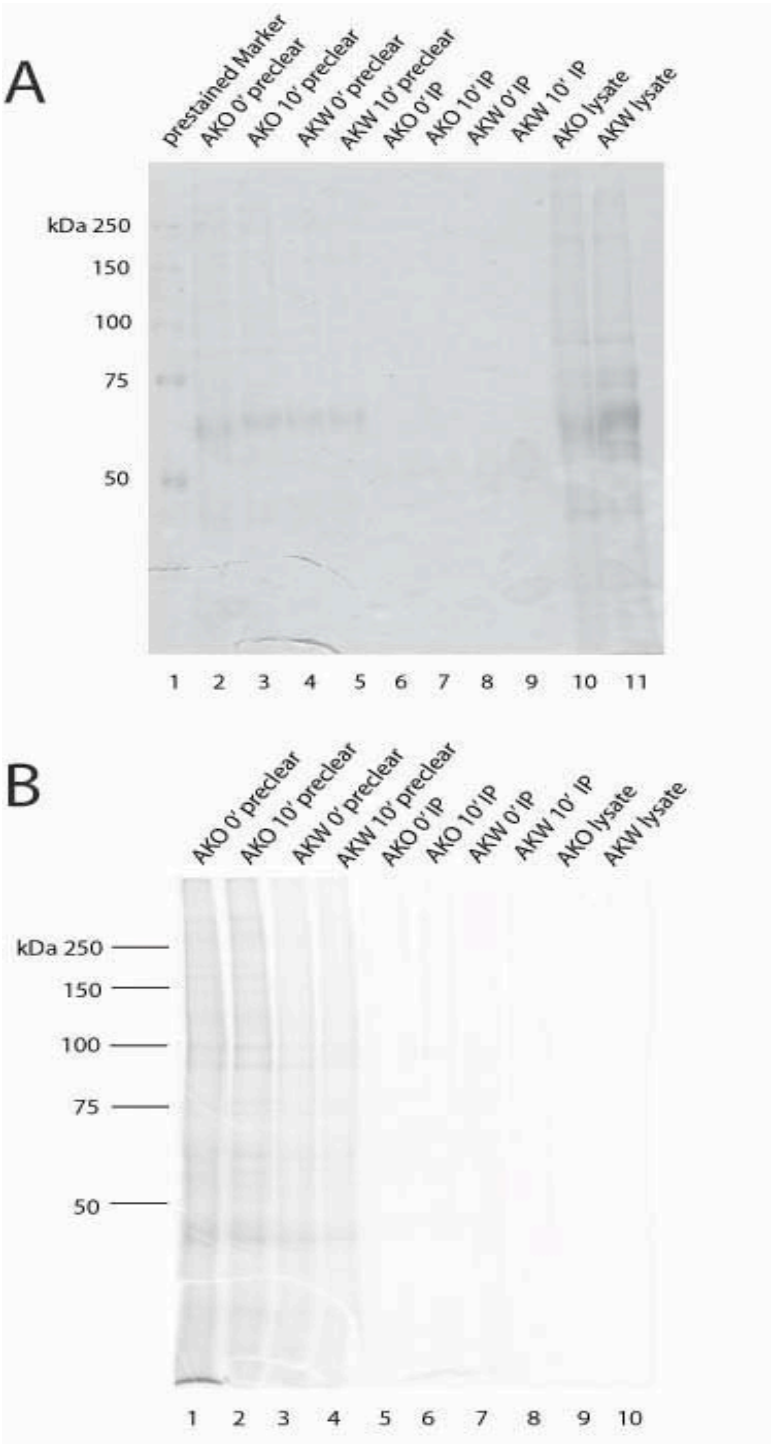

Figure 3.14: Coomassie Blue staining and autoradiogram of pulse/chase immunoprecipitation (PC IP). (A): Coomassie Blue staining of PC IP. Lane 1: prestained marker; lanes 2 and 3: precleared samples of AKO lysates at various chase time points; lanes 4 and 5: precleared samples of AKW lysates at various chase time points; lane 6 and 7: immunoprecipitation samples of AKO lysates at various chase time points; lanes 8 and 9: immunprecipitation samples of AKW lysates at various chase time points; lane 10: unlabelled AKO lysates; lane 11: unlabeled AKW lysates; **(B)**: Autoradiogram of PC IP. Lanes 1 and 2: precleared samples of AKO lysates at various chase time points; lanes 3 and 4: precleared samples of AKW lysates at various chase time points; lane 5 and 6: immunoprecipitation samples of AKO lysates at various chase time points; lanes 7 and 8: immunprecipitation samples of AKW lysates at various chase time points; lane 9: unlabeled AKO lysates; lane 10: unlabeled AKW lysates;

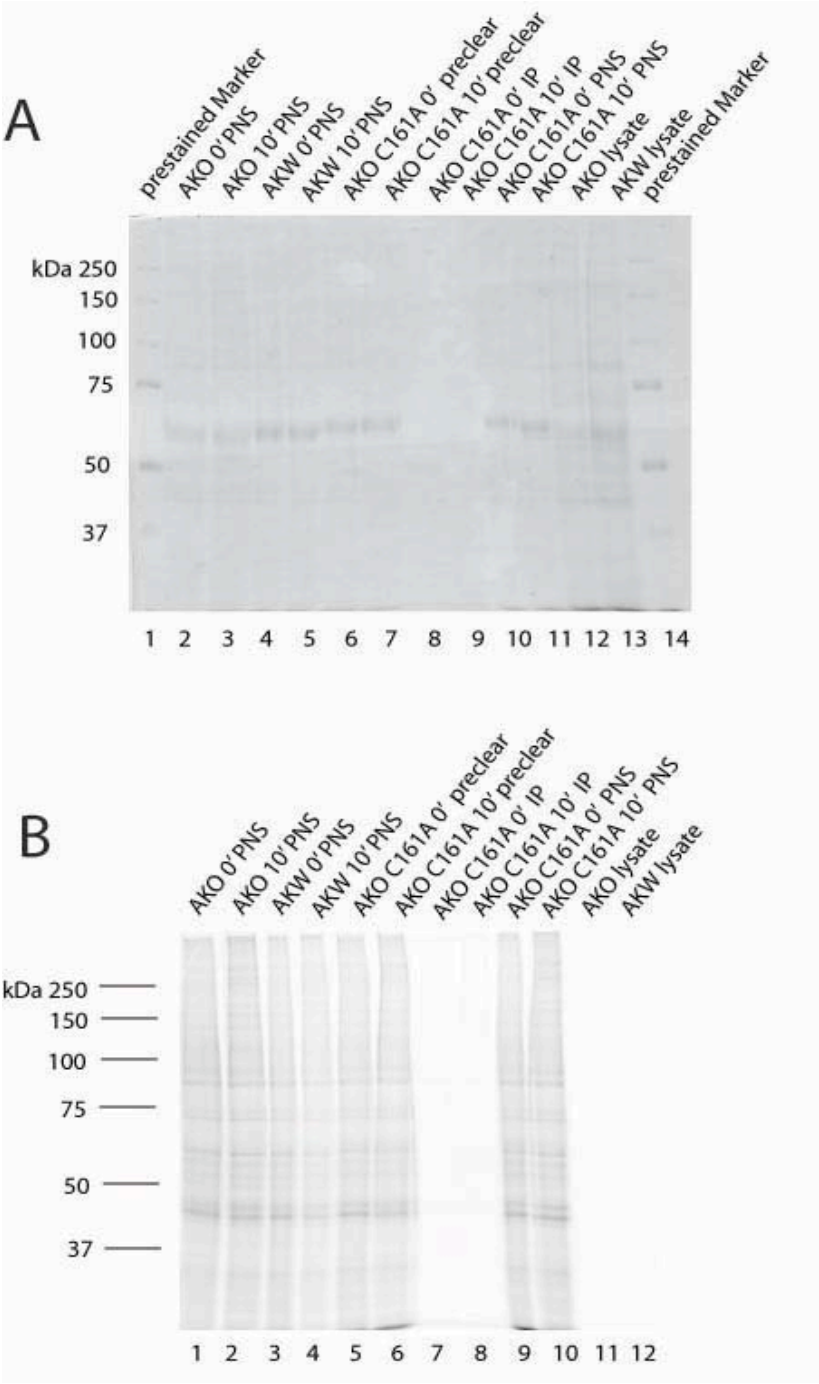

Figure 3.15: Coomassie Blue staining and autoradiogram of pulse/chase immunoprecipitation. (A): Coomassie Blue staining of PC IP. Lane 1: prestained marker; lanes 2 and 3: post nuclear supernatant samples of AKO lysates at various chase time points; lanes 4 and 5: post nuclear supernatant samples of AKW lysates at various chase time points; lanes 6 and 7: precleared samples of AKO lysates transfected with cnx C161A cDNA at various chase time points; lanes 8 and 9: immunprecipitation samples of AKO lysates transfected with cnx C161A cDNA at various chase time points; lanes 10 and 11: post nuclear supernatant samples of AKO lysates transfected with cnx C161A cDNA at various chase time points; lane 12: unlabeled AKO lysates; lane 13: unlabeled AKW lysates; lane 14: prestained marker; **(B)**: Autoradiogram of PC IP. Lanes 1 and 2: post nuclear supernatant samples of AKO lysates at various chase time points; lanes 3 and 4: post nuclear supernatant samples of AKW lysates at various chase time points; lanes 5 and 6: precleared samples of AKO lysates transfected with cnx C161A cDNA at various chase time points; lanes 7 and 8: immunprecipitation samples of AKO lysates transfected with cnx C161A cDNA at various chase time points; lanes 9 and 10: post nuclear supernatant samples of AKO lysates transfected with cnx C161A cDNA at various chase time points; lane 11: unlabeled AKO lysates; lane 12: unlabeled AKW lysates;

Coomassie Blue staining of the proteins was performed to check if the amounts of protein A-bound IgG were comparable (Figure 3.14, Panel A, and Figure 3.15, Panel A). The autoradiogram was analyzed for immunoprecipitated cnx as well as for proteins possibly having interacted with cnx (Figure 3.14, Panel B, and Figure 3.15, Panel B).

With our fibroblasts, we were using a protocol (kindly provided by Dr. Maurizio Molinari, Bellinzona), which was originally designed for HepG2 cells. Unfortunately, I was not able to obtain interpretable results in my pulse/chase experiments.

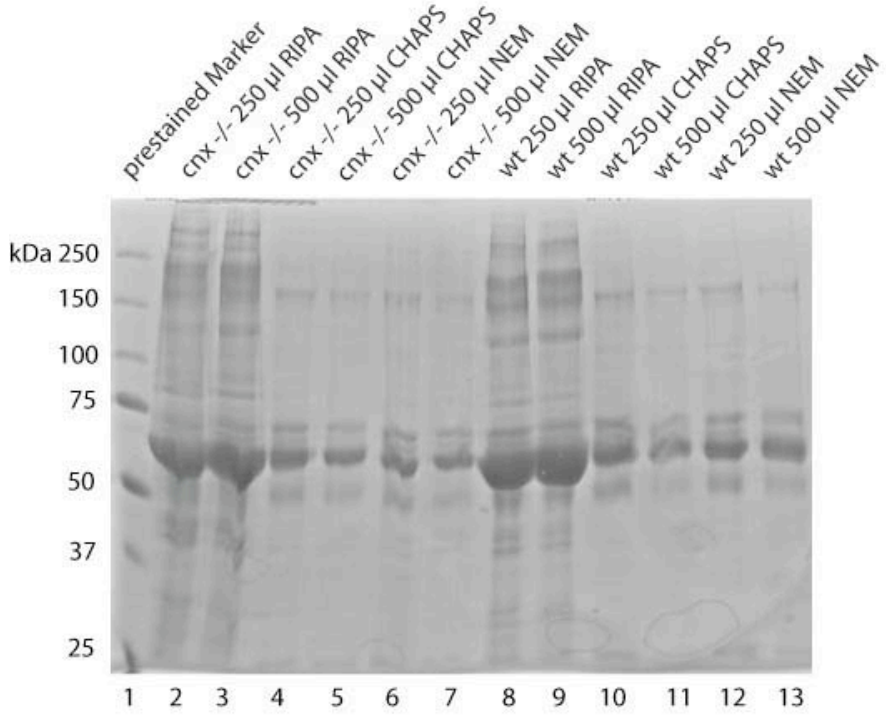

Figure 3.16: Coomassie Blue staining of cell lysates using various lysis buffers. Lane 1: prestained marker; lanes 2 and 3: AKO lysates using RIPA buffer at different volumes; lanes 4 and 5: AKO lysates using CHAPS buffer at different volumes; lanes 6 and 7: AKO lysates using NEM buffer at different volumes; lanes 8 and 9: AKW lysates using RIPA buffer at different volumes; lanes 10 and 11: AKW lysates using CHAPS buffer at different volumes; lanes 12 and 13: AKW lysates using NEM buffer at different volumes;

We thought the difficulty may have been due to the lysis buffer, and thus a lysis assay was performed, in which I tested 3 buffers. Already on Coomassie Blue staining (Figure 3.16), the effects of the lysis buffers are visible: RIPA buffer works best (lanes 2, 3, 8, and 9). Examining the Western blotting [Figure 3.17 (lanes 5 and 7) and Figure 3.18], the results become even clearer: only in samples lysed with RIPA buffer, cnx was detected by the antibody (Figure 3.17, lanes 5 and 7).

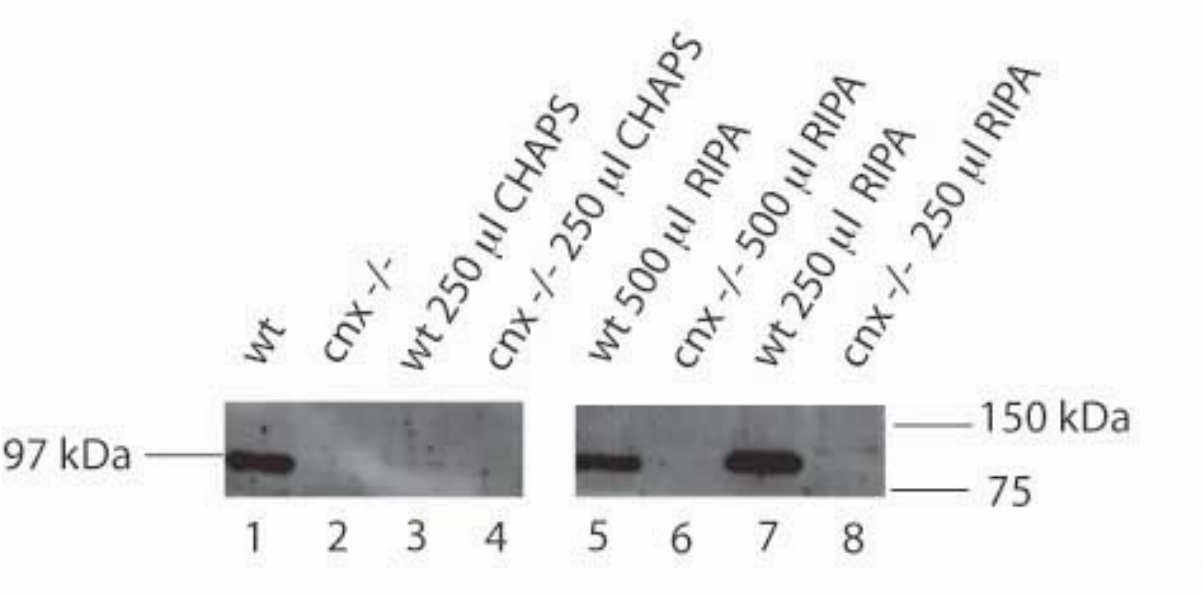

Figure 3.17: Western blot analysis of cell lysates using different lysis buffers. Lane 1: AKW lysates (see Materials and Methods, section 2.3.1); lane 2: AKO cell lysates (see Materials and Methods, section 2.3.1); lane 3: AKW lysates using CHAPS; lane 4: AKO lysates using CHAPS; lane 5: AKW lysates using 500 µl RIPA buffer; lane 6: AKO lysates using 500 µl RIPA buffer; lane 7: AKW lysates using 250 µl RIPA buffer; lane 8: AKO lysates using 250 µl RIPA buffer; band at 90 kDa is cnx (Anti cnx: 1:1000; anti-β-tubulin: 1:8000; sec. Ab: 1:500). For detection of the cnx, secondary HRP-conjugated goat α-rabbit antibody was used, and visualization was performed using ECL.

Assuming that the buffer choice caused the failure of the pulse/chase immunoprecipitations, we performed immunoprecipitations of unlabeled cell proteins with the RIPA buffer; however, still no clear results were obtained (no bands visible in IP samples on Coomassie staining Figure 3.19, Panel A, lanes 6 and 7, or any bands in PNS and IP samples on Western blot, Figure 3.19, Panel B, lanes 1, 2, 5, and 6).

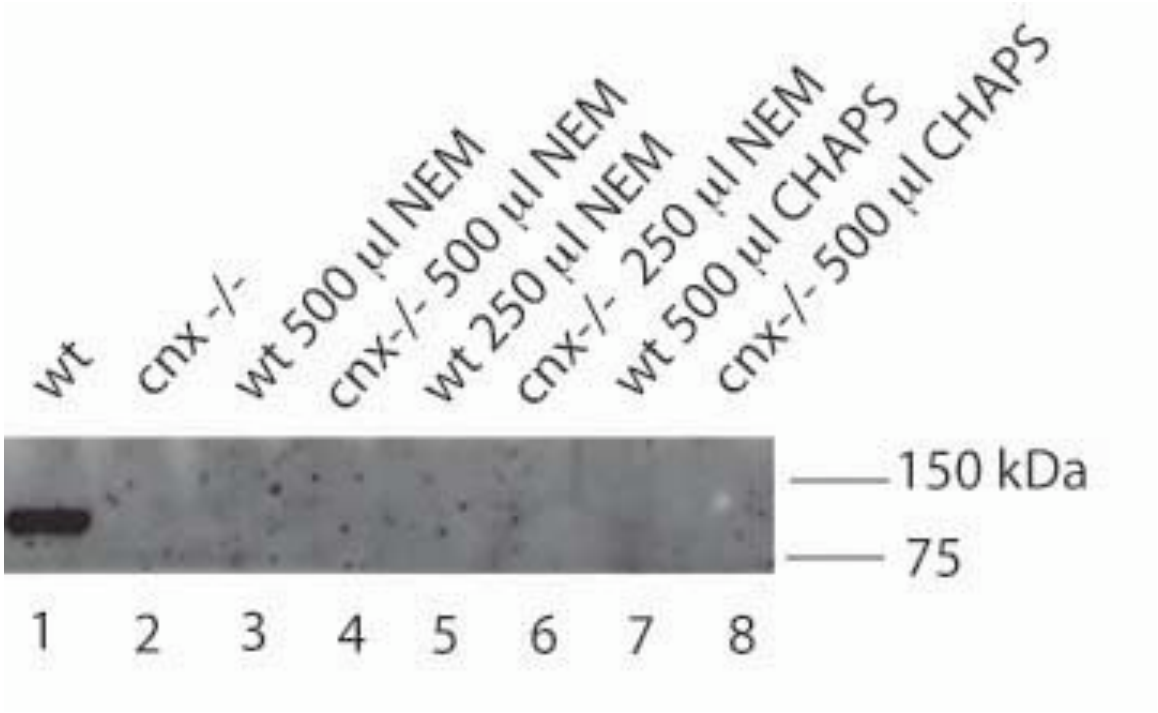

Figure 3.18: Western blot analysis of cell lysates using different lysis buffers. Lane 1: AKW lysates; lane 2: AKO lysates; lane 3: AKW lysates using 500 µl NEM; lane 4: AKO lysates using 500 µl NEM; lane 5: AKW lysates using 250 µl NEM buffer; lane 6: AKO lysates using 250 µl NEM buffer; lane 7: AKW lysates using 500 µl CHAPS buffer; lane 8: AKO lysates using 500 µl CHAPS buffer; band at 90 kDa is cnx (Anti cnx: 1:1000; anti-β-tubulin: 1:8000; sec. Ab: 1:500). For detection of the cnx, secondary HRP-conjugated goat α-rabbit antibody was used, and visualization was performed using ECL.

Currently, Helen Coe is continuing this work with HepG2 cells and with an altered protocol with AKO and AKW cells, see Discussion.

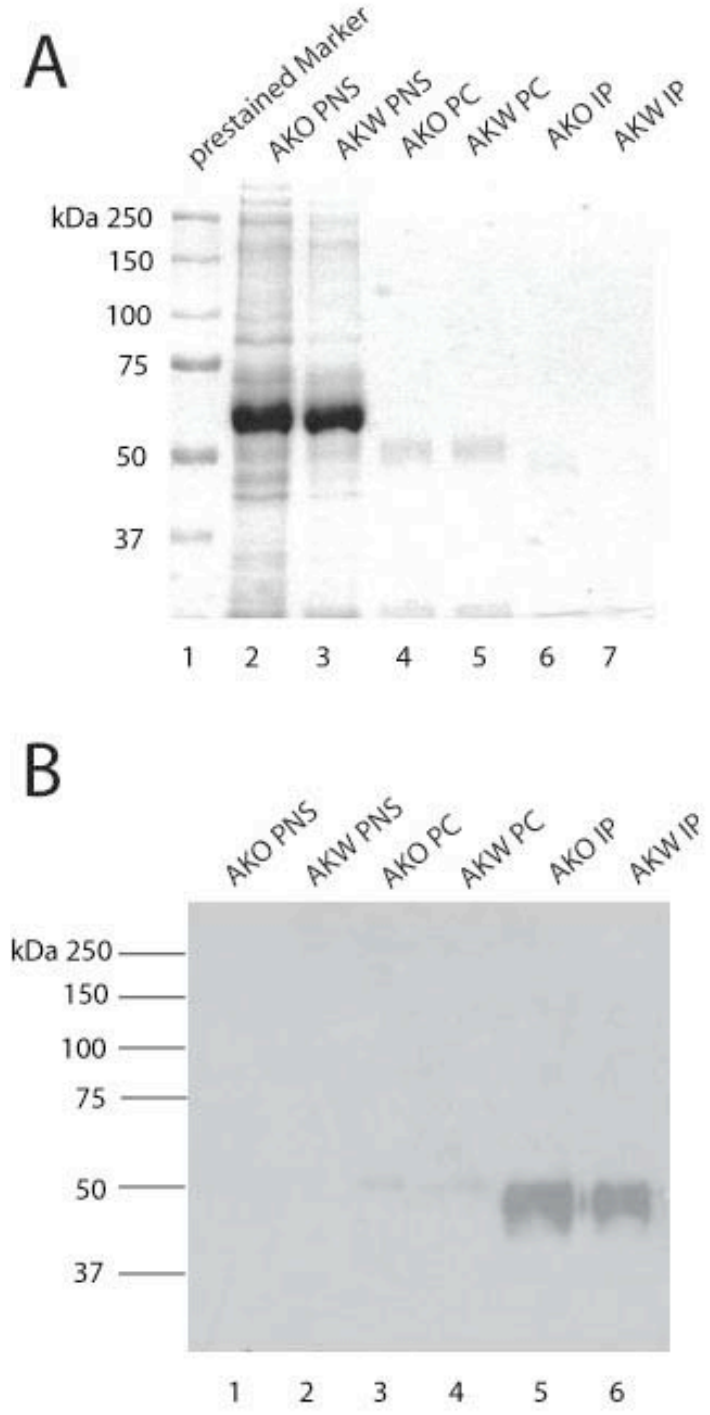

Figure 3.19: Coomassie staining and Western blot of Immunoprecipitation of cnx. (A): Lane 1: prestained marker; lane 2: post nuclear supernatant samples of AKO lysates; lane 3: post nuclear supernatant samples of AKW lysates; lane 4: precleared samples of AKO lysates; lane 5: precleared samples of AKW lysates; lane6: immunoprecipitation samples of AKO lysates; lane 7: immunoprecipitation samples of AKW lysates; **(B**): Western blot of Immunoprecipitation of cnx (Anti cnx: 1:1000; anti-β-tubulin: 1:8000; sec. Ab: 1:500). Lane 1: post nuclear supernatant samples of AKO lysates; lane 2: post nuclear supernatant samples of AKW lysates; lane 3: precleared samples of AKO lysates; lane 4: precleared samples of AKW lysates; lane 5: immunoprecipitation samples of AKO lysates; lane 6: immunoprecipitation samples of AKW lysates; (Anti cnx: 1:1000; sec. Ab: 1:500) For detection of cnx, secondary HRP-conjugated goat α-rabbit antibody was used, and visualization performed using ECL.

3.8 Trypsin sensitivity of mutated calnexin compared to wild-type calnexin

As setting up an assay to monitor protein activity and function of the cnx mutants (Pulse Chase IP or Tyrosinase assay) was unsuccessful, we decided to evaluate the mutants' sensitivity to trypsin digestion, previously shown to detect structural perturbations of proteins (Thomson and Williams, 2005);(Guo et al., 2003). The serine protease trypsin cleaves proteins at lysines and arginines, except when a proline follows.

Comparative protease digests were carried out under different conditions. EGTA and $CaCl_2$, $ZnCl_2$, or Mg-ATP was added to the basic buffer, buffer A, to show possible differences in trypsin sensitivity between wild-type and mutant cnx. As trypsin degrades the protein, new sites of the protein become accessible, depending on the amino acid sequence, resulting in fragments of different size. Thus, if protein is misfolded, we predict that different fragment sizes and/or degradation at different rates would be observed.

In Buffer A (Figure 3.20), more fragments were generated from wild-type cnx than from the two mutant proteins. Mutant H202A is degraded slower than the other two proteins. Both mutants display fewer protein bands at time point 0,5 min (at about 50 kDa) and show stronger bands than the wild-type at 60 kDa at all time points.

The patterns observed in Buffer B are similar, especially for the mutant cnxs (Figure 3.21). In the wild-type, fewer bands compared to Buffer A appear, however there are now bands at 60 kDa as well.

The property of wild-type cnx in Buffer C is comparable with that of wild-type cnx in Buffer A. In all 3 panels showing the results in Buffer C (Figure 3.22), there are distinct bands at 31 kDa. These bands also appear in other buffers, however here they are the most apparent. All in all, the bands seem to be clearest with Buffer C.

In Buffer D, the samples again look similar to the ones in Buffers A, B, or C (Figure 3.23).

In summary, regardless of buffer and wild-type or mutation, bands less sensitive to trypsin at about 31 and 55 kDa appear. These might be comparable to the protease-resistant species of crt (Thomson and Williams, 2005), suggesting that the tertiary structure of cnx exhibits parts of the protein that are inaccessible to the protease. Since there are no significant differences in the effects of the different buffers, nor

between wild-type and mutant cnxs, it can be hypothesized that the structures of these 2 mutants do not differ much from that of the wild-type protein.

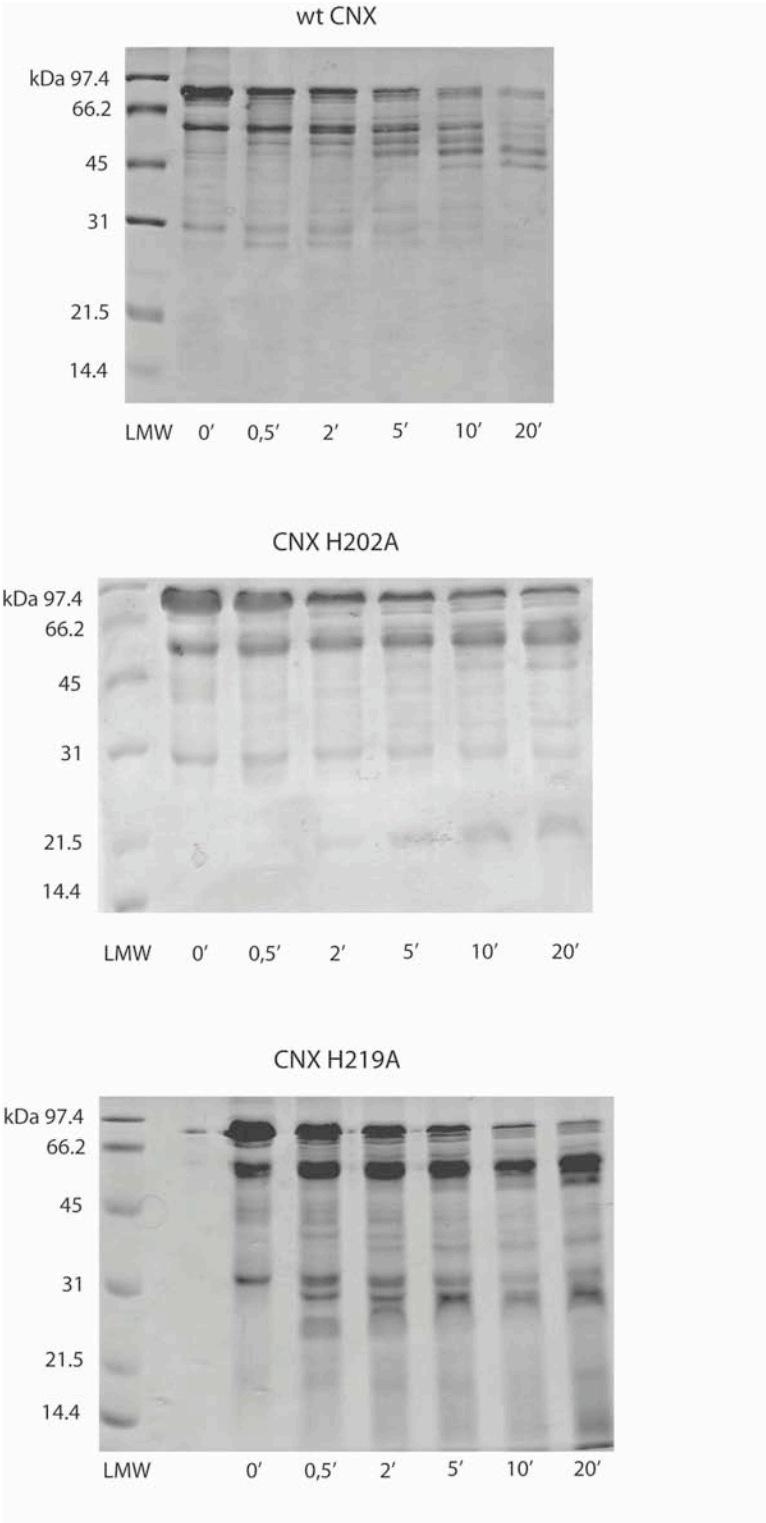

Figure 3.20: Coomassie Blue staining showing trypsin sensitivity of wild-type cnx and cnx mutants H202A and H219A. Trypsin digestion using Buffer A: Aliquots were taken at the indicated time points, and the proteins were separated on 12,5% acrylamide gels by SDS PAGE.

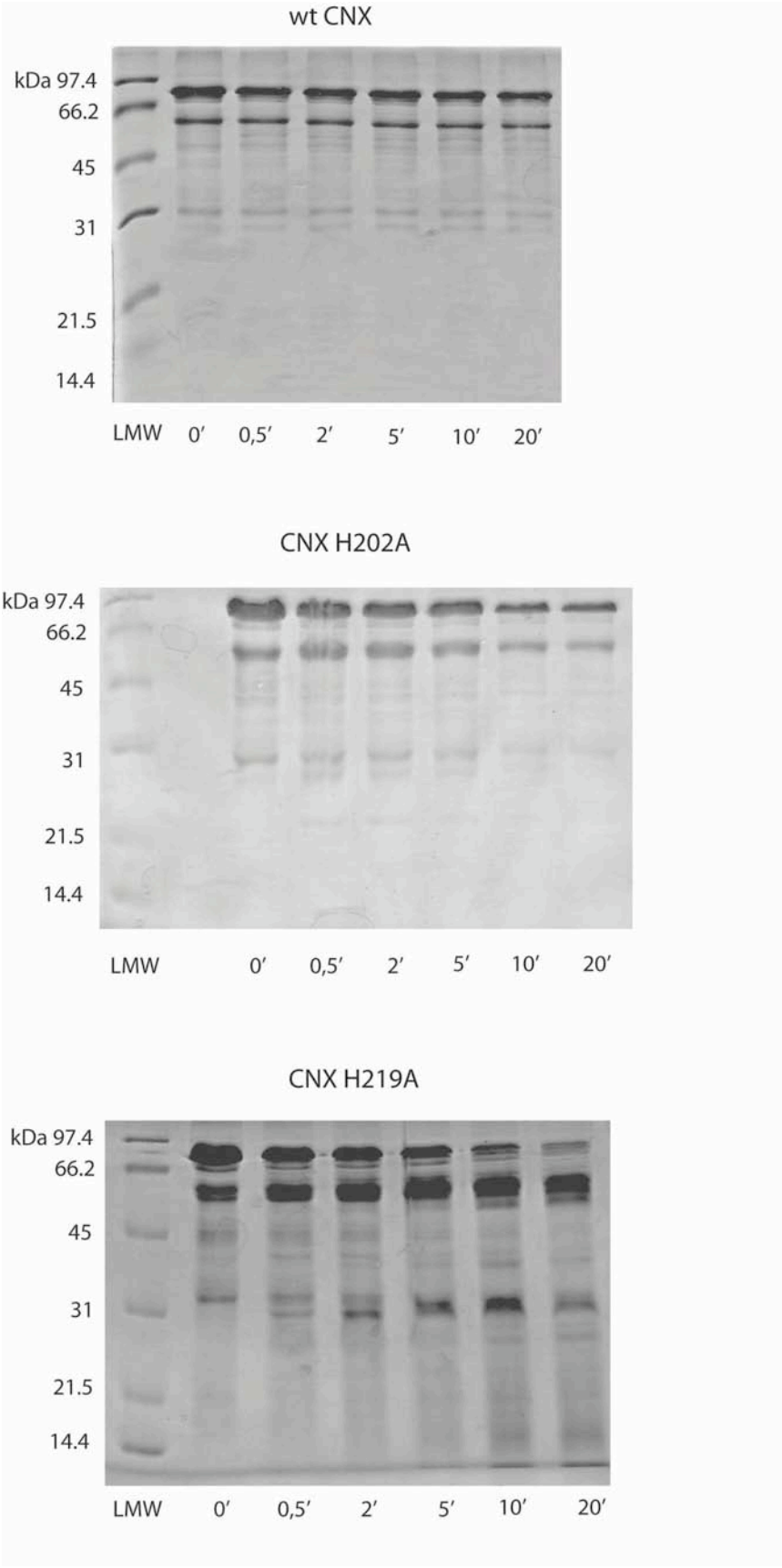

Figure 3.21: Coomassie Blue staining showing trypsin sensitivity of wild-type cnx and cnx mutants H202A and H219A. Trypsin digestion using Buffer B: Aliquots were taken at the indicated time points, and the proteins were separated on 12,5% acrylamide gels by SDS PAGE.

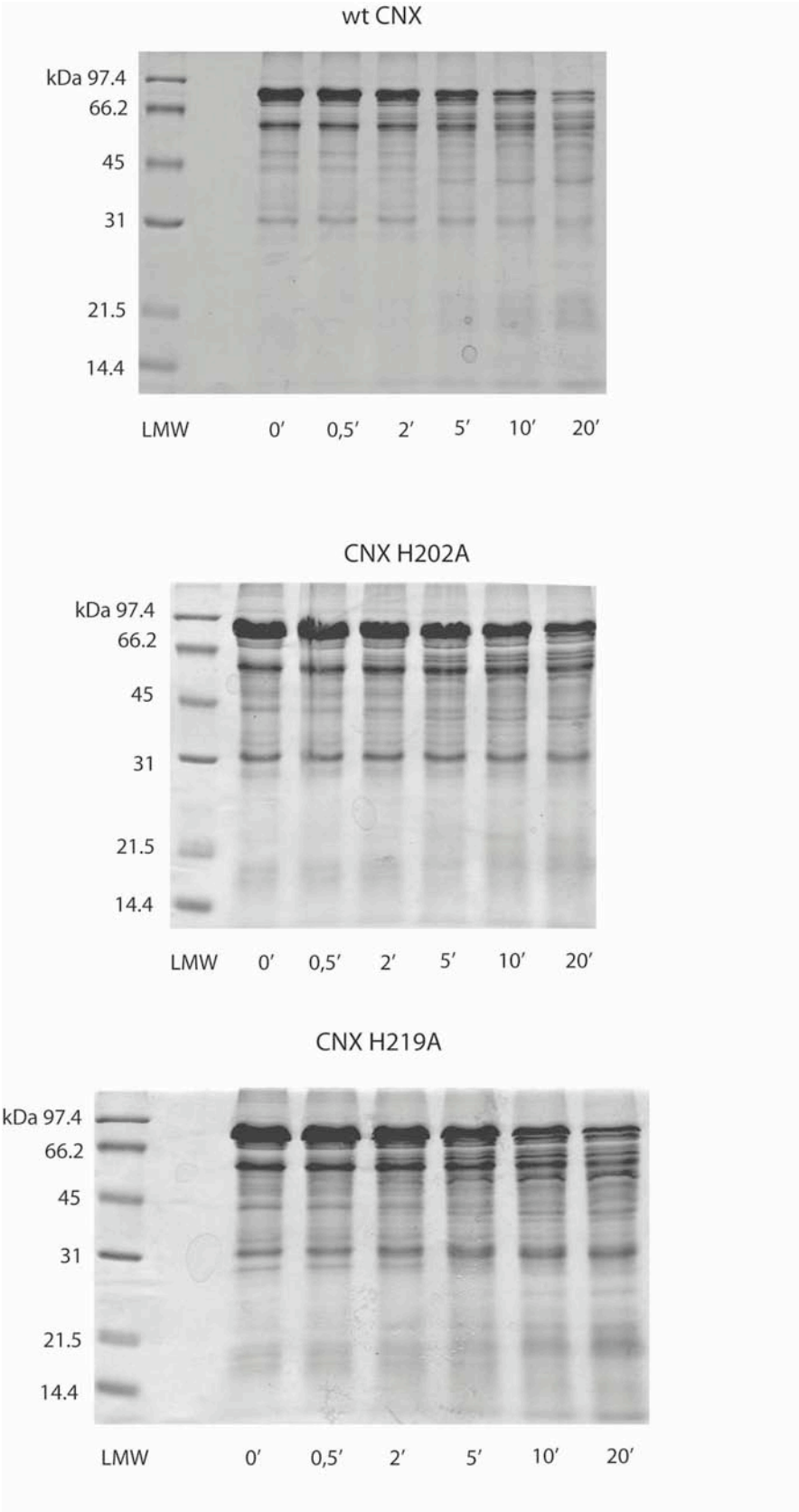

Figure 3.22: Coomassie Blue staining showing trypsin sensitivity of wild-type cnx and cnx mutants H202A and H219A. Trypsin digestion using Buffer C: Aliquots were taken at the indicated time points, and the proteins were separated on 12,5% acrylamide gels by SDS PAGE.

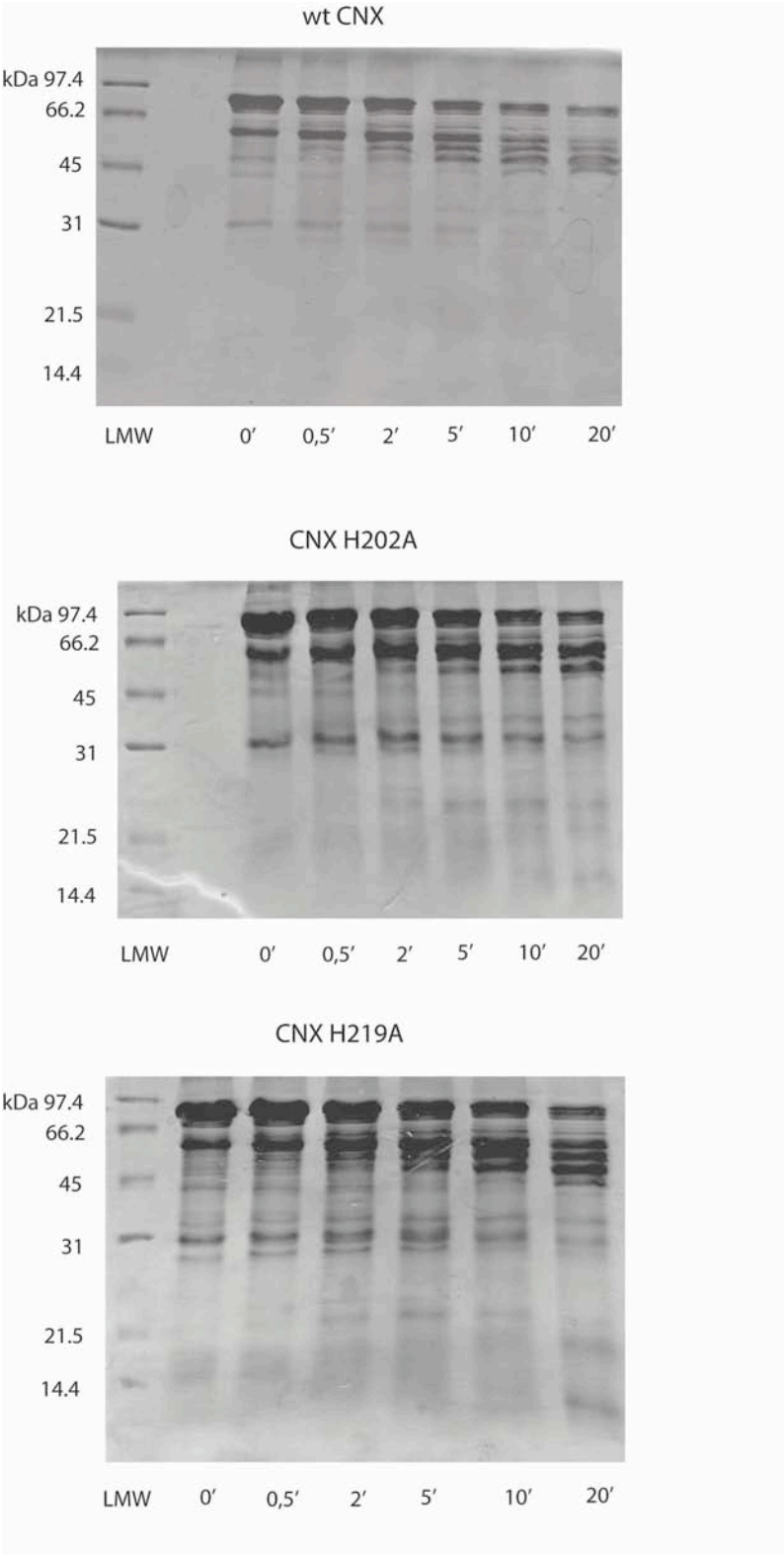

Figure 3.23: Coomassie Blue staining showing trypsin sensitivity of wild-type cnx and cnx mutants H202A and H219A. Trypsin digestion using Buffer D: Aliquots were taken at the indicated time points, and the proteins were separated on 12,5% acrylamide gels by SDS PAGE.

4 DISCUSSION

As reported by Pollock et al. (Pollock et al., 2004), the side chains of aspartic acids 342, 344, 346, and 348, as well as of methionine 347 and glutamic acid 352 (Figure 4.1), all located in the P-domain of cnx, are involved in cnx/ERp57 interactions. Possibly, Asp 344 and Glu 352 are the most important amino acids contributing to the cnx/ERp57 interaction, as shown by yeast two hybrid assays (Pollock et al., 2004). By mutating the amino acids selected in this study, we wanted to analyze the effects of theses changes on cnx/ERp57 complexes. As mentioned above, the amino acids chosen in this study were selected according to crt/ERp57 interactions.

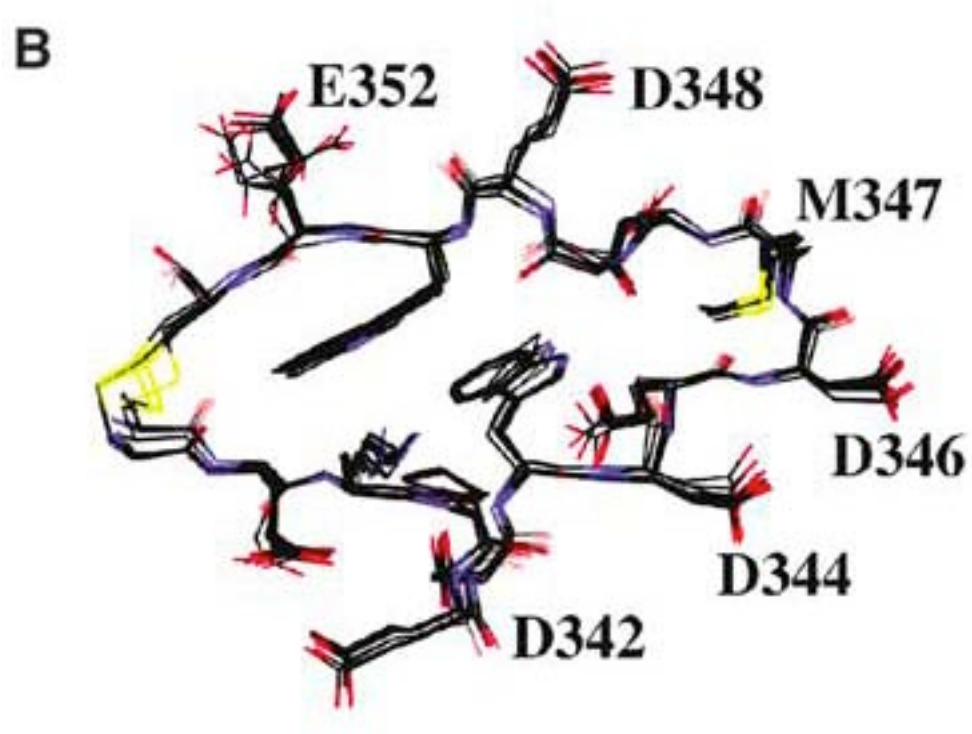

Figure 4.1: Overlay of the 20 lowest-energy structures of the cyclic peptide derived from the tip module sequence of the cnx P-domain (see Figure 1.2.B) when bound to ERp57. The residues involved in ERp57 interactions are labeled. (Figure 1, Panel B, from Pollock et al., 2004).

Whereas I was able to generate most of the (double) mutants and show expression and localization of the mutant cnx proteins (Figures 3.7-3.9 and Figures 3.11-3.13), there was not enough time to perform experiments in regards to studies on the binding between these and ERp57.

Generating mutant calnexins

While the generation of mutants Cys161Ala, Cys195Ala, His195Ala, Cys361Ala, and Cys367Ala was successful, unfortunately, several attempts to generate the double mutant C161/195A failed. However, using the original template (p2K7bsdEIFαCNX) and 2 mutagenic primer pairs in further attempts to generate double mutants, I was able to create the C361/367A cnx double mutant. On the other hand, since generating the cnx mutant H202A was unsuccessful, the production of the double mutant H202/219A was not possible either. Despite using different PCR programs, new template plasmids, and fresh primers, I was unable to generate these mutants. Especially with the double mutants I experienced unexpected difficulties. At first, I tried to use already mutated plasmids (i.e. p2K7bsdEIFαCNX with mutations C161A or C361A) as a template and then add a primer pair to perform the second mutation (C195A and C367A, respectively). However, after sequencing, neither of the mutations was integrated. One of the reasons for unefficient mutagenisis could be insufficient Dpn 1 digestion of the parental template. The incubation conditions for the endonuclease digestion were altered as suggested (QuikChange® XL Site-Directed Mutagenesis Kit instruction manual), but I was still not able to generate the double mutants. Therefore, I feel that, as listed in the QuikChange manual, the formation of secondary structures was inhibiting the mutagenesis reaction, although, as suggested, the annealing temperature of the PCR had been increased.

Western blot analysis

I was able to stably integrate the mutant cnxs (Cys161Ala, Cys195Ala, His195Ala, Cys361Ala, Cys367Ala, and Cys361/367Ala) into murine cnx-/- fibroblasts. The expression of the proteins was shown by Western blotting of cell extracts (Figures 3.7 - 3.9). As a control, β-tubulin was visualized as well. While most of these immunological visualization experiments worked well, in one case (Figure 3.8), the bands were somewhat weak. One likely explanation for weak signals is that the anti-β-tubulin antibody solution was re-used.

Immunofluorescence

As mentioned in Results (Figures 3.10 - 3.13), AKO cells not expressing cnx mutants are present in all immunostaining experiments (i.e., only ER-staining with Concanavalin A is visible). This is most likely due to limited selection efficiency of

blastacidin-S. Clearly, less than 80% of the cells expressed the proteins of interest following the lentiviral transfection and selection. Also, I noticed small circles of FITC staining in some of the images of control AKO cells, for example in Figure 3.10. These might be artifacts due to insufficient washing steps or to unspecific binding of the primary and/or secondary antibody.

Structure of mutated calnexin proteins

In most analyses of trypsin digests, regardless of the buffer used and whether wild-type or mutants were the substrates, bands less sensitive to trypsin were observed, which had sizes of approximately 31 and 55 kDa (Figures 3.20 - 3.23).

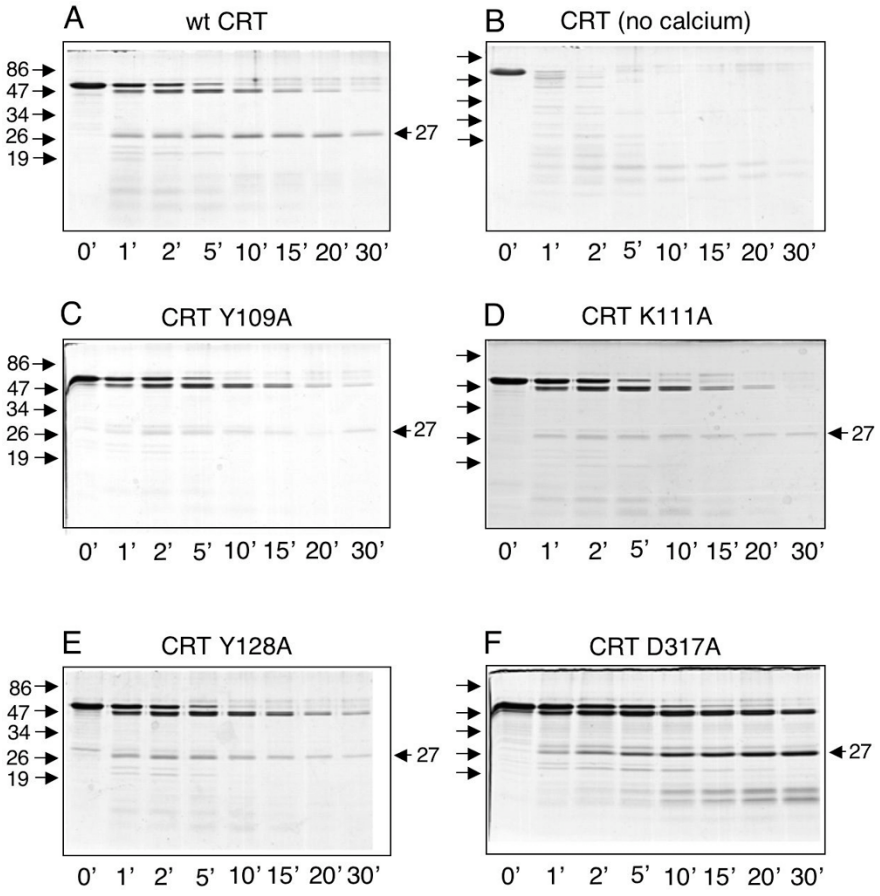

Figure 4.2: Trypsin sensitivity of oligosaccharide binding–deficient CRT mutants. Wild-type CRT and CRT point mutants Y109A, K111A, Y128A, and D317A were incubated with trypsin at a ratio of 1:50 (trypsin:protein, wt/wt) in 0.5 mM $CaCl_2$ (panels A, C–F) or in the absence of calcium (panel B). Aliquots were taken at the time points indicated, and the proteins were separated by reducing SDS-PAGE using 15% acrylamide gels. The arrow indicates the 27-kDa protease-resistant fragment of CRT. The mobilities of molecular weight markers are shown. CRT, calreticulin; SDS-PAGE, sodium dodecylsulfate–polyacrylamide gel electrophoresis. Figure 3. From (Thomson and Williams, 2005):

These might be comparable to the 27 kDa protease-resistant species of crt [Figure 4.2, (Thomson and Williams, 2005), see above]. This suggests that the tertiary structure of cnx, as well as of its mutants, comprises parts of the protein that are inaccessible to trypsin. Overall, the results suggest that the 2 mutants do not differ much from the wild-type in structure.

Although wild-type cnx and the two cnx mutant proteins (H202A and H219A) were similarly sensitive to the trypsin digestion (Figures 3.20 - 3.23), it might be useful, and for the sake of completeness, to also analyze the other mutant proteins, especially the double mutants. Currently, these experiments are being performed by Helen Coe.

Functionality of calnexin mutants

Based on the results derived from the current experiments, the pulse/chase immunoprecipitation protocol has been modified by Helen Coe and performed with HepG2 cells. With the adapted protocol, the experiment showed the expected results, i.e., the IP samples showed few bands likely representing substrates of cnx (Figure 4.3, arrows). The main adaptations to the original protocol are 5% FBS and L-glutamine were added to the depletion medium, NEM instead of RIPA buffer, and only a 5 min pulse-label period.

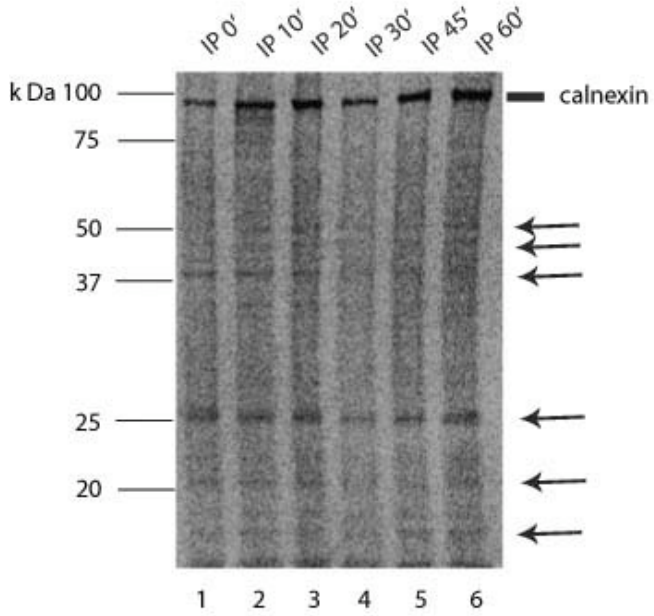

Figure 4.1: Autoradiogram of pulse/chase immunoprecipitation using HepG2 cells performed by Helen Coe. Lane 1-6: IP samples of HepG2 cells biosynthetically pulse-labeled for 5 min and chased for the indicated times; Arrows indicate possible substrates/binding partners of cnx.

Given the properties of cnx as chaperone for tyrosinase (see below), an alternative approach to functional analysis of cnx mutants would be the tyrosinase assay. Tyrosinase is a copper-containing type I membrane-bound enzyme involved in the production of melanin, the primary pigment found in vertebrates. It oxidizes L-tyrosine to L-dopaquinone using L-3,4-dihydroxyphenylalanine (L-DOPA) as an intermediate product (Lavado et al., 2006). L-dopaquinone then undergoes non-enzymatic reactions leading to precursors of melanin pigments (Land et al., 2003). Since tyrosinase is a substrate of cnx (Toyofuku et al., 1999);(Branza-Nichita et al., 1999), one can use this assay to show functionality of cnx mutants: if there is a color reaction, tyrosinase is correctly folded by cnx (mutants) because only then it oxidizes tyrosine to L-dopaquinone. L-dopaquinone forms a pink adduct with 3-methyl-2-benzothiazolinone hydrazone (MBTX), which can be quantitated by densitometric analysis, showing tyrosinase activity due to proper folding by calnexin.

In summary, mutant forms of cnx (C161A, C195A, H219A, C361A, C367A, and C361/367A) were generated. Following transfection into cnx-knockout murine fibroblasts, expression and intracellular localization of the proteins were investigated by Western blotting and immunohistochemistry, respectively. Possible differences in structure between mutant cnxs and wild-type cnx were analyzed via trypsin digestion, and their function in terms of interaction with substrates with pulse/chase immunoprecipitation experiments. The single and the double cnx mutants (Cys161/195 Ala, His202/219Ala, and Cys361/367Ala) showed only minor, if any, differences in behaviour in comparison to the wildtype protein.

Future studies aimed at production and analysis of additional cnx mutants, at the identification of proteins that co-immunoprecipitate with wild-type- and mutant cnxs, and at their ability to bind to ERp57, can be expected to reveal further details of the structure/function relationship between cnx and its partners.

5 ABBREVIATIONS

A

APMSF	(4-Amidinophenyl)-methanesulfonyl fluoride hydrochloride monohydrate
ATP	adenosine tri phosphate

B

bp	base pair
BiP	immunoglobulin heavy chain binding protein
BGS	bovine growth serum
BSA	bovine serum albumine

C

CFTR	cystic fibrosis transmembrane conductance regulator
CHAPS	3-[(3-Cholamidopropyl)dimethylammonio]-1-propanesulfonate
crt, CRT	calreticulin
cnx, CNX	calnexin
C-terminal	carboxy terminal

D

ddH_2O	double destilled water
DMEM	Dulbecco's Modified Eagle Medium
DMSO	dimethyl sulfoxide
DNA	desoxyribonucleinsäure
dNTP	deoxyribonucleotide triphosphate
DOC	deoxycholate

E

E-64	(2*S*,3*S*)-3-(*N*-{(*S*)-1-[*N*-(4-guanidinobutyl)carbamoyl]3-methylbutyl}carbamoyl)oxirane-2-carboxylic acid
ECL	enhanced chemoluminescence
EDTA	ethylenediaminetetraacetic acid
EDEM	endoplasmic reticulum degradation-enhancing α-mannosidase-like lectins
EGTA	ethylene glycol tetraacetic acid

ER	endoplasmatic reticulim
ERAD	endoplasmic reticulum associated protein degradation
ERp57	endoplasmic reticulum protein 57 kDa

F

FBS	fetal bovine serum
FITC	fluorescein isothiocyanate

G

g	gram
GFP	green fluorescent protein
GSH	glutathione

H

HEBS	4-(2-hydroxyethyl)-1-piperazineethanesulfonic acid buffered saline
HEPES	4-(2-hydroxyethyl)-1-piperazineethanesulfonic acid
HMG-CoA	3-hydroxy-3-methyl-glutaryl-CoA reductase
hr	hour(s)
HRP	horseradish peroxidase
Hsp	heat shock protein

I

IgG	immunglobulin
IP	immunoprecipitation

K

kDa	kilo Dalton
kb	kilobases

L

l	litre
LB	Luria-Bertani
L-DOPA	l-3,4-dihydroxyphenylalanine

M

M	methionine or molar
mA	milliampere

MHC	major histocompatibility complex
mM	millimolar
ml	millilitre
MBTX	3-methyl-2-benzothiazolinone
min	minute(s)
µg	microgram
µl	microlitre
µM	micromolar

N

NaDOC	sodium deoxycholate
NEM	N-Ethylmaleimide
NP-40	nonyl phenoxylpolyethoxylethanol
nm	nanometer
N-terminal	amino terminal

P

PAGE	polyacrylamide gel electrophoresi
PBS	phosphate buffered saline
PBS-T	phosphate buffered saline with Tween 20
PC	preclear
PCR	polymerase chain reaction
PDI	protein disulfide isomerase
PNS	post nuclear supernatant
PMSF	phenylmethylsulfonyl fluoride

R

RIPA	radioimmunoprecipitation assay buffer
RNA	ribonucleic acid
rpm	rounds per minute

S

sec	second(s)
SDS	sodium dodecyl sulfate

T

TAE	Tris-acetate-EDTA buffer
TAP	transporter associated with antigen processing
TLCK	Nα-Tosyl-Lys-chloromethylketone·HCl
T_m	melting temperature
TEMED	N,N,N',N' - tetramethylethylendiamine

U

U	unit
UPR	unfolded protein response

V

V	volt

W

w/v	weight per volume

%GC	guanine cytosine content
ºC	degrees celsius

6 REFERENCES

Anderson, K.S., and Cresswell, P. (1994). A role for calnexin (IP90) in the assembly of class II MHC molecules. The EMBO journal *13*, 675-682.

Antoniou, A.N., Ford, S., Alphey, M., Osborne, A., Elliott, T., and Powis, S.J. (2002). The oxidoreductase ERp57 efficiently reduces partially folded in preference to fully folded MHC class I molecules. The EMBO journal *21*, 2655-2663.

Argon, Y., and Simen, B.B. (1999). GRP94, an ER chaperone with protein and peptide binding properties. Semin Cell Dev Biol *10*, 495-505.

Arnaudeau, S., Frieden, M., Nakamura, K., Castelbou, C., Michalak, M., and Demaurex, N. (2002). Calreticulin differentially modulates calcium uptake and release in the endoplasmic reticulum and mitochondria. J Biol Chem *277*, 46696-46705.

Baksh, S., Spamer, C., Heilmann, C., and Michalak, M. (1995). Identification of the Zn2+ binding region in calreticulin. FEBS letters *376*, 53-57.

Barnes, J. A., and Smoak, I. W. (1997). Immunolocalization and heart levels of GRP94 in the mouse during post-implantation development. Anat Embryol (Berl) *196*, 335-341.

Biederer, T., Volkwein, C., and Sommer, T. (1997). Role of Cue1p in ubiquitination and degradation at the ER surface. Science *278*, 1806-1809.

Booth, C., and Koch, G.L. (1989). Perturbation of cellular calcium induces secretion of luminal ER proteins. Cell *59*, 729-737.

Bohley, P., and Seglan, P.O. (1992). Proteases and proteolysis in the lysosome. Experientia 48, 151-7.

Branza-Nichita, N., Petrescu, A.J., Dwek, R.A., Wormald, M.R., Platt, F.M., and Petrescu, S.M. (1999). Tyrosinase folding and copper loading in vivo: a crucial role for calnexin and alpha-glucosidase II. Biochemical and biophysical research communications *261*, 720-725.

Brodsky, J.L., Goeckeler, J., and Schekman, R. (1995). BiP and Sec63p are required for both co- and posttranslational protein translocation into the yeast endoplasmic reticulum. Proc Natl Acad Sci U S A *92*, 9643-9646.

Bu, G., Geuze, H.J., Strous, G.J., and Schwartz, A.L. (1995). 39 kDa receptor-associated protein is an ER resident protein and molecular chaperone for LDL receptor-related protein. The EMBO journal *14*, 2269-2280.

Cai, H., Wang, C.C., and Tsou, C.L. (1994). Chaperone-like activity of protein disulfide isomerase in the refolding of a protein with no disulfide bonds. J Biol Chem *269*, 24550-24552.

Cheetham, M.E., and Caplan, A.J. (1998). Structure, function and evolution of DnaJ: conservation and adaptation of chaperone function. Cell Stress Chaperones *3*, 28-36.

Cheng, S.H., Gregory, R.J., Marshall, J., Paul, S., Souza, D.W., White, G.A., O'Riordan, C.R., and Smith, A.E. (1990). Defective intracellular transport and processing of CFTR is the molecular basis of most cystic fibrosis. Cell *63*, 827-834.

Christianson, J.C., Shaler, T.A., Tyler, R.E., and Kopito, R.R. (2008). OS-9 and GRP94 deliver mutant alpha1-antitrypsin to the Hrd1-SEL1L ubiquitin ligase complex for ERAD. Nature cell biology *10*, 272-282.

Corbett, E.F., Michalak, K.M., Oikawa, K., Johnson, S., Campbell, I.D., Eggleton, P., Kay, C., and Michalak, M. (2000). The conformation of calreticulin is influenced by the endoplasmic reticulum luminal environment. J Biol Chem *275*, 27177-27185.

Corbett, E.F., and Michalak, M. (2000). Calcium, a signaling molecule in the endoplasmic reticulum? Trends Biochem Sci *25*, 307-311.

Corbett, E.F., Oikawa, K., Francois, P., Tessier, D.C., Kay, C., Bergeron, J.J., Thomas, D.Y., Krause, K.H., and Michalak, M. (1999). Ca2+ regulation of interactions between endoplasmic reticulum chaperones. J Biol Chem *274*, 6203-6211.

Coux, O., Tanaka, K., and Goldberg, A.L. (1996). Structure and functions of the 20S and 26S proteasomes. Annual review of biochemistry *65*, 801-847.

Credle, J.J., Finer-Moore, J.S., Papa, F.R., Stroud, R.M., and Walter, P. (2005). On the mechanism of sensing unfolded protein in the endoplasmic reticulum. Proc Natl Acad Sci U S A *102*, 18773-18784.

Danilczyk, U.G., and Williams, D.B. (2001). The lectin chaperone calnexin utilizes polypeptide-based interactions to associate with many of its substrates in vivo. J Biol Chem *276*, 25532-25540.

David, V., Hochstenbach, F., Rajagopalan, S., and Brenner, M.B. (1993). Interaction with newly synthesized and retained proteins in the endoplasmic reticulum suggests a chaperone function for human integral membrane protein IP90 (calnexin). J Biol Chem *268*, 9585-9592.

Degen, E., Cohen-Doyle, M.F., and Williams, D.B. (1992). Efficient dissociation of the p88 chaperone from major histocompatibility complex class I molecules requires both beta 2-microglobulin and peptide. J Exp Med *175*, 1653-1661.

Denzel, A., Molinari, M., Trigueros, C., Martin, J.E., Velmurgan, S., Brown, S., Stamp, G., and Owen, M.J. (2002). Early postnatal death and motor disorders in mice congenitally deficient in calnexin expression. Molecular and cellular biology *22*, 7398-7404.

Ellgaard, L., and Helenius, A. (2001). ER quality control: towards an understanding at the molecular level. Curr Opin Cell Biol *13*, 431-437.

Ellgaard, L., Molinari, M., and Helenius, A. (1999). Setting the standards: quality control in the secretory pathway. Science *286*, 1882-1888.

Fassio, A., and Sitia, R. (2002). Formation, isomerisation and reduction of disulphide bonds during protein quality control in the endoplasmic reticulum. Histochem Cell Biol *117*, 151-157.

Feng, H.P., and Gierasch, L.M. (1998). Molecular chaperones: clamps for the Clps? Curr Biol *8*, R464-467.

Fink, A.L. (1999). Chaperone-mediated protein folding. Physiol Rev *79*, 425-449.

Fliegel, L., Burns, K., MacLennan, D.H., Reithmeier, R.A., and Michalak, M. (1989). Molecular cloning of the high affinity calcium-binding protein (calreticulin) of skeletal muscle sarcoplasmic reticulum. J Biol Chem *264*, 21522-21528.

Frey, S., Leskovar, A., Reinstein, J., and Buchner, J. (2007) The ATPase cycle of the endoplasmic chaperone Grp94. J Biol Chem *282*, 35612-35620.

Frickel, E.M., Frei, P., Bouvier, M., Stafford, W.F., Helenius, A., Glockshuber, R., and Ellgaard, L. (2004). ERp57 is a multifunctional thiol-disulfide oxidoreductase. J Biol Chem *279*, 18277-18287.

Frickel, E.M., Riek, R., Jelesarov, I., Helenius, A., Wuthrich, K., and Ellgaard, L. (2002). TROSY-NMR reveals interaction between ERp57 and the tip of the calreticulin P-domain. Proc Natl Acad Sci U S A *99*, 1954-1959.

Gao, B., Adhikari, R., Howarth, M., Nakamura, K., Gold, M.C., Hill, A.B., Knee, R., Michalak, M., and Elliott, T. (2002). Assembly and antigen-presenting function of MHC class I molecules in cells lacking the ER chaperone calreticulin. Immunity *16*, 99-109.

Garbi, N., Tanaka, S., Momburg, F., and Hammerling, G.J. (2006). Impaired assembly of the major histocompatibility complex class I peptide-loading complex in mice deficient in the oxidoreductase ERp57. Nature immunology *7*, 93-102.

Gething, M.J., and Sambrook, J. (1992). Protein folding in the cell. Nature *355*, 33-45.

Guo, L., Groenendyk, J., Papp, S., Dabrowska, M., Knoblach, B., Kay, C., Parker, J.M., Opas, M., and Michalak, M. (2003). Identification of an N-domain histidine essential for chaperone function in calreticulin. J Biol Chem *278*, 50645-50653.

Haas, I.G., and Wabl, M. (1983). Immunoglobulin heavy chain binding protein. Nature *306*, 387-389.

Hamman, B.D., Hendershot, L.M., and Johnson, A.E. (1998). BiP maintains the permeability barrier of the ER membrane by sealing the lumenal end of the translocon pore before and early in translocation. Cell *92*, 747-758.

Hammond, C., Braakman, I., and Helenius, A. (1994). Role of N-linked oligosaccharide recognition, glucose trimming, and calnexin in glycoprotein folding and quality control. Proc Natl Acad Sci U S A *91*, 913-917.

Hampton, R.Y., Gardner, R.G., and Rine, J. (1996). Role of 26S proteasome and HRD genes in the degradation of 3-hydroxy-3-methylglutaryl-CoA reductase, an integral endoplasmic reticulum membrane protein. Mol Biol Cell *7*, 2029-2044.

Haslbeck, M. (2002). sHsps and their role in the chaperone network. Cell Mol Life Sci *59*, 1649-1657.

Hebert, D.N., and Molinari, M. (2007). In and out of the ER: protein folding, quality control, degradation, and related human diseases. Physiol Rev *87*, 1377-1408.

Helenius, A., and Aebi, M. (2001). Intracellular functions of N-linked glycans. Science *291*, 2364-2369.

Helenius, J., and Aebi, M. (2002). Transmembrane movement of dolichol linked carbohydrates during N-glycoprotein biosynthesis in the endoplasmic reticulum. Semin Cell Dev Biol *13*, 171-178.

Hendershot, L., Wei, J., Gaut, J., Melnick, J., Aviel, S., and Argon, Y. (1996). Inhibition of immunoglobulin folding and secretion by dominant negative BiP ATPase mutants. Proc Natl Acad Sci U S A *93*, 5269-5274.

High, S., Lecomte, F.J., Russell, S.J., Abell, B.M., and Oliver, J.D. (2000). Glycoprotein folding in the endoplasmic reticulum: a tale of three chaperones? FEBS letters *476*, 38-41.

Hiller, M.M., Finger, A., Schweiger, M., and Wolf, D.H. (1996). ER degradation of a misfolded luminal protein by the cytosolic ubiquitin-proteasome pathway. Science *273*, 1725-1728.

Hochstrasser, M. (1996). Protein degradation or regulation: Ub the judge. Cell *84*, 813-815.

Hong, M., Luo, S., Baumeister, P., Huang, J.M., Gogia, R.K., Li, M., and Lee, A.S. (2004). Underglycosylation of ATF6 as a novel sensing mechanism for activation of the unfolded protein response. J Biol Chem *279*, 11354-11363.

Hosokawa, N., Wada, I., Hasegawa, K., Yorihuzi, T., Tremblay, L.O., Herscovics, A., and Nagata, K. (2001). A novel ER alpha-mannosidase-like protein accelerates ER-associated degradation. EMBO Rep *2*, 415-422.

Ihara, Y., Cohen-Doyle, M.F., Saito, Y., and Williams, D.B. (1999). Calnexin discriminates between protein conformational states and functions as a molecular chaperone in vitro. Mol Cell *4*, 331-341.

Jakob, C.A., Bodmer, D., Spirig, U., Battig, P., Marcil, A., Dignard, D., Bergeron, J.J., Thomas, D.Y., and Aebi, M. (2001). Htm1p, a mannosidase-like protein, is involved in glycoprotein degradation in yeast. EMBO Rep *2*, 423-430.

Jentsch, S., and Schlenker, S. (1995). Selective protein degradation: a journey's end within the proteasome. Cell *82*, 881-884.

Jessop, C.E., Chakravarthi, S., Garbi, N., Hammerling, G.J., Lovell, S., and Bulleid, N.J. (2007). ERp57 is essential for efficient folding of glycoproteins sharing common structural domains. The EMBO journal *26*, 28-40.

Kelley, W.L. (1998). The J-domain family and the recruitment of chaperone power. Trends Biochem Sci *23*, 222-227.

Kelley, W.L. (1999). Molecular chaperones: How J domains turn on Hsp70s. Curr Biol *9*, R305-308.

Kimura, M., Takatsuki, A., and Yamaguchi, I. (1994). Blasticidin S deaminase gene from Aspergillus terreus (BSD): a new drug resistance gene for transfection of mammalian cells. Biochim Biophys Acta *1219*, 653-659.

Kleizen, B., and Braakman, I. (2004). Protein folding and quality control in the endoplasmatic reticulum. Curr Opin Cell Biol *16*, 343-349.

Ladiges, W.C., Knoblaugh, S.E., Morton, J.F., Korth, M.J., Sopher, B.L., Baskin, C.R., MacAuley, A., Goodman, A.G., LeBoeuf, R.C., and Katze, M.G. (2005). Pancreatic beta-cell failure and diabetes in mice with a deletion mutation of the endoplasmic reticulum molecular chaperone gene P58IPK. Diabetes *54*, 1074-1081.

Land, E.J., Ramsden, C.A., and Riley, P.A. (2003). Tyrosinase autoactivation and the chemistry of ortho-quinone amines. Accounts of chemical research *36*, 300-308.

Lau, M.M., and Neufeld, E.F. (1989). A frameshift mutation in a patient with Tay-Sachs disease causes premature termination and defective intracellular transport of the alpha-subunit of beta-hexosaminidase. J Biol Chem *264*, 21376-21380.

Lavado, A., Jeffery, G., Tovar, V., de la Villa, P., and Montoliu, L. (2006). Ectopic expression of tyrosine hydroxylase in the pigmented epithelium rescues the retinal abnormalities and visual function common in albinos in the absence of melanin. Journal of neurochemistry *96*, 1201-1211.

Le, A., Graham, K.S., and Sifers, R.N. (1990). Intracellular degradation of the transport-impaired human PiZ alpha 1-antitrypsin variant. Biochemical mapping of the degradative event among compartments of the secretory pathway. J Biol Chem *265*, 14001-14007.

Leach, M.R., Cohen-Doyle, M.F., Thomas, D.Y., and Williams, D.B. (2002). Localization of the lectin, ERp57 binding, and polypeptide binding sites of calnexin and calreticulin. J Biol Chem *277*, 29686-29697.

Lehrman, M.A., Schneider, W.J., Brown, M.S., Davis, C.G., Elhammer, A., Russell, D.W., and Goldstein, J.L. (1987). The Lebanese allele at the low density lipoprotein receptor locus. Nonsense mutation produces truncated receptor that is retained in endoplasmic reticulum. J Biol Chem *262*, 401-410.

Li, Y., and Camacho, P. (2004). Ca2+-dependent redox modulation of SERCA 2b by ERp57. The Journal of cell biology *164*, 35-46.

Li, Z., and Srivastava, P. (2004). Heat-shock proteins. Current protocols in immunology / edited by John E. Coligan ... [et al *Appendix 1*, Appendix 1T.

Lindquist, J.A., Hammerling, G.J., and Trowsdale, J. (2001). ER60/ERp57 forms disulfide-bonded intermediates with MHC class I heavy chain. Faseb J *15*, 1448-1450.

Liu, C.Y., Schroder, M., and Kaufman, R.J. (2000). Ligand-independent dimerization activates the stress response kinases IRE1 and PERK in the lumen of the endoplasmic reticulum. J Biol Chem *275*, 24881-24885.

Lowry, O.H., Rosebrough, N. J., Farr, A. L., and Randall, R. J. (1951) Protein measurement with the Folin phenol reagent. J Biol Chem 193, 265-75.

Lukacs, G.L., Chang, X.B., Bear, C., Kartner, N., Mohamed, A., Riordan, J.R., and Grinstein, S. (1993). The delta F508 mutation decreases the stability of cystic fibrosis transmembrane conductance regulator in the plasma membrane. Determination of functional half-lives on transfected cells. J Biol Chem *268*, 21592-21598.

Luo, S., Mao, C., Lee, B., and Lee, A.S. (2006). GRP78/BiP is required for cell proliferation and protecting the inner cell mass from apoptosis during early mouse embryonic development. Molecular and cellular biology *26*, 5688-5697.

Lyman, S.K., and Schekman, R. (1995). Interaction between BiP and Sec63p is required for the completion of protein translocation into the ER of Saccharomyces cerevisiae. The Journal of cell biology *131*, 1163-1171.

Mao, C., Dong, D., Little, E., Luo, S., and Lee, A.S. (2004). Transgenic mouse model for monitoring endoplasmic reticulum stress in vivo. Nature medicine *10*, 1013-1014; author reply 1014.

Mao, C., Tai, W.C., Bai, Y., Poizat, C., and Lee, A.S. (2006). In vivo regulation of Grp78/BiP transcription in the embryonic heart: role of the endoplasmic reticulum stress response element and GATA-4. J Biol Chem *281*, 8877-8887.

Martin, V., Groenendyk, J., Steiner, S.S., Guo, L., Dabrowska, M., Parker, J.M., Muller-Esterl, W., Opas, M., and Michalak, M. (2006). Identification by mutational analysis of amino acid residues essential in the chaperone function of calreticulin. J Biol Chem *281*, 2338-2346.

Matlack, K.E., Mothes, W., and Rapoport, T.A. (1998). Protein translocation: tunnel vision. Cell *92*, 381-390.

Mayer, M.P., Brehmer, D., Gassler, C.S., and Bukau, B. (2001). Hsp70 chaperone machines. Adv Protein Chem *59*, 1-44.

Mayer, T.U., Braun, T., and Jentsch, S. (1998). Role of the proteasome in membrane extraction of a short-lived ER-transmembrane protein. The EMBO journal *17*, 3251-3257.

Meldolesi, J., and Pozzan, T. (1998). The heterogeneity of ER Ca2+ stores has a key role in nonmuscle cell signaling and function. The Journal of cell biology *142*, 1395-1398.

Mesaeli, N., Nakamura, K., Opas, M., and Michalak, M. (2001). Endoplasmic reticulum in the heart, a forgotten organelle? Molecular and cellular biochemistry *225*, 1-6.

Mesaeli, N., Nakamura, K., Zvaritch, E., Dickie, P., Dziak, E., Krause, K.H., Opas, M., MacLennan, D.H., and Michalak, M. (1999). Calreticulin is essential for cardiac development. The Journal of cell biology *144*, 857-868.

Michalak, M., Groenendyk, J., Szabo, E., Gold, L.I., and Opas, M. (2009). Calreticulin, a multi-process calcium-buffering chaperone of the endoplasmic reticulum. Biochem J *417*, 651-666.

Molinari, M., Calanca, V., Galli, C., Lucca, P., and Paganetti, P. (2003). Role of EDEM in the release of misfolded glycoproteins from the calnexin cycle. Science *299*, 1397-1400.

Molinari, M., Eriksson, K.K., Calanca, V., Galli, C., Cresswell, P., Michalak, M., and Helenius, A. (2004). Contrasting functions of calreticulin and calnexin in glycoprotein folding and ER quality control. Mol Cell *13*, 125-135.

Molinari, M., Galli, C., Vanoni, O., Arnold, S.M., and Kaufman, R.J. (2005). Persistent glycoprotein misfolding activates the glucosidase II/UGT1-driven calnexin cycle to delay aggregation and loss of folding competence. Mol Cell *20*, 503-512.

Molinari, M., and Helenius, A. (1999). Glycoproteins form mixed disulphides with oxidoreductases during folding in living cells. Nature *402*, 90-93.

Nadanaka, S., Okada, T., Yoshida, H., and Mori, K. (2007). Role of disulfide bridges formed in the luminal domain of ATF6 in sensing endoplasmic reticulum stress. Molecular and cellular biology *27*, 1027-1043.

Nagata, K., and Hosokawa, N. (1996). Regulation and function of collagen-specific molecular chaperone, HSP47. Cell Struct Funct *21*, 425-430.

Naldini, L., Blomer, U., Gage, F.H., Trono, D., and Verma, I.M. (1996a). Efficient transfer, integration, and sustained long-term expression of the transgene in adult rat brains injected with a lentiviral vector. Proc Natl Acad Sci U S A *93*, 11382-11388.

Naldini, L., Blomer, U., Gallay, P., Ory, D., Mulligan, R., Gage, F.H., Verma, I.M., and Trono, D. (1996b). In vivo gene delivery and stable transduction of nondividing cells by a lentiviral vector. Science *272*, 263-267.

Nakamura, K., Zuppini, A., Arnaudeau, S., Lynch, J., Ahsan, I., Krause, R., Papp, S., De Smedt, H., Parys, J.B., Muller-Esterl, W.*, et al.* (2001). Functional specialization of calreticulin domains. The Journal of cell biology *154*, 961-972.

Nakatsukasa, K., Nishikawa, S., Hosokawa, N., Nagata, K., and Endo, T. (2001). Mnl1p, an alpha -mannosidase-like protein in yeast Saccharomyces cerevisiae, is required for endoplasmic reticulum-associated degradation of glycoproteins. J Biol Chem *276*, 8635-8638.

Newman, R.H., Whitehead, P., Lally, J., Coffer, A., and Freemont, P. (1996). 20S human proteasomes bind with a specific orientation to lipid monolayers in vitro. Biochim Biophys Acta *1281*, 111-116.

Ni, M., and Lee, A.S. (2007). ER chaperones in mammalian development and human diseases. FEBS letters *581*, 3641-3651.

Nishikawa, S., and Endo, T. (1997). The yeast JEM1p is a DnaJ-like protein of the endoplasmic reticulum membrane required for nuclear fusion. J Biol Chem *272*, 12889-12892.

Nishikawa, S.I., Fewell, S.W., Kato, Y., Brodsky, J.L., and Endo, T. (2001). Molecular chaperones in the yeast endoplasmic reticulum maintain the solubility of proteins for retrotranslocation and degradation. The Journal of cell biology *153*, 1061-1070.

Noiva, R. (1999). Protein disulfide isomerase: the multifunctional redox chaperone of the endoplasmic reticulum. Semin Cell Dev Biol *10*, 481-493.

Oda, Y., Senaha, T., Matsuno, Y., Nakajima, K., Naka, R., Kinoshita, M., Honda, E., Furuta, I., and Kakehi, K. (2003). A new fungal lectin recognizing alpha(1-6)-linked fucose in the N-glycan. J Biol Chem *278*, 32439-32447.

Olivari, S., and Molinari, M. (2007). Glycoprotein folding and the role of EDEM1, EDEM2 and EDEM3 in degradation of folding-defective glycoproteins. FEBS letters *581*, 3658-3664.

Oliver, J.D., van der Wal, F.J., Bulleid, N.J., and High, S. (1997). Interaction of the thiol-dependent reductase ERp57 with nascent glycoproteins. Science *275*, 86-88.

Ortmann, B., Copeman, J., Lehner, P.J., Sadasivan, B., Herberg, J.A., Grandea, A.G., Riddell, S.R., Tampe, R., Spies, T., Trowsdale, J., and Cresswell, P. (1997). A critical role for tapasin in the assembly and function of multimeric MHC class I-TAP complexes. Science *277*, 1306-1309.

Ou, W.J., Cameron, P.H., Thomas, D.Y., and Bergeron, J.J. (1993). Association of folding intermediates of glycoproteins with calnexin during protein maturation. Nature *364*, 771-776.

Palleros, D.R., Reid, K.L., Shi, L., Welch, W.J., and Fink, A.L. (1993). ATP-induced protein-Hsp70 complex dissociation requires K+ but not ATP hydrolysis. Nature *365*, 664-666.

Palmer, A., Rivett, A.J., Thomson, S., Hendil, K.B., Butcher, G.W., Fuertes, G., and Knecht, E. (1996). Subpopulations of proteasomes in rat liver nuclei, microsomes and cytosol. Biochem J *316 (Pt 2)*, 401-407.

Parodi, A.J. (2000a). Protein glucosylation and its role in protein folding. Annual review of biochemistry *69*, 69-93.

Parodi, A.J. (2000b). Role of N-oligosaccharide endoplasmic reticulum processing reactions in glycoprotein folding and degradation. Biochem J *348 Pt 1*, 1-13.

Peaper, D.R., Wearsch, P.A., and Cresswell, P. (2005). Tapasin and ERp57 form a stable disulfide-linked dimer within the MHC class I peptide-loading complex. The EMBO journal *24*, 3613-3623.

Picard, D. (2002). Heat-shock protein 90, a chaperone for folding and regulation. Cell Mol Life Sci *59*, 1640-1648.

Pind, S., Riordan, J.R., and Williams, D.B. (1994). Participation of the endoplasmic reticulum chaperone calnexin (p88, IP90) in the biogenesis of the cystic fibrosis transmembrane conductance regulator. J Biol Chem *269*, 12784-12788.

Plemper, R.K., and Wolf, D.H. (1999a). Endoplasmic reticulum degradation. Reverse protein transport and its end in the proteasome. Mol Biol Rep *26*, 125-130.

Plemper, R.K., and Wolf, D.H. (1999b). Retrograde protein translocation: ERADication of secretory proteins in health and disease. Trends Biochem Sci *24*, 266-270.

Pollock, S., Kozlov, G., Pelletier, M.F., Trempe, J.F., Jansen, G., Sitnikov, D., Bergeron, J.J., Gehring, K., Ekiel, I., and Thomas, D.Y. (2004). Specific interaction of ERp57 and calnexin determined by NMR spectroscopy and an ER two-hybrid system. The EMBO journal *23*, 1020-1029.

Qu, D., Teckman, J.H., Omura, S., and Perlmutter, D.H. (1996). Degradation of a mutant secretory protein, alpha1-antitrypsin Z, in the endoplasmic reticulum requires proteasome activity. J Biol Chem *271*, 22791-22795.

Quinones, Q.J., de Ridder, G.G., and Pizzo, S.V. (2008). GRP78: a chaperone with diverse roles beyond the endoplasmic reticulum. Histol Histopathol *23*, 1409-1416.

Rapoport, T.A., Rolls, M.M., and Jungnickel, B. (1996). Approaching the mechanism of protein transport across the ER membrane. Curr Opin Cell Biol *8*, 499-504.

Rivett, A.J., Palmer, A., and Knecht, E. (1992). Electron microscopic localization of the multicatalytic proteinase complex in rat liver and in cultured cells. J Histochem Cytochem *40*, 1165-1172.

Rubin, D.M., and Finley, D. (1995). Proteolysis. The proteasome: a protein-degrading organelle? Curr Biol *5*, 854-858.

Russell, S.J., Ruddock, L.W., Salo, K.E., Oliver, J.D., Roebuck, Q.P., Llewellyn, D.H., Roderick, H.L., Koivunen, P., Myllyharju, J., and High, S. (2004). The primary substrate binding site in the b' domain of ERp57 is adapted for endoplasmic reticulum lectin association. J Biol Chem *279*, 18861-18869.

Saito, Y., Ihara, Y., Leach, M.R., Cohen-Doyle, M.F., and Williams, D.B. (1999). Calreticulin functions in vitro as a molecular chaperone for both glycosylated and non-glycosylated proteins. The EMBO journal *18*, 6718-6729.

Scheuner, D., Vander Mierde, D., Song, B., Flamez, D., Creemers, J.W., Tsukamoto, K., Ribick, M., Schuit, F.C., and Kaufman, R.J. (2005). Control of mRNA translation preserves endoplasmic reticulum function in beta cells and maintains glucose homeostasis. Nature medicine *11*, 757-764.

Schlenstedt, G., Harris, S., Risse, B., Lill, R., and Silver, P.A. (1995). A yeast DnaJ homologue, Scj1p, can function in the endoplasmic reticulum with BiP/Kar2p via a conserved domain that specifies interactions with Hsp70s. The Journal of cell biology *129*, 979-988.

Schrag, J.D., Bergeron, J.J., Li, Y., Borisova, S., Hahn, M., Thomas, D.Y., and Cygler, M. (2001). The Structure of calnexin, an ER chaperone involved in quality control of protein folding. Mol Cell *8*, 633-644.

Schroder, M., and Kaufman, R.J. (2005). The mammalian unfolded protein response. Annual review of biochemistry *74*, 739-789.

Silvennoinen, L., Myllyharju, J., Ruoppolo, M., Orru, S., Caterino, M., Kivirikko, K.I., and Koivunen, P. (2004). Identification and characterization of structural domains of human ERp57: association with calreticulin requires several domains. J Biol Chem *279*, 13607-13615.

Smith, M.J., and Koch, G.L. (1989). Multiple zones in the sequence of calreticulin (CRP55, calregulin, HACBP), a major calcium binding ER/SR protein. The EMBO journal *8*, 3581-3586.

Solda, T., Garbi, N., Hammerling, G.J., and Molinari, M. (2006). Consequences of ERp57 deletion on oxidative folding of obligate and facultative clients of the calnexin cycle. J Biol Chem *281*, 6219-6226.

Sommer, T., and Wolf, D.H. (1997). Endoplasmic reticulum degradation: reverse protein flow of no return. Faseb J *11*, 1227-1233.

Stevens, F.J., and Argon, Y. (1999). Protein folding in the ER. Semin Cell Dev Biol *10*, 443-454.

Suter, D. M., Cartier, L., Bettiol, E., Tirefort, D., Jaconi, M. E., Dubois-Dauphin, M., and

Krause, K. H. (2006) Rapid generation of stable transgenic embryonic stem cell lines using modular lentivectors. Stem Cells *24*, 615-23.

Thomson, S.P., and Williams, D.B. (2005). Delineation of the lectin site of the molecular chaperone calreticulin. Cell Stress Chaperones *10*, 242-251.

Toyofuku, K., Wada, I., Hirosaki, K., Park, J.S., Hori, Y., and Jimbow, K. (1999). Promotion of tyrosinase folding in COS 7 cells by calnexin. Journal of biochemistry *125*, 82-89.

Trombetta, E.S., and Helenius, A. (1998). Lectins as chaperones in glycoprotein folding. Current opinion in structural biology *8*, 587-592.

Trombetta, E.S., and Helenius, A. (1999). Glycoprotein reglucosylation and nucleotide sugar utilization in the secretory pathway: identification of a nucleoside diphosphatase in the endoplasmic reticulum. The EMBO journal *18*, 3282-3292.

van Huizen, R., Martindale, J.L., Gorospe, M., and Holbrook, N.J. (2003). P58IPK, a novel endoplasmic reticulum stress-inducible protein and potential negative regulator of eIF2alpha signaling. J Biol Chem *278*, 15558-15564.

van Leeuwen, J.E., and Kearse, K.P. (1996). Deglucosylation of N-linked glycans is an important step in the dissociation of calreticulin-class I-TAP complexes. Proc Natl Acad Sci U S A *93*, 13997-14001.

Varki, A. (1993). Biological roles of oligosaccharides: all of the theories are correct. Glycobiology *3*, 97-130.

Vembar, S.S., and Brodsky, J.L. (2008). One step at a time: endoplasmic reticulum-associated degradation. Nature reviews *9*, 944-957.

Wada, I., Rindress, D., Cameron, P.H., Ou, W.J., Doherty, J.J., 2nd, Louvard, D., Bell, A.W., Dignard, D., Thomas, D.Y., and Bergeron, J.J. (1991). SSR alpha and associated calnexin are major calcium binding proteins of the endoplasmic reticulum membrane. J Biol Chem *266*, 19599-19610.

Walter, S., and Buchner, J. (2002). Molecular chaperones--cellular machines for protein folding. Angew Chem Int Ed Engl *41*, 1098-1113.

Ward, C.L., Omura, S., and Kopito, R.R. (1995). Degradation of CFTR by the ubiquitin-proteasome pathway. Cell *83*, 121-127.

Ward, P.L., Campadelli-Fiume, G., Avitabile, E., and Roizman, B. (1994). Localization and putative function of the UL20 membrane protein in cells infected with herpes simplex virus 1. Journal of virology *68*, 7406-7417.

Ware, F.E., Vassilakos, A., Peterson, P.A., Jackson, M.R., Lehrman, M.A., and Williams, D.B. (1995). The molecular chaperone calnexin binds Glc1Man9GlcNAc2 oligosaccharide as an initial step in recognizing unfolded glycoproteins. J Biol Chem *270*, 4697-4704.

Wiertz, E.J., Tortorella, D., Bogyo, M., Yu, J., Mothes, W., Jones, T.R., Rapoport, T.A., and Ploegh, H.L. (1996). Sec61-mediated transfer of a membrane protein from the endoplasmic reticulum to the proteasome for destruction. Nature *384*, 432-438.

Williams, D.B. (2006). Beyond lectins: the calnexin/calreticulin chaperone system of the endoplasmic reticulum. J Cell Sci *119*, 615-623.

Yan, W., Frank, C.L., Korth, M.J., Sopher, B.L., Novoa, I., Ron, D., and Katze, M.G. (2002). Control of PERK eIF2alpha kinase activity by the endoplasmic reticulum stress-induced molecular chaperone P58IPK. Proc Natl Acad Sci U S A *99*, 15920-15925.

Zapun, A., Darby, N.J., Tessier, D.C., Michalak, M., Bergeron, J.J., and Thomas, D.Y. (1998). Enhanced catalysis of ribonuclease B folding by the interaction of calnexin or calreticulin with ERp57. J Biol Chem *273*, 6009-6012.

Zhang, J.X., Braakman, I., Matlack, K.E., and Helenius, A. (1997). Quality control in the secretory pathway: the role of calreticulin, calnexin and BiP in the retention of glycoproteins with C-terminal truncations. Mol Biol Cell *8*, 1943-1954.

Zhang, Y., Kozlov, G., Pocanschi, C.L., Brockmeier, U., Ireland, B.S., Maattanen, P., Howe, C., Elliott, T., Gehring, K., and Williams, D.B. (2009). ERp57 Does Not Require Interactions with Calnexin and Calreticulin to Promote Assembly of Class I Histocompatibility Molecules, and It Enhances Peptide Loading Independently of Its Redox Activity. J Biol Chem *284*, 10160-10173.

Zhang, Y., and Williams, D.B. (2006). Assembly of MHC class I molecules within the endoplasmic reticulum. Immunologic research *35*, 151-162.

Zhou, J., Liu, C.Y., Back, S.H., Clark, R.L., Peisach, D., Xu, Z., and Kaufman, R.J. (2006). The crystal structure of human IRE1 luminal domain reveals a conserved

dimerization interface required for activation of the unfolded protein response. Proc Natl Acad Sci U S A *103*, 14343-14348.

ACKNOWLEDGEMENTS

First, I want to express my appreciation for my supervisor Prof. Marek Michalak for giving me the opportunity to work in his group at the University of Alberta, for providing me with the interesting topic, and for strongly supporting me during my stay.

Also, my thanks go to Helen Coe in the Michalak lab, who always answered all my questions and provided valuable feedback. The other members of the Michalak were also very kind and helpful, of course, and I apologize for not mentioning each of you. Thank you for making my time in the lab such a positive and memorable experience!

I want to particularly thank Prof. Obinger of BOKU for agreeing to be my supervisor and for helping with paper work and the final steps of the completion of my thesis.

Of course, I will never be able to express how thankful I am towards my parents. Thank you for always being there for me, in all situations. Without you, I would have never gotten this far. You are so generous in so many ways. Hopefully you know that you are the best!

I also want to thank my friends for accompanying me throughout my studies. Thanks (Marlene) for the time that provided distraction from university. I am glad I met you (Diana, Verena, Edi, only to mention a few) during my time at BOKU, it made things much easier.

And last but not at all at least, I want to thank Kevin. You are such an important part of my life! You always make me smile and help me over those rocky roads. Thanks for being there.

DANKE